Universitat Autònoma de Barcelona

Departament de Física
Grup de Física Teòrica

Compositeness from Holography and beyond

A dissertation presented by

Oriol Domènech Cots

in partial fulfillment of the requirements
for the degree of

Doctor of Philosofy

in the subject of

Physics

Advisor: Alex Pomarol Clotet

Universitat Autonoma de Barcelona
Bellaterra, Barcelona
June 2012

Abstract

The search for compositeness is a paramount goal in particle physics. Since the discovery of the atom, more and more fundamental structures have been discovered in nature in which matter is compound. The Standard Model of particle physics assumes the existence of a set of fundamental particles, including the Higgs boson, that possess no structure. Nevertheless there are strong motivations to believe that at least some of them could be composite and indeed its nature could be unraveled at the LHC. The main di culty of theories of composite particles is that, in certain regimes, their constituents are strongly coupled. Dealing with strongly coupled theories is a major puzzle in theoretical physics since they can not be understood in the usual framework of Quantum Field Theories, which is the main tool available in theoretical high energy physics. Fortunately, the study of extra dimensional theories has allowed us to gain deeper insights on this issue since these models can be viewed as `holographic' theories exhibiting strong dynamics. The purpose of this thesis is the study of different composite systems which exhibit strong dynamics. We focus on the development and study of extra dimensional models which can be interpreted as analogs of some strongly interacting systems present in nature, these are Quantum Chromodynamics and superconducting systems. Moreover we also analyze the case of quark compositeness in a model independent way by studying the effects of explicit models at energies below the cut-off scale of New Physics.

Resum

La recerca dels components fonamentals de la natura es l'objectiu primordial de la f sica de part cules. Des del descobriment de l'atom, estructures mes i mes fonamentals s'han descobert, les quals componen la materia. El Model Estandar de la f sica de part cules assumeix l'existencia d'una serie de part cules considerades fonamentals, incloent el boso de Higgs. No obstant, hi ha fortes motivacions per creure que almenys algunes d'aquestes part cules son compostes i, de fet, la seva naturalesa es podria revelar a l'LHC. El principal problema de les teories que descriuen part cules compostes es el fet de que, en certs regims, els constituents d'aquestes estan fortament acoblats. El tractament de teories fortament acoblades es un dels reptes mes importants en la f sica de part cules actual ja que aquest tipus de teories no poden esser tractades en el marc de la Teoria Quantica de Camps, que es l'eina principal en la f sica teorica d'altes energies. L'estudi de models en dimensions extra ha aportat una visio mes profunda d'aquest problema, ja que aquests models es poden entendre com teories `holografiques' que exhibeixen una dinamica d'acoblament fort. El proposit d'aquesta tesis es l'estudi de diferents sistemes de part cules compostes. Ens centrem en el desenvolupament de models en dimensions extra que es poden considerar com analegs a sistemes fortament acoblats presents a la natura, aquests son la Cromodinamica Quantica y els sistemes superconductors. A mes tambe analitzem el cas de la naturalesa composta dels quarks de manera generica a traves de l'estudi dels efectes de models expl cits a energies inferiors a l'escala de nova f sica.

Contents

Preface

Theoretical Particle Physics is at the frontier of our knowledge of nature. What could be branded as an speculative branch of science turns out to be the fascinating quest of the margin in which nature can operate. Pushing this margin to the limit, in all senses, is both challenging and exciting and leads to the proliferation of revolutionary ideas and pioneering technology that not only serve to gain deeper insights on nature but also have strong impact in other areas of knowledge. A clear example are the theories with Extra Dimensions (ED) that constitute possible completions of our present understanding of nature and, moreover, they can be used as a tool to progress towards the issue of calculability in strongly coupled systems, in which our current understanding of Quantum Field Theories (QFT) does not apply.

The novel idea of ED models pionereed by Kaluza and Klein in the twenties [1] as an attempt to unify all fundamental forces known at that time has been revisited in the recent past and indeed has received a strong boost in the last 15 years mainly due to the appearance of revolutionary work done by several authors among which we cite Maldacena, Witten, Randall, Arkani-Hamed, Dvali and a long etc. these has led to a vast amount of literature in this subject, trying to exploit the idea of ED to its last consequences.

The first part of this thesis mainly focuses on the construction of theories with ED as an attempt to effectively describe quantum field theories that exhibit strong dynamics. We will will be able to find 5D analogs of certain strongly coupled theories and relate them via the celebrated AdS/CFT correspondence, that we will explain below.

The second part of this thesis is devoted to the study of the feasibility of a class of models inspired by ED theories and intended to describe the quarks, the most fundamental particles we know in nature, as composite objects with an underlying

structure.

The contents of this thesis are based on the work done during four years (from 2008 to 2012) at the *Institut de Física d'Altes Energies* (IFAE) under the supervision of Professor Alex Pomarol. This is the fruit of collaborations with several researchers; Marc Montull (IFAE), Giuliano Panico (Zurich U.), Alex Pomarol (IFAE), Alberto Salvio (Scuola Normale Superiore di Pisa), Javi Serra (Cornell U.), Pedro J. Silva (IFAE) and Andrea Wulzer (Padova U.) that have materialized in published articles corresponding to Refs. [2 4].

Acknowledgements

This thesis is the result of the work made in four wonderful years at the `Institut de F sica d'Altes Energies' and throughout this time I feel really lucky to have shared a lot of time with my collegues which, in most of the cases, have become my friends as well. To all of them I would like to show my most sincere gratitude; Mariona, Jordi, Felix, Alessio, Alvise, Sebastian, Clara, Diogo, Oriol, Simone, Luca, Pere, Llu s, Volker, Juanjo, Marc R., Germano, Max, etc. Among them I would like to thank my Ph.D. `brothers' Javi and Marc and also my o cemate Joan Antoni not just for the stimulating discussions about physics in all this time but for their kindness and for the good moments we have lived together.

I would also like to thank all my collaborators, the ones already cited and also Andrea, Giuliano, Alberto and Pedro for letting me be part on the birth and development of the ideas that in the end cristalize as original research work, from each of them I have learned important lessons. I specially thank my supervisor, Alex Pomarol, for his guidance.

During these years I have had also the opportunity to know researchers from other institutions that have left a deep imprint on me. From my stay at Lausanne I would like to cite Riccardo R. for hosting me at the EPFL and also mi fellows Diego and Marco. From Rome I would like to thank my collegues Alex and Jamison. From Granada it has been a sincere pleasure to know Roberto and Adrian. I would also like to dedicate few special words to Roberto Contino, whose kindness and generosity were really helpful during my stay in Rome and left a profound mark on me.

I would also like to dedicate a words of gratitude to all my friends outside the academia for all the experiences lived throughout this wonderful years and that, for sure, have helped me to face the challenge of the Ph.D. in a more optimistic way. Among them I feel forced to cite a person that has been of paramount importance during this time for his patience, comprehension and support in all senses, I am not able to imagine what would have been about me without his presence; thanks Andres.

Finally and most importantly I feel really in debt with my family for his unconditional support; my father Xavier, my mother Carme and my sister Marta whose comprehension, kindness and faith on me has been of crucial importance during the years.

Chapter 1

Introduction

Our deepest understanding of the laws that govern nature is based on symmetry principles. This beautiful and illuminating formulation give rise to the most fundamental and successful theories we can nowadays handle. Just to give a flavor of the power of this tool let us enumerate two basic examples. The Standard Model of particle physics (SM) is the paradigm of a theory based on symmetries and behind its simplicity it hides one of the most successful theories in the history of science, being the anomalous magnetic moment of the electron its standard bearer, observable that has been proven to an unprecedented level of accuracy. The second example of theory that pushes the idea of symmetry to its limits is General Relativity (GR) in which the Lorenz group of transformations plays a central role.

These two examples involve theories that are at the basis of our most fundamental knowledge of the laws of nature and they are both based on symmetry principles. Therefore it is natural to try to push this idea further and it is actually what it has been done in the last years where theories beyond the SM (BSM) have been constructed in an attempt to address inconsistencies and naturalness problems of the SM. Examples of BSM models based on symmetry principles are Grand Unified Theories (GUT), Supersymmetry and Composite Higgs Models.

The framework in which the SM and its completions are constructed is based on Quantum Field Theories (QFT). This theoretical framework allows us to describe quantum mechanical systems parametrized by an infinte number of degrees of freedom. The combination of this powerful technology with the deep insight provided by symmetries leads us to an amazingly successful description of the weak, stong and Electromagnetic (EM) interactions, three of the four fundamental forces we know in nature so far. The key point for our understanding of QFT is the notion of perturbativity. The fact that the interactions in a quantum mechanical system

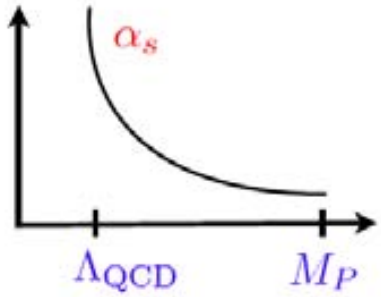

Figure 1.1: Running of $_s$ and the appearence of Λ_{QCD}.

of fields can be treated as small perturbations is crucial for expanding their effects around the free theory (without interactions) in order to determine the dynamics that govern the system, this is known as Perturbation Theory (PT). In order for the interactions to be small we need the value of the associated coupling constant to have a small value and in this way we can consider the coupling constant itself as a sensible parameter expansion. Unfortunately this is not always the case. We do know many systems in nature that become strongly coupled under certain circumstances. A paradigmatic example is QCD where the running of the strong coupling constant g_s due to quantum effects leads to the loss of a sensible perturbative expansion below a certain energy scale Λ_{QCD}, as can be seen in Fig. 1.1.[1]

Dealing with strongly coupled systems is a major puzzle in theoretical physics. The lack of perturbativity makes impossible to understand a quantum dynamical system of fields in terms of standard QFT tools. Luckily, the study of models involving Extra Dimensions (ED) has led us to gain deeper insights into this subject. These models are predicted by models of quantum gravity like String Theory and, moreover, constitute sensible Ultra-Violet (UV) completions of the SM in the sense that the scale of quantum gravity is reduced down to the Tera-electronVolt (TeV) thus getting rid of the large hierarchy between the EW scale and the Planck scale. But the interest on ED models goes far beyond these considerations, since the advent of the String/Gauge duality conjectured by Maldacena in 1997 that has allowed us to gain deeper insights towards the calculability issue of strongly coupled theories [6]. The original Maldacena conjecture relates type IIB String Theory in an AdS_5 S^5 background and $\mathcal{N} = 4$ SU(N) 4D gauge theory, what has been called the AdS/CFT correspondence, where AdS stands for Anti-de-Sitter and CFT for Conformal Field Theory. However, a more phenomenological

[1] A perturbative expansion in these enrgy regimes is indeed possible by taking the number of colors N_c as the expansion parameter. This will be explained in more detail in Sec 2.1.1

approach is still possible by considering 5D models of AdS space. This more modest attempt is clearly inspired in the AdS/CFT correspondence and from it we can still capture the essential features of the more involved string models. In this context, one of the motivations of the thesis is the construction of predictive frameworks for different strongly coupled systems that exhibit certain symmetry breaking patterns through the elaboration of 5D models and exploiting the ideas of the AdS/CFT correspondence. The generality of this holographic prescriptions will allow us to implement this framework in completely independent systems involving very different physics like Condensed Matter Systems exhibiting properties of Superconductivity or models of low energy QCD with spontaneous and explicit breaking of the chiral symmetry. The first part of the thesis is devoted to the construction of explicit 5D warped models with the aim of addressing the calculability issue on the aforementioned systems.

The common point in the two systems enumerated previously, apart from its strongly coupled nature, is the fact that the constituent fields of these theories are composite, in the sense that they possess an underlying structure that determine their properties. The search for underlying structure and the fundamental particles in nature is a major goal of particle physics. From atoms to quarks we have always found new structures and at this point in the SM of particle physics it is assumed that nature is composed by a set of elementary particles: quarks, leptons, gauge bosons and the Higgs. The question then is obvious; why stopping here in our search for compositeness? Could it be that the story does not end at this point?

Not just because of these naive arguments but, moreover, naturalness problems on the mass of the Higgs boson suggest that indeed this particle could have a composite nature, arising from a strongly coupled sector very much in the same way as the pion is made of quarks and gluons in the context of QCD. Also the heaviness of the Top quark in comparison to the other particles in the SM suggests that these particle could have an underlying structure related to the same strong sector. At this point it seems fair to look for compositeness in all the fundamental particles we know so far, *i.e.* , quarks, leptons and gauge bosons. Nevertheless, the fact that the sector of New Physics (NP) is strongly coupled makes di cult its study from a theoretical point of view. To overcome this problem explicit realizations of Composite models have been constructed in the context of the AdS/CFT correspondence. The expectation that the physics associated to this new composite sector should arise at the TeV scale makes feasible its search at the LHC. Luckily, when we probe NP at energies much less than the mass of the new heavy resonances that could arise from the strong sector we can parametrize all the effects and deviations from the SM predictions by a set of higher dimensional operators involving SM fields. Therefore it is not necessary to go to the full extra dimensional theory to compute these deviations but just to its simpler low energy

realization in terms of higher dimensional operators, where the heavy resonances have been integrated out.

The second part of the thesis is devoted to the study of NP effects parametrized through higher dimensional operators in a model independent way. We will see that these operators can be studied and constrained with the LHC data. Moreover, these operators arise in many completions of the SM and specifically they parametrize models of compositeness of the SM particles. Through their analysis we will be able to study the feasibiltity of different composite scenarios of the SM particles inspired in ED models.

The thesis is organized as follows, in Chap. 2 we introduce the models with warped Extra Dimensions and the AdS/CFT correspondence. We also look at three particular systems where this correspondence can be applied, they are Quantum Chromodynamics, the theory of Superconductivity and models of Higgs as a pseudo-Nambu-Goldstone boson. For each of these systems we make a brief introduction and discuss the necessity of an extra dimensional point of view. in Chap. **??** we introduce a 5D model that will allow us to describe both the meson and the baryon sector. In this holographic analog of QCD we will be able to derive properties of hadrons and find that they are in very good agreement with present experimental data. In Chap. **??** we will study an Extra Dimensional theory of Superconductivity in 2+1 and 3+1 dimensions in which a dynamical gauge field is present in the system. This fact will allow us to study some very important phenomenology associated to the gauge field and its interaction with the superconducting system. Finally, in Chap. 3 we will study the feasibility of the compositeness of the SM particles arising from a strongly coupled sector responsible of the Electro-Weak symmetry breaking, through the study of dijet events at the LHC. This analysis will allow us to put constraints on some higher dimensional operators that typically parametrize quark compositeness. Moreover, we will be able to study and constrain other BSM models in the same context.

Chapter 2

Warped Extra Dimensions and Holography

In the last fifteen years Extra Dimensional theories have been proven to be very useful in the context of particle physics and even beyond. There exist many models in the literature that, based on ED, are able to address the Hierarchy problem of the SM [7 10], that is the fact that the natural mass of the Higgs boson is much above its expected value. Therefore, these models can be considered as sensible candidates for completing the SM at the TeV scale. But the interest on ED models goes far beyond that since the advent of the AdS/CFT correspondence (see Ref. [5] for a nice comprehensive on this subject). The first to realize about the correspondence between gravity and gauge theories was Maldacena in 1997 [6]. He conjectured that,

$$\begin{array}{c}\text{type IIB string theory}\\ \text{on } \mathrm{AdS}_5 \quad S^5\end{array} \qquad \overset{\text{DUAL}}{\Longleftrightarrow} \qquad \mathcal{N}=4 \;\; \text{SU(N) 4D gauge theory}$$

where $\mathcal{N}$ is the number of supersymmetry generators and S^5 is the five-dimensional sphere. In the context of this duality the parameters of both theories are related by,

$$R^4_{AdS} = 4\pi g^2_{YM} N l^4_s, \tag{2.1}$$

where R_{AdS} is the curvature radius of the AdS_5 space, l_s the string length and g_{YM} is the coupling constant for the Yang-Mills theory. Of course this is a very particular example that is relating a specific type of string theory with a Supersymmetric SU(N) Yang-Mills theory. Actually, due to its high degree of Supersymmetry the dual theory presents Conformal invariance, that is associated to the isometries of the AdS_5 space in the gravity side.

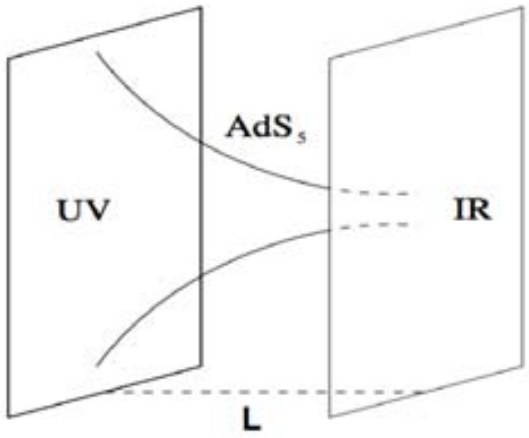

Figure 2.1: AdS_5 space in the Randall-Sundrum type 1 model.

This correspondence can be generalized to encompass a wider class of theories. The first thing to note is that the string modes are not crucial for the duality to take place. They can actually be decoupled by taking the limit

$$R_{AdS} \gg l_s \quad \Rightarrow \quad g_{YM}^2 N \gg 1, \tag{2.2}$$

which means that we are working at distances much larger than the string length and because of this reason the string modes can be decoupled and we end up getting a purely gravitational theory. This automatically implies that the 't Hooft coupling of the dual theory is much larger than one.

After decoupling the string modes and remaining with the low energy effective theory we end up with the more generic correspondence

$$\begin{array}{ccc} \text{5D AdS gravity} & \text{DUAL} & \text{4D CFT} \\ \text{weakly coupled} & \Longleftrightarrow & \text{strongly coupled} \end{array}$$

or more generically

$$\begin{array}{ccc} \text{nD AdS gravity} & \text{DUAL} & \text{(n-1)D CFT} \\ \text{weakly coupled} & \Longleftrightarrow & \text{strongly coupled} \end{array}$$

This is precisely what we are going to use throughout this Chapter in order to relate ED models with AdS geometry to their strongly coupled duals. Because the CFT is defined in one less dimension respect to the AdS space this theory is usually called "holographic".

Up to this point we have been very qualitative when describing the correspondence between these two classes of theories. One can actually be more quantitative

and get predictions from one theory to the other by relating the generating functionals of both theories. The idea is that every field we put in the AdS background when defining the 5D theory will be associated to some operator, $\mathcal{O}$, in the 4D side, that will specify the CFT [11, 12]. Let us define $\ _0$ as the UV boundary value of some bulk field

$$(x\ , z)\ _{z=z_{UV}} \qquad _0(x\ ). \tag{2.3}$$

When taking the limit z_{UV} $\quad$ 0 we can formally state the AdS/CFT correspondence at the quantitative level as,

$$Z[\ _0] = \int \mathcal{D}\ _{CFT}\ e^{-S_{CFT}[\ _{CFT}]-\int d^4x\ _0\mathcal{O}} = \int_{\ _0} \mathcal{D}\quad e^{-S_{bulk}[\ ]}\quad e^{iS_{eff}[\ _0]}\ , \tag{2.4}$$

where S_{CFT} is the CFT action with $\ _{CFT}$ generically denoting the CFT fields and S_{bulk} is the bulk 5D action. Note that, as stated above, $\ _0$ acts as a source for the operator $\mathcal{O}$. The on-shell gravity action, S_{eff} is obtained by integrating out the bulk degrees of freedom for suitably chosen IR boundary conditions. This is formally done by solving the 5D Equations of Motion (EOM) with fixed values for the source fields $\ _0$ and then substituting back into the action to obtain $\mathcal{L}_{eff}$.

Basically this equation relates the generating fuctional of the 4D CFT sourced by $\ _0$ with the 5D AdS theory when integrating out the bulk dynamics. This relation allows us to make calculations in one theory and relate them to the other. n-point functions can be calculated as in the usual path integral formalism, by considering $\ _0$ as a source

$$\mathcal{O}\ldots\mathcal{O}\ = \frac{^nS_{eff}}{_{0\cdots}\quad _0}\ . \tag{2.5}$$

So far we have just considered a general AdS_5 space and found that its properties can be related to a 4D CFT. It is interesting to focus on a slice of AdS space, where the presence of a UV and an IR brane chomp the space along the z direction. The metric in this particular case is given by,

$$ds^2 = \mathrm{e}^{-2ky}\quad dx\ dx\ + dy^2\ , \tag{2.6}$$

where the parameter k is the curvature scale of the warped extra dimension. We can also write this solution for the metric in conformal coordinates

$$ds^2 = a(z)^2(\quad x\ x\ - dz^2)\quad g_{MN}x^Mx^N\ , \tag{2.7}$$

being $a(z) = 1/kz$ is the warp factor. How the AdS/CFT picture changes in this slice of AdS? This question has been extensively studied in the literature [13 15].

The first thing to realize is that, because of the fact that the AdS_5 geometry is associated with conformal invariance in the 4D side, the abrupt cut in the ED due to the presence of the two branes will introduce two scales in the 4D theory related with a breaking of the conformal invariance. The presence of the UV brane will reflect in the CFT as an explicit breaking at some UV scale, Λ_{UV}, while the IR brane will generate a spontaneous breaking of the conformal invariance at the scale Λ_{IR}. Because of the spontaneous breaking a Nambu-Goldstone boson has to be present in the spectrum of particles, this is the dilaton, which is dual to the radion in the gravity side.

Finally, another consequence of placing a UV brane in the AdS_5 background is that the source $_0$ will become dynamical because the bulk dynamics will generate a kinetic term for this field when the 5D fields are integrated over. In this case $_0$ cannot just be considered as an external source but a truly dynamical field that is coupled to some operator in the CFT through the mixing term $_0\mathcal{O}$. Therefore the mass eigenstates will be mixtures of `elementary' $_0$ and `composite' CFT states. The fact that this kinetic term is generated for the source field $_0$ is a consequence of placing the UV brane at a finite position in the extra dimension. This term could actually be sent to zero if we place the UV brane at y_{UV} $-$.

In the following sections of this chapter we will study two specific examples that will serve us to exploit the virtues of the AdS/CFT correspondence and extra dimensional models in order to address the issue of calculability in strongly coupled systems. In Sec. 2.1 we study the case of QCD at energies in which the theory exhibits strong dynamics, while in Sec. 2.2 we analyze the superconducting and the superfluid systems through an extra dimensional point of view.

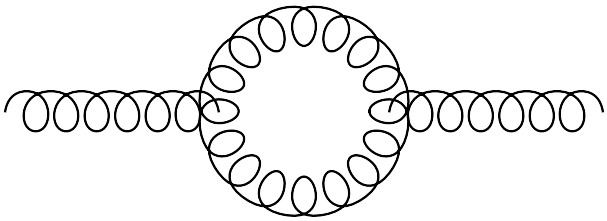

Figure 2.2: Vacuum polarization diagram for the gluon at the one-loop level.

2.1 Holographic QCD

The strong interaction is one of the fundamental forces we know in nature and the theory which describes it is QCD. Due to its non-abelian nature this theory is just known at high energy scales, this is a consequence of the fact that QCD is asymptotically free, which means that its coupling constant, when considering quantum effects, runs towards small values at high energies. For the very same reason this coupling gets bigger as we go to lower energies until a point in which the theory can not be considered perturbative anymore. We then reach the region in which QCD is strongly coupled ($g_s \quad 4\pi$). This automatically generates a scale in the theory which is precisely the energy scale at which PT brakes down, $\Lambda_{QCD} \sim 1$ GeV. This is a dynamical mechanism for generating scales in quantum field theories, known as *dimensional transmutation*. Below this scale the strong interaction seems to be well described in terms of baryons and mesons, what suggests a duality between these composite particles and the `fundamental' degrees of freedom in QCD, *i.e.* the quarks and the gluons. This consideration seems to point out that a successful theory of strong interactions at low energies have to describe hadron physics in some way.

2.1.1 Low Energy QCD and the large N_c limit

Though QCD reaches a scale below which the theory exhibits strong dynamics a perturbative expansion in this regime is still possible by considering a `hidden' parameter of the theory: the number of colors, N_c, [16]. Troughout this section we will see that by taking the limit of large number of colors ($N_c \quad$) we will be able to qualitatively derive many properties of hadron physics in a purely QCD framework, suggesting that this limit could lead to a successful description of low energy QCD.

Let us very briefly review the main properties of Large N_c QCD. A complete discussion about this topic can be found in Ref. [17].

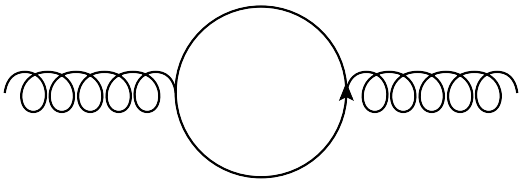

Figure 2.3: One-loop quark contribution to the gluon propagator.

First of all let us consider the one loop gluon vacuum polarization amplitude, Fig. 2.2. A naive estimate tells us that this diagram will scales as $g^2 N_c$ where the N_c factor comes from the number of possible colors running in the loop. If we want this diagram to have a smooth value when taking the limit of large N_c we should impose that $g^2 N_c$ approaches a constant value as N_c , what implies that

$$g \sim \frac{}{\overline{N_c}} \,. \tag{2.8}$$

where is known as the 't Hooft coupling. The lesson we learn from the scaling property of the coupling constant is that just diagrams with large enough N_c combinatoric factors will survive in the large N_c limit. Actually, by a naive counting of powers of N_c we can see that only planar diagrams survive while non-planar diagrams are always suppressed respect to the former. What we mean here by planar is a kind of diagrams that can be written in the plane without line crossing at points where there are not interaction vertices. This criterium defines a class of topologies called *planar*. The fact that only this kind of diagrams survives simplifies very much this approach.

Another important consideration is the fact that loops of quarks are also suppressed by powers of N_c. Again, this can be seen by a simple N_c power counting. Consider the diagram in Fig. 2.3, since quarks and gluons are coupled with coupling constant g this diagram has to scale like $\sim 1/N_c$. The main difference with respect to the gluon self energy is basically the fact that the color of the quarks inside the loop is fixed by the external gluon legs and therefore there is no N_c combinatoric factor in the numerator in this case.

Let us consider another important case that is the one current-current correlator JJ of quark bilinears like qq or $q \quad q$. In this case we will unavoidably have a quark loop running in the diagram. Similarly to the previous cases, only some particular diagrams will survive in the large N_c limit. It is easy to see by NDA arguments that they will be the planar ones in which the quark loop is placed at the edge of the diagram.

The above considerations about the type of diagrams that survive in the large N_c limit define a set of selection rules that, in the case of two point functions, can

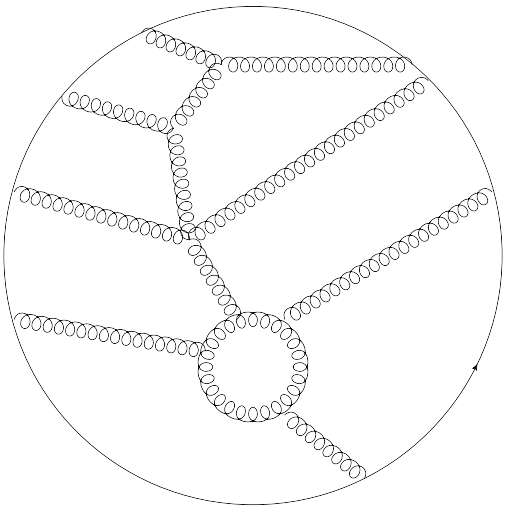

Figure 2.4: Leading contribution to quark bilinears in powers of N_c.

be summarized with the following statement

> *The dominant contributions to matrix elements of quark bilinears will come from planar diagrams with quarks placed only at the edge.*

A general diagram giving a leading contribution in the parameter N_c is shown in Fig. 2.4.

The fact that quarks can only be placed at the edge of the diagram has a very important consequence, that is; the intermediate states in the current-current matrix element JJ involve always just one q and one q fields. Since mesons are qq bound states we can a rm that the intermediate states are always meson resonances. Moreover we can quantify this statement in the following way

$$J(p)J(-p) \ = \sum_n \frac{f_n^2}{p^2 - m_n^2}, \tag{2.9}$$

where $f_n = \ 0 \ J \ a_n$ is the decay constant for the n'th resonance and m_n its mass and the sum runs over mesons.

Many important properties of the meson sector can be derived from the above equation. First of all, the large energy behavior of JJ is known to be logarithmic. This can only match with Eq. (2.9) if the sum is infinite, which means that there is an infinite tower of meson resonances in this limit. We can also see from Fig. 2.4 that the dominant contributions to the current-current correlator are of order N_c, $JJ \ \sim N_c$. This leads to the conclusion that the decay constant of meson

resonances scales like $f_n \sim \sqrt{N_c}$. Finally, the smooth dependence on N_c in both sides also implies that the mass of the meson resonances should be independent of N_c, $m_n \sim N_c^0$.

So far we have just talked about mesons in the large N_c approach. How baryons look like in this limit? To answer this question first note that for a SU(N) theory of strong interactions we can construct singlets of quark fields by taking a qq pair or considering N_c (anti-)quark bound states. The first option would correspond to a meson resonance while the second would be associated with a baryon in the large N_c limit. The fact that the baryon is composed by N_c quarks leads us to the conclusion that the baryon mass scales like $M_B \sim N_c \sim 1/g^2$. This particular scaling of M_B with the coupling very much resembles the one of solitons, what suggests that in the large N_c expansion, baryons could arise as topological solutions of the theory, in a similar way as postulated by T.H.R. Skyrme in the 60's [18].

Many other interesting properties can be derived in the context of the large N_c limit, but let us just summarize what we found so far:

> The large N_c expansion describes a theory of infinite, stable and narrow meson resonances which moreover are non-interacting.
>
> Baryons arise as topological solutions of the theory.
>
> The physical properties of baryons and mesons present a definite scaling with N_c ($m_n \sim N_c^0$, $M_B \sim N_c$, $f_n \sim \sqrt{N_c}$, etc.).

$$
\begin{aligned}
&m_n \sim N_c^0 \\
&M_B \sim N_c \\
&f_n \sim \sqrt{N_c} \\
&g \sim \sqrt{N_c} \\
&. \\
&. \\
&.
\end{aligned}
$$

2.1.2 Large N_c realization in Extra Dimensions

So far we have just derived qualitative features of then large N_c expansion that we can relate to hadron physics. Though they are very encouraging, we do not posses a quantitative insight on this framework. This leads us to wonder if an explicit realization of this limit can be constructed. In order to guess if this is possible let us look more closely to the properties of large N_c theories described above.

A set of infinite, stable and non-interacting resonances appears naturally in the large N_c approach.

This very much resembles the behavior of a 5D theory when integrating out the extra dimension. The result is the appearance of a KK tower of stable resonances. Moreover, from Eq. (2.2) we can see that in the large N_c limit of the 4D CFT we can obtain a coupling g 1.

Baryons arise as solitons in the large N_c limit.

Recently, it has been seen that ED models can accommodate for stable topological solutions [19 21] and therefore they could be candidates for describing baryon physics.

From these considerations we can see that ED models very much resemble large N_c QCD. It would be nice if, in addition, we could mimic the N_c scalings of meson and baryon properties. let us try to do this exercise in a simple way. We consider a simple 5D model with a chiral $SU(2)_L$ $SU(2)_R$ symmetry in the bulk

$$\mathcal{L}_{5D} = \int dx^5 \quad \overline{-g} M_5 \mathrm{Tr}[-L^{MN} L_{MN} - R^{MN} R_{MN}], \tag{2.10}$$

where $M, N = (\ , 5)$ refer to the five coordinates. We can also define

$$\begin{aligned} V_M &= L_M + R_M, \\ A_M &= L_M - R_M, \end{aligned} \tag{2.11}$$

associated to vector and axial fields.

Let us very briefly flash the properties of this model and try to relate them with large N_c QCD. When integrating out the extra dimension this model leads to resonances with the same quantum numbers as the QCD mesons (, $a1$, , etc.). Moreover, the holographic 4D theory possesses a global $\mathrm{SU}(2)_L$ $\mathrm{SU}(2)_R$ symmetry analogously to the QCD chiral one. Now, we can wonder if from this simple Lagrangian we can mimic the N_c scalings of masses and decay constants of hadron resonances.

The first thing to note is that we have factored out a M_5 factor in front of the Lagrangian, which plays the role of $1/g^2$. If we assume that M_5 scales like, $M_5 \sim N_c$ in order for the coupling to mimic the behaviour of the large N_c QCD case, Eq. (2.8), we will be able to deduce the scalings of the other hadron properties.

From the holographic description stated above, Eq. (2.4), we see that we can calculate properties of the holographic theory by integrating out the bulk dynamics

keeping the source term fixed. For this reason we are going to impose the following boundary conditions in the UV brane

$$\begin{aligned} V_{z_{UV}} &= v \ , \\ A_{z_{UV}} &= a \ , \end{aligned} \tag{2.12}$$

It can be seen that, when solving the EOM's keeping these boundary values fixed (and choosing suitable boundary conditions to cancel the IR boundary terms), we formally obtain an effective Lagrangian of the form [22]:

$$\mathcal{L}_{eff} = M_5 P \ \mathrm{Tr}[v \ \ _V(p^2) v \ + a \ \ _A(p^2) a \ ], \tag{2.13}$$

where $P = - p \ p \ /p^2$ is a projector. The explicit form of the $_{V\,A}$ can be obtained in the case of an AdS_5 space [22, 23]. It is not our goal to derive the exact value for these functions but just to sketch the properties of this solution. Is for this reason that we have factored out the M_5 factor in front of the Lagrangian, Eq. (2.10).

In view of Eq. (2.5) we can relate $_{V\,A}$ with the two point correlation functions of the quark currents $J_{V\,A} J_{V\,A}$. In the large N_c limit these functions are expected to be expressed as a sum over narrow resonances as in Eq. (2.9), which means that the poles of these correlators can be interpreted as the mass of the resonances in the 4D theory, while the residues of the poles would correspond to their decay constants. Since the functions $_{V\,A}$ come purely from solving the 5D EOM and they are independent of M_5 since this parameter is factored in front of the Lagrangian, we conclude that the poles of these functions should also be independent of M_5, which means that $m_n \sim N_c^0$.

On the other hand the residues of these poles have to absorbe the M_5 factor in front of the effective Lagrangian, Eq. (2.13) and for this reason $f_n \sim \overline{M_5} \sim \overline{N_c}$.

Finally, if we believe that topological solutions can be found stable in this AdS_5 background we could associate them with baryon, in the spirit of [18], and therefore, baryons could be accommodated in this set up[1] . Moreover let us guess how the mass of a baryon would scale in this ED approach. Since topological solutions at the classical level are associated to non-trivial configurations of the 5D fields, their energy would be calculated as the integral of the energy density, *i.e.* the Hamiltonian density $\mathcal{H}$, of this particular configuration of fields over all the space. For static field configurations the baryonic energy would correspond exactly to its mass and, therefore

$$M_B = \int dx^3 dz \mathcal{H} = \int dx^3 dz \ \ \overline{-g} M_5 \mathrm{Tr}[L^{MN} L_{MN} + R^{MN} R_{MN}] \, . \tag{2.14}$$

[1] This is what it has been actually found in Ref. [19] for the same Lagrangian, Eq. (2.10).

As we can see, the mass of the baryon will scale like $M_B \sim N_c \sim 1/g^2$. The particular scaling of the mass with the coupling constant is also a feature of solitons so, in some sense, this behavior was already expected.

So far we have seen that with a simple 5D model we are able to reproduce many of the properties of the large N_c limit of QCD. Of course, we could add more elements in this framework in order to make more contact with the real theory of QCD like the spontaneous and the explicit breaking of the chiral symmetry. All these features suggest that we should be able to find a dual theory of low energy QCD based on extra dimensions by making an appropriate matching between the hadron properties and the parameters of the 5D model. This is precisely the aim of the next Section, where we study the possibility of obtaining a unified description of baryons and mesons by making use of a 5D model analog to QCD where chiral symmetry is spontaneously and explicitly broken.

2.1.3 Hadron physics in Holographic QCD with Chiral Symmetry Breaking

5D approach to QCD

Throughout the previous Section we have discussed the virtues of 5d models and specifically their resemblance to the large-N_c expansion of QCD, what suggests that we could be able to find an analog version of this theory based on Extra Dimensions. This possibility has been widely discussed in the literature [19 22, 34 37] and can be briefly summarized as follows. From the theoretical point of view, these models resemble large-N_c QCD in that they contain infinite towers of weakly interacting mesons while the baryons are solitons, similar to the Skyrmions of the non-linear -model. Differently from ordinary Skyrmions, however, the 5d soliton size remains finite in the weak coupling (large-N_c) limit and is therefore parametrically larger than the length scale at which the 5d model enters the strongly coupled regime. The 5d Skyrmions are genuinely macroscopic objects, whose physics is perfectly within the reach of the effective theory as it must also be the case for the baryons in the true theory of large-N_c hadrons [17].

For what concerns phenomenology, it is already quite remarkable that the holographic implementation of the QCD chiral symmetry and of its breaking automatically leads to towers of vector and scalar mesons with the quantum numbers of the observed , , a_1, f_1, a_0, f_0, $\pi(1300)$ and (1295), but even more remarkable is that, when extrapolating the model to the physically relevant case of $N_c = 3$, an agreement at less than 10% with observations is found. This success is non-trivial because the model contains an extremely limited number of free parameters that

can be adjusted to reproduce many observed meson couplings and masses, and is mainly due to a set of phenomenologically successful "sum rule" relations among the predictions. The latter originate from the 5d structure of the theory and are independent of many details of the model, such as the background 5d metric, whose choice is therefore unessential for phenomenology as discussed in [38]. The overall agreement is less good in the baryonic sector, but still compatible with the expected $1/N_c \sim 30\%$ deviations. Furthermore, one recovers in a non-trivial way several features of the large-N_c QCD baryons such as the scaling of the currents form factors with N_c, the fact that the isovector electric and magnetic radii diverge in the chiral limit (as in QCD [39]) and other large-distance behaviors [40]. In holographic QCD an important role is played by the Chern Simons (CS) term of the 5d action whose presence is required, with a fixed coe cient, by the need of reproducing the QCD global anomalies. The CS is therefore the 5d analog of the gauged Wess Zumino Witten (WZW) term of the standard 4d chiral theory and, like the WZW, it is responsible for the π decay and for "naive parity" breaking in the Goldstone interactions [41]. The CS actually contains the WZW, in the sense that it reduces to it in the low-energy description of the Goldstones obtained from the 5d theory, but it also contains other interactions such as the well-measured "anomalous parity" couplings g , g and g . As a result of the 5d structure of the theory, these couplings are predicted and are found to be in good agreement with the observations. In the case of exact chiral symmetry (and only in that case, as we will show) the CS term is also crucial for the physics of the baryons because it stabilizes the 5d Skyrmion solution and makes its size scale like a constant for large N_c.

Many of the above-mentioned results, and in particular the ones related with the CS term and with the baryons, have however been only established in the minimal holographic QCD model with exact chiral symmetry; the aim of this article is to generalize them to the more realistic case of explicit chiral breaking (and therefore non-vanishing mass for the Goldstones) and to check if the previously outlined general picture survives. In order to complete this program we first of all need a model with explicit breaking, but we cannot simply employ the original one of [22, 35, 36]. A very simple variation is needed in order to incorporate the CS term and the 5d Skyrmions that were not considered in the original literature. Like in [22, 35, 36], our model will be a 5d $U(2)_L$ $U(2)_R$ gauge theory with a 5d scalar field in the bifundamental of the group, whose presence is necessary to parametrize the breaking of the chiral symmetry due to the quark mass term. The only difference with [22, 35, 36] is in the boundary conditions for the gauge fields at the IR brane, where we break the chiral group to vector (as in [37]) instead of preserving it and making the spontaneous chiral symmetry breaking arise exclu-

sively from the VEV of . [2] This choice of boundary conditions would be a priori equivalent to the original one from the model-building perspective, and costs no more parameters, but is necessary if willing to incorporate the CS term. As we will discuss in more details in the following section (see also [42]), the reason is that the CS gauge variation is an integral on the boundaries of the 5d space and therefore receives contribution from both the UV and the IR brane. While the UV term is welcome because it reproduces the QCD global anomalies, the IR one must cancel because the IR group is gauged and a non-vanishing variation would have on the model the same effects of a gauge anomaly. The symmetry-breaking boundary conditions, which are actually equivalent to gauging only the vector subgroup at the IR, enforce this cancellation. On top of this, symmetry-preserving IR boundary conditions could make the 5d Skyrmion unstable or even the classical 5d Skyrmion solution not to exist at all because the baryonic charge [3]

$$B = \frac{1}{32\pi^2}\int d^3x \int_{z_{\rm UV}}^{z_{\rm IR}} dz \quad \mathrm{Tr}\left[\mathbf{L}\ \ \mathbf{L}\ \ -\mathbf{R}\ \ \mathbf{R}\ \right] \int_r \left[\ {}_3(l) - \ {}_3(r)\right] + \int_{z=z_{\rm IR}} \left[\ {}_3(l) - \ {}_3(r)\right] , \tag{2.15}$$

would not be quantized and therefore not topologically conserved. It is indeed possible to change continuously the IR contribution to B (the last term in the equation above) without affecting the rest by a local variation of the fields at the IR boundary. This is impossible with symmetry-breaking boundary conditions because the IR contribution vanishes identically and the baryonic charge is quantized as shown in [19 21].

Troughout this chapter we will study the implications of chiral symmetry breaking for hadron physics in Holographic QCD. In Section 2.1.4 we first of all describe the model which is the first one containing at the same time the explicit chiral breaking, the QCD anomalies (*i.e.* the CS term) and the 5d Skyrmion. We also discuss its phenomenological implications for the physics of vector and scalar mesons, which because of the change in the boundary conditions are a priori different from the ones derived in [22, 35, 36]. We actually find a quite similar phenomenology, the only remarkable difference being in the mass of the $\pi(1300)$ pseudoscalar meson that was impossible to fit in the original model [36] while it is easily accommodated in our case. We obviously also take into account the processes mediated by the CS term that were absent in the original model, and eventually perform a complete fit of the meson observables which allows us to fix the parameters and to quantify the level of agreement with observations. In Section 2.1.5 we study the physics of the

[2] Actually, another di erence with [22, 35, 36] is that the gauge group was taken there to be the chiral $SU(2)$ while our model is based on $U(2)$.

[3] For the notation, see [19 21] or the following Section.

baryons, generalizing the analysis of [19 21] where the chiral case was considered. In that section we check that the existence and calculability of the 5d Skyrmion is maintained in the non-chiral case, and see how much the predictions change after the deformations required to incorporate the chiral breaking in the holographic model. The latter deformation is not mild because the newly introduced 5d scalar does not decouple from the vector mesons, and therefore from the 5d Skyrmion solution, even when the chiral symmetry is restored. We also compute the isovector form factor radii which were divergent in the chiral case and become now finite, as expected in QCD, due to the chiral breaking. Finally, in Section 2.1.6, we present our conclusions.

2.1.4 Meson sector in Holographic QCD

As a starting point for the description of the model, let us consider the QCD partition function $Z_{QCD}[l, r, M]$ in the presence of sources for the left and right global currents and for the quark mass operator. The latter reads

$$Z_{QCD}\left[\mathbf{l}, \mathbf{r}, M\right] \;=\; \int \mathcal{D} \quad \exp\left[iS_{QCD}[\quad] + i\int d^4x\, \mathrm{Tr}\left(\mathbf{l}\;\; j_L + \mathbf{r}\;\; j_R - Ms - s\;\; M\;\;\right)\right], \tag{2.16}$$

where collectively indicates the QCD fundamental fields, S_{QCD} is the massless QCD action, $\left(j_{L\,R}\right)_{ij} = \overline{q}^j_{L\,R} \quad q^i_{L\,R}$ are the currents of the $U(2)_L \quad U(2)_R$ chiral group and $s_{ij} = \overline{q}^j_L q^i_R$ is the quark bilinear. Due to anomalies, the partition function changes under local chiral transformations as [4]

$$Z_{QCD}\left[\mathbf{l}^{(\widehat{g}_L)}, \mathbf{r}^{(\widehat{g}_R)}, \widehat{g}_L M\, \widehat{g}_R\right] \;=\; e^{i\mathcal{A}} Z_{QCD}\left[\mathbf{l}, \mathbf{r}, M\right], \tag{2.17}$$

where the vector sources transform as gauge fields (*i.e.*, $\mathbf{l}^{(\widehat{g}_L)} = \widehat{g}_L[\mathbf{l} \;\; + i \quad]\widehat{g}_L$ and analogously for $\mathbf{r}$) and $\mathcal{A}$ stands for the QCD global anomaly which, as discussed in appendix C, can be put in the form

$$\mathcal{A} = \frac{N_c}{24\pi^2}\int \left[{}^{-1}_{4}(\boldsymbol{\alpha}_L, \mathbf{l}) - {}^{-1}_{4}(\boldsymbol{\alpha}_R, \mathbf{r})\right] \tag{2.18}$$

by the addition of suitable local counterterms. In words, what eqs. (2.16) and (2.17) mean is that 2-flavor (large-N_c) QCD is a theory endowed with an $U(2)_L$

[4] The equation which follows is only valid in the large-N_c limit in which the $U(1)_A \;\; SU(N_c)^2$ anomaly can be neglected and the $'$ only gets its mass from the explicit chiral symmetry breaking. Given that the expansion parameter of the 5d theory is interpreted as $1 \;\; N_c$, it is completely correct to stick to eq. (2.17) at the leading order, though it would be interesting to see what kind of next-to-leading order corrections the inclusion of the $U(1)_A$ anomaly leads to. The problem of incorporating the $'$ mass in holographic QCD has already been addressed in [43], though its connection with the anomalies and the $1 \;\; N_c$ expansion has not been outlined.

$U(2)_R$ anomalous global symmetry and with a non-dynamical spurion field M, associated with the quark mass operator, in the bifundamental of the group. This symmetry, with its explicit breaking parameter M, must obviously be present in any phenomenological description of hadrons such as the one we want to construct.

Following the holographic method, we incorporate the chiral symmetry and the spurion by introducing 5d fields with appropriate quantum numbers ($\mathbf{L}_M$, $\mathbf{R}_M$ and) associated respectively to the sources $\mathbf{l}$, $\mathbf{r}$ and M, and identify the latter with the values of these fields at the UV-boundary. For the gauge fields the model is exactly as in [20], and all what we have to add is the scalar which, according to the holographic prescription, transforms as

$$^{(g_L\, g_R)} \qquad g_L \quad g_R\,, \tag{2.19}$$

under the local 5d $U(2)_L$ $U(2)_R$ group and is subject to the following UV boundary conditions

$$_{z=z_{\rm UV}} = \left(\frac{z_{\rm UV}}{z_{\rm IR}}\right)^{\ -} M\,, \tag{2.20}$$

with $^{-}$ defined in eq. (2.33). The need for the rescaling in M is a technicality associated with our choice of the AdS_5 geometry, and will be explained in the following. For simplicity, and since we are considering the two-flavor case in which the vector symmetry breaking is negligible, we take the spurion VEV to be of the form

$$M \;=\; M_q\, \mathbb{1}\,,$$

which respects $U(2)_V$.

The partition function of the 5d model, which we would like to identify with the QCD one in eq. (2.16), is defined as

$$Z\,[\mathbf{l},\mathbf{r},M] \qquad \int \mathcal{D}L_M \mathcal{D}R_M \mathcal{D} \quad \exp \;\; i\,S_5[L,R,\;\;]\;\;, \tag{2.21}$$

where the dependence of the r.h.s. on the sources arises from the boundary conditions on the allowed field configurations. The gauge part of the 5d action is given by a kinetic part

$$S_g = -\int d^4x \int_{z_{\rm UV}}^{z_{\rm IR}} dz\, a(z)\, \frac{M_5}{2} \left\{ {\rm Tr}\left[L_{MN}L^{MN}\right] \,+\, \frac{1}{2}\widehat{L}_{MN}\widehat{L}^{MN} \,+\, \quad L \qquad R \right\}, \tag{2.22}$$

and a Chern Simons part

$$S_{CS} \;=\; \frac{N_c}{16\pi^2}\int d^5x \left\{ \frac{1}{4}\;^{MNOPQ}\widehat{L}_M\, {\rm Tr}\left[L_{NO}L_{PQ}\right] \,+\, \frac{1}{24}\;^{MNOPQ}\widehat{L}_M\widehat{L}_{NO}\widehat{L}_{PQ} \,-\, \quad L \qquad R \right\}, \tag{2.23}$$

having parametrized the fields as $\mathbf{L} = L^a \ ^a/2 + \widehat{L} \ \mathbb{1}/2$ and analogously for $\mathbf{R}$. As discussed before, the UV boundary conditions for the gauge fields are

$$\mathbf{L} \ _{z=z_{\rm UV}} = \mathbf{l} \ , \qquad \mathbf{R} \ _{z=z_{\rm UV}} = \mathbf{r} \ . \tag{2.24}$$

The action for the scalar is

$$S \ = M_5 \int d^4x \int_{z_{\rm UV}}^{z_{\rm IR}} dz \, a^3(z) \left\{ {\rm Tr} \left[(D_M \ ) \ D^M \ \right] - a(z)^2 M_{Bulk}^2 {\rm Tr} \left[\ \ \right] \right\} , \tag{2.25}$$

where we defined the covariant derivative

$$D_M \ \ _M \ - i \, \mathbf{L}_M \ + i \ \mathbf{R}_M \, . \tag{2.26}$$

If a local 4d chiral transformation is performed on the sources, as in eq. (2.17), the UV boundary conditions get modified but this change can be reabsorbed in a change of variable in the path integral of the form of a local 5d gauge transformation $g_{L\,R} = \exp(i \ _{L\,R})$ which does not reduce to the identity at the UV brane. The kinetic part of the gauge action S_g and the scalar action S are invariant under this transformation, while the CS part (as discussed in appendix C) gives the variation

$$S_{CS} = \frac{N_c}{24\pi^2} \left(\int_{z=z_{\rm UV}} \left[{}^{-1}_{4}(\boldsymbol{\alpha}_L, \mathbf{l}) - {}^{-1}_{4}(\boldsymbol{\alpha}_R, \mathbf{r}) \right] - \int_{z=z_{\rm IR}} \left[{}^{-1}_{4}(\boldsymbol{\alpha}_L, \mathbf{L}) - {}^{-1}_{4}(\boldsymbol{\alpha}_R, \mathbf{R}) \right] \right) . \tag{2.27}$$

The UV contribution in the above expression is welcome, because it coincides with the anomalous variation in eq. (2.17). On the other hand, the IR terms in S_{CS} have no counterpart in 4d QCD and must be cancelled. The chiral-breaking conditions

$$(\mathbf{L} \ - \mathbf{R} \ )_{\ z=z_{\rm IR}} = 0 \ , \qquad (\mathbf{L}_{\ 5} + \mathbf{R}_{\ 5})_{\ z=z_{\rm IR}} = 0 \tag{2.28}$$

enforce this cancellation, which, on the contrary, would not occur in the case of the symmetry-preserving Neumann conditions considered in [22, 35, 36]. The choice (2.28) of boundary conditions is motivated not only by the need of correctly reproducing the QCD anomaly, as the previous discussion shows, but also by the consistency of the theory in the presence of the CS term. We can introduce a term in the action only if it respects all the symmetries which are gauged. As can be seen from es. (2.27), the CS term in eq. (2.23) is not invariant under local axial transformations which do not vanish at the IR boundary, thus it can be consistently introduced only if the local axial symmetry at the IR boundary is not gauged, as implied by the conditions in eq. (2.28).

For the scalar we impose the IR boundary condition

$$_{z=z_{\rm IR}} = \qquad \mathbb{1} \, , \tag{2.29}$$

where is a positive parameter and fields satisfying eq. (2.29) with both signs, associated to two disconnected sectors, coexist in the theory. These boundary conditions (with their sign ambiguity) can be thought to originate (as in [22, 35, 36]) from an IR localized potential of the form $V = \quad ((\mathrm{Re\,Tr}[\ ])^2 - 4\ ^2)^2 + \left(2\mathrm{Tr}[\quad\ ] - (\mathrm{Re\,Tr}[\ ])^2\right)$. The latter would enforce eq. (2.29) in the , limit. When dealing with small field fluctuations around the vacuum, the subtle sign ambiguity is irrelevant, because only one of the two sectors contains a stable stationary point and the dynamics entirely takes place around it. This is because of the $-$ symmetry of the lagrangian, which implies that a simultaneous sign change of M_q and of the boundary condition (2.29) is unobservable. The pion mass squared is therefore $m^2 \sim \quad M_q\ \ f(z_{IR}\ ) + \mathcal{O}(M_q^2)$ which, depending on the sign of M_q, can be positive or negative implying that only one of the two sectors can be tachyon-free. For $M_q > 0$ the vacuum is in the "plus-sign" sector and the physics of mesons, described by small fluctuations around the vacuum, is totally insensitive to the presence of the other (minus-sign) sector. We will show in the following section that the baryons live, on the contrary, in the minus-sign sectors so that the sign ambiguity in eq. (2.29) has to be maintained.

Having described the model, we can now study its phenomenological implications for the physics of mesons, with the aim of comparing it with the observations and of fixing its parameters. With respect to the massless case of [20], three new parameters (M_q, and M_{Bulk}) have been introduced, but also new predictions can be extracted from the model. The scalar describes scalars and pseudo-scalars with the isospin quantum numbers of, respectively, the $a_0(980)$, the $f_0(980)$, the $\pi(1300)$ and the (1295); we will use their masses, plus of course the pion mass, to fit the new parameters. [5]

To study the meson spectrum, we have first of all to find the vacuum configuration, which is given by the solution of the bulk equation of motion for

$$D_M\left(a^3(z)D^M\ \ \right) = -a^5(z)M_{Bulk}^2\quad , \tag{2.30}$$

for vanishing 4d momenta and with the boundary conditions in eqs. (2.20) and (2.29). The result is

$$= c_+\left(\frac{z}{z_{\mathrm{IR}}}\right)^{\ +} + c_-\left(\frac{z}{z_{\mathrm{IR}}}\right)^{\ -}\qquad v(z)\mathbb{1}, \tag{2.31}$$

[5] In our model the axial field A_M gives rise to towers of resonances with the quantum numbers of the f_1 and of the mesons. These states are predicted to be degenerate in mass with the corresponding mesons of the a_1 and the tower. Although the masses predicted for the $f_1(1285)$ and for the (1295) are close to the experimental ones, we decided not to include these predictions in the fit because, in principle, they could receive sizable corrections when a proper treatment of the $U(1)_A$ anomaly is included (see footnote 4).

with

$$\begin{cases} c_+ = \dfrac{z_{\rm IR}^2}{z_{\rm IR}^2 - z_{\rm UV}^2}\,(\ - M_q)\,\mathbb{1}\,, \\ c_- = \dfrac{1}{z_{\rm IR}^2 - z_{\rm UV}^2}\left(z_{\rm IR}^2\, M_q - z_{\rm UV}^2\ \right)\mathbb{1}\,, \end{cases} \tag{2.32}$$

where we normalized the warp factor as $a(z) = z_{\rm IR}/z$ and we defined

$$= 2 \quad \sqrt{4 + M^2} = 2 \qquad , \tag{2.33}$$

with $M^2 \qquad z_{\rm IR}^2 M_{Bulk}^2$. To obtain a real value for and to avoid a singular behavior of the $z^{\ -}$ piece in eq. (2.31) at the UV boundary in the $z_{\rm UV} \qquad 0$ limit, we must impose the constraint $-4 \qquad M^2 \qquad 0$. Notice that it is only because of the rescaling in eq. (2.20) that we obtain a finite VEV in the $z_{\rm UV} \qquad 0$ limit while keeping all the other parameters finite. The rescaling has allowed us to define a finite quantity, M_q, which controls the departure from the chiral limit.

The Mesons Wavefunctions

In order to study the properties of the mesonic sector, it is useful to rewrite the scalar field as

$$= (v\,\mathbb{1} + S)\, e^{iP\ v}\,, \tag{2.34}$$

where S and P are Hermitian matrices of respectively scalar and pseudoscalar fields. Under the unbroken $U(2)_V$ symmetry S and P can both be decomposed as $\mathbf{1} + \mathbf{3}$. Form the boundary conditions on the field in eqs. (2.20) and (2.29) we immediately find the boundary conditions for the S and the P fields

$$S\ _{z_{\rm UV}} = S\ _{z_{\rm IR}} = P\ _{z_{\rm UV}} = P\ _{z_{\rm IR}} = 0\,. \tag{2.35}$$

A convenient gauge fixing choice for studying the properties of the mesons is the R gauge which eliminates the mixing between the gauge bosons A , V and the scalars A_5, P. This gauge is obtained by introducing in the Lagrangian the terms

$$\mathcal{L}_{gf}^V = -\frac{2M_5 a(z)}{V}\mathrm{Tr}\left[\ V\ - \frac{V}{a(z)}\ {}_z(a(z)V_5)\right]^2\,, \tag{2.36}$$

$$\mathcal{L}_{gf}^A = -\frac{2M_5 a(z)}{A}\mathrm{Tr}\left[\ A\ - \frac{A}{a(z)}\ {}_z(a(z)A_5) - \ {}_A a^2(z) v(z) P\right]^2\,, \tag{2.37}$$

where $V_M = (\mathbf{L}_M + \mathbf{R}_M)/2$ and $A_M = (\mathbf{L}_M - \mathbf{R}_M)/2$. The wavefunctions and the masses of the mesons can be determined by solving the quadratic equations of

motion for the 5d fields and imposing the appropriate boundary conditions. The computation is analogous to the one described in [22, 36], so we will skip here most of the details. The physical degrees of freedom are easily identified using the unitary gauge, which corresponds to the limit $_{A\,V}$. In this gauge the fields A_5, V_5 and P satisfy the constraints

$$_z(a(z)V_5) = 0\,, \qquad P = -\frac{1}{a^3(z)v}\ _z(a(z)A_5)\,, \tag{2.38}$$

and the pion field can be identified with the lightest KK mode of A_5.

The vector mesons, namely the and the mesons and their resonances, are described by the KK modes of the vector gauge field V . In the unitary gauge the V_5 component of the vector gauge field is forced to vanish due to the boundary condition $V_5\ _{z_{\rm IR}\ z_{\rm UV}} = 0$, while the 4d components V satisfy the bulk equation of motion

$$V\ - \qquad V\ - \frac{1}{a(z)}\ _z\,(a(z)\ _zV\ ) = 0\,, \tag{2.39}$$

and the boundary conditions

$$V\ _{z_{\rm UV}} = 0\,, \qquad _zV\ _{z_{\rm IR}} = 0\,. \tag{2.40}$$

As expected, the equation of motion for the vector mesons is independent of the VEV of the 5d scalar , and the masses and the wavefunctions for these states are exactly the same as in [20].

The equation of motion for the scalar field S is independent of v as well

$$S - \frac{1}{a^3(z)}\ _z\left(a^3(z)\ _zS\right) + a^2(z)M^2_{Bulk}S = 0\,, \tag{2.41}$$

and the corresponding boundary conditions are given in eq. (2.35). The KK modes of the S field are interpreted as the parity-even scalar mesons, whose lightest states are the $a_0(980)$ and the $f_0(980)$.

On the other hand the axial fields, which are interpreted as the $a_1(1260)$ and $f_1(1285)$ mesons and their heavier resonances, are sensitive to the symmetry breaking induced by the VEV of , as can be seen from the equation of motion

$$A\ - \qquad A\ - \frac{1}{a(z)}\ _z\,(a(z)\ _zA\ ) + 2a^2(z)v^2(z)A\ = 0\,. \tag{2.42}$$

The boundary conditions are

$$A\ _{z_{\rm UV}} = A\ _{z_{\rm IR}} = 0\,. \tag{2.43}$$

Finally, the pion and the other pseudoscalar mesons are described, for finite $_A$, by the fields A_5 and P. These fields mix in the quadratic Lagrangian and it is not totally straightforward to obtain their equations of motion in the unitary gauge limit $_A$. If one simply removes the P field from the Lagrangian through the constraint in eq. (2.38) and then varies the action with respect to A_5, one obtains indeed the bulk equation of motion

$$\mathcal{D}\Big[\quad A_5 + 2a^2(z)v^2(z)\mathcal{D}A_5\Big] = 0\,, \tag{2.44}$$

which is of fourth order in the z derivatives, having defined the differential operator

$$\mathcal{D} \quad 1 - \ _z\left(\frac{1}{2a^3(z)v^2(z)} \ _z a(z)\right) . \tag{2.45}$$

From the boundary conditions on P and from the gauge fixing constraint one also gets the boundary conditions

$$_z(a(z)A_5)\ _{z_{\rm UV}} = \ _z(a(z)A_5)\ _{z_{\rm IR}} = 0\,, \tag{2.46}$$

which however are only two while four conditions would be needed for the fourth order bulk equation (2.44) to have a unique solution. The two remaining boundary conditions cannot be obtained directly in the unitary gauge, they arise from the equations of motion at finite $_A$ by carefully taking the $_A$ limit. From this procedure we recover the bulk equation (2.44) and the boundary conditions in (2.46), plus the additional constraints

$$_z\Big\{a(z)\Big[\quad + 2a^2(z)v^2(z)\mathcal{D}\Big]A_5\Big\}\Big|_{z_{\rm UV}\ z_{\rm IR}} = 0\,. \tag{2.47}$$

By the above equation one can prove that the bulk equation (2.44) can be replaced by the reduced second-order one

$$A_5 + 2a^2(z)v^2(z)\mathcal{D}A_5 = 0\,, \tag{2.48}$$

with the boundary conditions given in eq. (2.46). The pseudoscalar spectrum, and in particular the pion, its lighter state, obviously depends on $v(z)$ and therefore on M_q and . We have checked that for positive M_q (and) all the squared masses are strictly positive, while for $M_q < 0$ the lightest state is tachyonic as anticipated in the discussion below eq. (2.29).

Fit on the Meson Observables

Before performing the complete fit, an estimate of the five parameters of our model ($L \quad z_{\rm IR} - z_{\rm UV}$, M_5, M_{Bulk}, and M_q) can be obtained as follows. The length of the

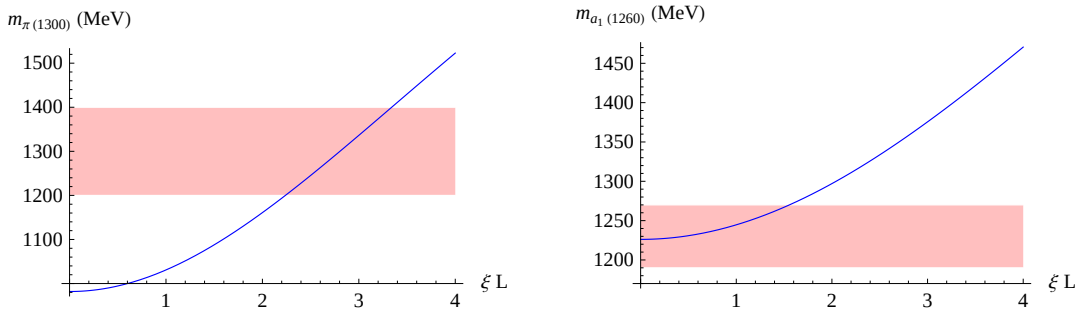

Figure 2.5: Mass of the (1300) meson (left) and $a_1(1260)$ meson (right) as a function of L for $L^{-1} = 320$ MeV and $L^2 M_{Bulk}^2 \simeq -3.8$. The shaded band shows the experimental values $m_{(1300)} = (1300 \quad 100)$ MeV and $m_{a_1(1260)} = (1230 \quad 40)$ MeV.

compact dimension is fixed by the meson mass through the relation $m \simeq 2.4/L$, from which we derive $L^{-1} \simeq 320$ MeV [22]. The bulk mass parameter is determined by the mass of the $a_0(980)$ meson. The relation between these two quantities can be derived by solving analytically the equation of motion for S (eq. (2.41)) and then imposing the corresponding boundary conditions. This leads to an approximate relation

$$m_{a_0(980)} \simeq 1.3 \frac{^+}{L}, \tag{2.49}$$

which gives $^+ \simeq 2.4$ or, equivalently, $L^2 M_{Bulk}^2 \simeq -3.8$. An estimate of the value of the parameter can be obtained from the values of the masses of the $\pi(1300)$ and of the $a_1(1260)$ mesons, which we determine numerically using the previously determined values for L and M_{Bulk}. As can be seen from the plots in fig. 2.5, fitting the value of the $a_1(1260)$ mass points towards the region of small , $L \quad 2$, while reconstructing the $\pi(1300)$ mass favours larger value of the parameter $2 \quad L \quad 3$. Combining the two regions we get as a rough estimate $L \simeq 2$. The values of M_5 and M_q can be extracted respectively from the pion decay constant f and the pion mass m . These two quantities can be determined by computing the holographic Lagrangian for the pion field as explained in appendix A. We find that the series expansion for small L is given by

$$f^2 \simeq 4 \frac{M_5}{L} \left(1 + \frac{(\ L)^2}{^+(\ ^{+2} - 1)} \right), \qquad m^2 \simeq 2(\ ^+ - 2) \ M_q \, . \tag{2.50}$$

Using the experimental values [6] $f^2 = 92$ MeV and $m \ = 135$ MeV, we get $M_5 L \simeq 0.015$ and $M_q \simeq 35$ MeV.

[6] We did not include the electroweak correction in the determination of the observables. For this reason we compare the predictions of our model with the experimental value for pion decay constant with subtracted electroweak contributions [44] and with the mass of the ^{0}, whose electroweak corrections are negligible [45].

	Experiment	AdS_5	Deviat.
m	135 MeV	134 MeV	0.6%
$m_{\ (1300)}$	1300 MeV	1230 MeV	5.6%
m	775 MeV	783 MeV	1.0%
m	782 MeV	783 MeV	0.1%
$m_{a_1(1260)}$	1230 MeV	1320 MeV	7.6%
$m_{a_0(980)}$	980 MeV	1040 MeV	6.5%
$m_{f_0(980)}$	980 MeV	1040 MeV	6.5%
f	92 MeV	89 MeV	3.6%
f	153 MeV	149 MeV	2.7%
f	140 MeV	149 MeV	6.4%
g	6.0	4.89	22.7%
g	0.72	0.71	1.1%
g	0.22	0.24	7.9%
g	15.0	15.6	3.7%
RMSE			7.7%

	Experiment	AdS_5	Deviat.
m	135 MeV	133 MeV	1.2%
$m_{\ (1300)}$	1300 MeV	1207 MeV	7.7%
m	775 MeV	842 MeV	8.6%
m	782 MeV	842 MeV	7.7%
$m_{a_1(1260)}$	1230 MeV	1387 MeV	12.7%
$m_{a_0(980)}$	980 MeV	1099 MeV	12.1%
$m_{f_0(980)}$	980 MeV	1099 MeV	12.1%
f	92 MeV	89 MeV	3.1%
f	153 MeV	158 MeV	3.1%
f	140 MeV	158 MeV	12.7%
g	6.0	5.33	12.5%
g	0.72	0.74	3.2%
g	0.22	0.25	12.6%
g	15.0	16.8	11.8%
RMSE			9.6%

2

Table 2.1: Meson observables used for the fit of the microscopic parameters. The table on the left shows the results of a fit which minimizes the overall root mean square error (shown in the last line). The values of the parameters obtained in this way are $L^{-1} = 325$ MeV, $M_5 L = 0.014$, $L^2 M_{Bulk}^2 = -3.7$, $L = 2.1$ and $M_q = 31$ MeV. The table on the right gives the list of results obtained by minimizing the largest deviation from the experiments. With this procedure we get $L^{-1} = 350$ MeV, $M_5 L = 0.014$, $L^2 M_{Bulk}^2 = -3.8$, $L = 1.5$ and $M_q = 40$ MeV.

A more precise determination of the microscopic parameters can be obtained by performing a fit on a larger set of well measured mesonic observables. This procedure provides also a way to estimate the level of agreement of the model with the experimental results. As a simple fitting procedure, we chose to minimize the root mean square error (RMSE) of our predictions with respect to the experimental data (see [38] for details on the fitting procedure). We remark that for our analysis we take into account only the deviation of the theoretical predictions of our model from the central value of the experimental results. A more refined procedure, which however would be beyond the scope of our work, should also take into account the experimental error with which the various observables have been measured.

The list of observables used in the fit includes the masses of the lightest mesonic resonances as well as some of their decay constants and couplings. The predictions of the model and the experimental values are shown in the list on the left of table 2.1. We found that the best agreement with the data is obtained for the following values of the parameters $L^{-1} = 325$ MeV, $M_5 L = 0.014$, $L^2 M_{Bulk}^2 = -3.7$, $L = 2.1$ and $M_q = 31$ MeV, which are close to the previously estimated ones.

The overall agreement with the experimental data is quite good and almost all the observables show a deviation from the experimental values smaller than 8%, resulting in a RMSE of 7.7%. A somewhat surprising result of the fit is the fact that only one observable, namely the g coupling seems to have a large deviation from the experiments. This deviation is however not completely unexpected. In the class of models we are considering one gets an approximate tree-level relation [22]

$$m^2 \simeq 3f^2g^2 \quad , \tag{2.51}$$

which differ by a factor 2/3 form the experimentally well satisfied KSRF relation $m^2 \simeq 2f^2g^2$. In our fit the predictions for the pion decay constant and for the meson mass are in excellent agreement with the data, thus the g coupling must necessarily deviate from the experiments in order for the relation (2.51) to be valid.

It is interesting to notice that the change in the IR boundary conditions for the gauge fields with respect to the original model of [36] has some relevant consequences on the predictions of the theory. In the original set-up the mass of the $\pi(1300)$ resonance could not be reproduced and the first resonance of the axial gauge field was identified with the $\pi(1800)$ state. In the present model, on the contrary, the $\pi(1300)$ meson can be naturally accomodated.

To check the stability of our predictions, we can compare the previous results with the ones obtained by using an alternative fitting procedure. For this purpose, we chose to minimize the largest deviation of our predictions from the experiments. In this way we obtained the list of result shown in the right panel of table 2.1. The deviations from the experiments are now more uniformly spread among the various observables, with a maximal deviation of $\sim 13\%$. The overall RMSE is 9.6%, which is still reasonable and only slightly higher than the one found in the previous fit. The corresponding values of the microscopic parameters are $L^{-1} = 350$ MeV, $M_5 L = 0.014$, $L^2 M_{Bulk}^2 = -3.8$, $L = 1.5$ and $M_q = 40$ MeV, which are in good agreement with the previous determination.

The heavier resonances, which have not been included in the fits, show larger deviations from the experimental values. For example the predicted mass for the $\pi(1800)$ is 2140 MeV with an 18% deviation and for the $a_0(1450)$ it is 2070 MeV with a 40% deviation. We remark, however, that the heavy resonances, being close to the cut-off of the theory, are expected to have larger theoretical uncertainties.

Other quantities that we can extract from the model are the coe cients of the $\mathcal{O}(p^4)$ terms in the **PT** Lagrangian, which describe the interactions of the pions with the left and right sources and with the spurion field related to the quark masses. The computation can be performed by following the holographic procedure outlined in appendix A. Due to the non negligible experimental uncertainty,

	Experiment		AdS_5
L_1	0.4	0.3	0.47
L_2	1.4	0.3	0.95
L_3	−3.5	1.1	−2.8
L_4	−0.3	0.5	0.0
L_5	1.4	0.5	0.72
L_6	−0.2	0.3	0.0
L_8	0.9	0.3	0.45
L_9	6.9	0.7	6.0
L_{10}	−5.5	0.7	−6.0

	Experiment		AdS_5
L_1	0.4	0.3	0.43
L_2	1.4	0.3	0.87
L_3	−3.5	1.1	−2.4
L_4	−0.3	0.5	0.0
L_5	1.4	0.5	0.68
L_6	−0.2	0.3	0.0
L_8	0.9	0.3	0.39
L_9	6.9	0.7	5.6
L_{10}	−5.5	0.7	−5.6

Table 2.2: Predictions for the coe cients of the $\mathcal{O}(p^4)$ terms in the **PT** Lagrangian compared with the experimental values [46]. The values are given in units of 10^{-3}. The microscopic parameters are fixed by the fits on the observables in table 2.1 (RMSE fit for the left table and maximal deviation fit for the right table).

we decided not to include these observables in the fit for the microscopic parameters. We also excluded from the computation the L_7 coe cient which arises from integrating out the Goldstone boson singlet related to the $U(1)_A$ anomaly, whose complete treatment is not included in the present model (see footnote 4). In table 2.2 we listed the predictions of the model for two sets of microscopic parameters found with the RMSE and the `maximal deviation' fit. The numerical results in the two cases are quite similar and show a good agreement with the experimental data. The reduced $^2$ for the RMSE fit is 1.0, while for the `maximal deviation' fit it is 1.2, and the deviations from the experimental data are always below ~ 1.5 .

In the chiral-symmetric models without a bulk scalar field some phenomenologically successful relations were found among the coe cients of the **PT** Lagrangian [7]:

$$L_2 = 2L_1\,, \qquad L_9 = -L_{10}\,, \qquad L_4 = L_6 = 0\,, \qquad L_3 = -6L_1\,. \tag{2.52}$$

In our set-up all these relations remain valid, except for the last one $L_3 = -6L_1$, which receives some corrections but is still well satisfied (compare [22, 36]). Notice that the first and third relations in eq. (2.52), which are implied by the large N_c limit of QCD [47], are not modified in our model.

[7] See for example [37].

2.1.5 Baryon sector from 5d Skyrmions

The Static Solution

In the present model, baryons arise as 5d Skyrmions and studying their properties requires a slight modification of the methods of [19 21], where the massless case has been considered. As a first step we will consider the static soliton configuration. A convenient and automatically consistent 2d ansatz is obtained, as in the massless case, by imposing the solution to be invariant under a certain set of symmetry transformations. These are cylindrical symmetry (*i.e.*, the simultaneous action of 3-space and $SU(2)_V$ rotations), 3d parity and time-inversion, defined as a change of sign of all the temporal components combined with $\widehat{L} \quad -\widehat{L}$ and $\widehat{R} \quad -\widehat{R}$. This leads to the following ansatz for the gauge fields

$$\begin{cases} \overline{R}^a_j(\mathbf{x},z) = A_1(r,z)\widehat{x}_a\widehat{x}_j + \dfrac{1}{r}\ {}_{ajk}\widehat{x}_k - \dfrac{{}^{(x)}}{r}\ {}^{(x\,y)}\quad {}^{(y)\,aj}\,, \\ \overline{R}^a_5(\mathbf{x},z) = A_2(r,z)\widehat{x}^a\,, \\ \widehat{\overline{R}}_0(\mathbf{x},z) = \dfrac{s(r,z)}{r}\,, \end{cases} \tag{2.53}$$

where $r^2 = \sum_i x^i x^i$, $\widehat{x}^i = x^i/r$, ${}^{(x\,y)}$ is the antisymmetric tensor with ${}^{(1\,2)} = 1$ and the "doublet" tensors ${}^{(1\,2)}$ are

$${}^{(x)\,ab} = \begin{bmatrix} {}^{abc}\widehat{x}^c \\ \widehat{x}^a\widehat{x}^b - \quad {}^{ab} \end{bmatrix}. \tag{2.54}$$

Because of parity, eq. (2.53) also determines the ansatz for the **L** fields which are given by $L_i(\mathbf{x},z) = -R_i(-\mathbf{x},z)$, $L_{5\,0}(\mathbf{x},z) = R_{5\,0}(-\mathbf{x},z)$ and analogously for $\widehat{L}$, $\widehat{R}$.

The ansatz for is obviously obtained by imposing the same symmetries: cylindrical symmetry implies

$$^{-}(\mathbf{x},z) = \ {}_0(r,z)\frac{\mathbb{1}}{2} + i\ {}_a(r,z)\frac{{}^a}{2}\,, \tag{2.55}$$

where

$$\begin{cases} {}_0(r,z) = \ {}_2(r,z)\,, \\ {}_a(r,z) = \ {}_1(r,z)\,\widehat{x}_a\,. \end{cases} \tag{2.56}$$

It is easy to check that parity acts on as $(\mathbf{x},z,t) \quad (-\mathbf{x},z,t)$, while under time-inversion we have $(\mathbf{x},z,t) \quad {}_2 \quad (\mathbf{x},z,-t)\ {}_2$. Imposing to be invariant under these transformations simply implies that ${}_{1\,2}$ are real. It is useful to note that our ansatz preserves, again as in the massless case, a local $U(1)$ subgroup of

the original 5d chiral group corresponding to gauge transformations of the form $g_R = g$ and $g_L = g$ with

$$g = \exp[i \ (r, z) x^a \ _a/(2r)] \, . \tag{2.57}$$

Under this residual $U(1)$ the fields $= \ _1 + i \ _2$, s and $A-$ in eq. (2.53) are respectively one charged and one neutral scalar and a gauge field. It is easy to check that the field $= \ _1 + i \ _2$ in eq. (2.55) also transforms as a charge-one scalar; it will be convenient to define its 2d covariant derivative as

$$D \qquad - iA \quad . \tag{2.58}$$

It is straightforward to plug the ansatz in the 5d lagrangian and to obtain the energy of the Skyrmion. From the gauge part in eq. (2.22) and (2.23) we obtain, as in [20, 21],

$$\begin{aligned} E_G = 8\pi M_5 \int_0 \ dr \int_{z_{\rm UV}}^{z_{\rm IR}} dz \, \Big\{ a(z) \Big[\ D \ \ ^2 + \frac{1}{4} r^2 A^2 \ + \frac{1}{2r^2} \left(1 - \ \ ^2 \right)^2 - \frac{1}{2} (\ \ s)^2 \Big] \\ - \frac{L}{2} \frac{s}{r} \ \ \Big[\ \ (-i \ \ D \ \ + h.c.) + A \ \ \Big] \Big\} \, , \end{aligned} \tag{2.59}$$

where

$$\frac{N_c}{16\pi^2 M_5 L} \, , \tag{2.60}$$

while the new contribution coming from the scalar part in eq. (2.25) is

$$E \ = 8\pi M_5 \int dr \int dz \left\{ a^3(z) \left[\frac{r^2}{4} (D \ \ ) \ (D \ \ ) - \frac{1}{8} (\ \ \ - \ \ \ )^2 \right] + a^5(z) \frac{r^2}{4} M_{Bulk}^2 \ \ \right\} . \tag{2.61}$$

Notice that the total energy $E = E_G + E$ does not yet give the Skyrmion mass because the infinite energy of the vacuum needs to be subtracted in order to get an observable quantity. This zero-point energy is obtained from eq. (2.61) by plugging in the vacuum field configuration which is given by

$$= \ _V \ = 2 \, i \, v(z) \, , \qquad = \ _V \ = - \, i \, , \tag{2.62}$$

all other fields vanishing.

The 2d EOM for the Skyrmion are easily derived, at this point, by varying the energy in eq. (2.59,2.61), but in order for them to be solved suitable boundary conditions need to be specified at the four boundaries ($z = z_{\rm IR}$, $z = z_{\rm UV}$, $r = 0$ and $r \qquad$) of our 2d space. At $z = z_{\rm UV}$ and $z = z_{\rm IR}$ the boundary conditions are given, up to the sign ambiguity in eq. (2.29) that we will now fix, by the ones discussed

in the previous section. The presence of the $r = 0$ boundary merely results from a choice of coordinates, the physical 5d space being completely regular at $r = 0$. The boundary conditions will therefore result from just imposing regularity of the 5d fields, with no need for extra assumptions. At r we must require that the solution will have a finite mass, and this is ensured by imposing it to reduce, up to a symmetry transformation, to the vacuum configuration in eq. (2.62). We also want a $B = 1$ solution, where the baryon charge B is defined in eq. (2.15) and is given by

$$B = \frac{1}{2\pi} \int_0 \quad dr \int_{z_{\rm UV}}^{z_{\rm IR}} dz \quad \left[\quad (-i \quad D \quad + h.c.) + F \quad \right], \tag{2.63}$$

in terms of the 2d fields. The above equation can be easily rewritten (as it must, being the topological charge) as a 1d integral on the boundaries of the 2d space, and in order to get $B = 1$ from the r boundary we must have, as in the massless case, the following boundary conditions

$$r \qquad : \quad \begin{cases} \quad = -ie^{i \ (z - z_{\rm UV}) \ (z_{\rm IR} - z_{\rm UV})} \\ A_2 = \dfrac{\pi}{(z_{\rm IR} - z_{\rm UV})} \\ s = 0 \end{cases} , \tag{2.64}$$

which are obtained from the vacuum (2.62) by means of a residual $U(1)$ transformation in the form of eq. (2.57), with $= \pi(z - z_{\rm UV})/(z_{\rm IR} - z_{\rm UV})$.

Consistently, the boundary conditions for are obtained in the same way and read

$$r \qquad : \qquad = i\, e^{i \ (z - z_{\rm UV}) \ (z_{\rm IR} - z_{\rm UV})}\, 2\, v(z)\,. \tag{2.65}$$

At $z = z_{\rm IR}$, the above equation implies $(r = 0, z = z_{\rm IR}) = -2\,i$, because the "twist" $e^{i \ (z - z_{\rm UV}) \ (z_{\rm IR} - z_{\rm UV})}$ reduces to -1 at the IR while the vacuum respects the boundary condition (2.29) with the plus sign. This resolves the ambiguity and enforces the 5d Skyrmion to live in the minus-sign sector, with IR boundary conditions given by

$$z = z_{\rm IR} \ : \qquad = -2\,i \quad . \tag{2.66}$$

We stress, as mentioned in the discussion below eq. (2.29), that the sign ambiguity in the IR boundary conditions results from our choice of giving generalized Dirichlet conditions on , instead of treating it as a Neumann field and making its boundary conditions originate from a localized potential that would cost us more new parameters. If we had made the other choice, we would have had no ambiguity, and consequently no separated sectors in the field space. If studying this different setup in the limit of infinite strength for the coupling in the localized potential we expect that, while the vacuum and the meson's wave function will

be found to fulfill eq. (2.29) with the plus sign, the other boundary condition will be enforced on the Skyrmion solution and the results of the present paper will be recovered. Coming back to the boundary conditions, we must still specify the ones at $r = 0$ and at $z = z_{\rm UV}$. These are

$$r \quad 0 \; : \quad \begin{cases} {}_1 = 0 \\ {}_r \; {}_2 = 0 \end{cases} \qquad z = z_{\rm UV} \; : \qquad = 2\, i \left(\frac{z_{\rm UV}}{z_{\rm IR}}\right)^{\ -} M_q \tag{2.67}$$

where the ones for $r = 0$ arise, respectively, from asking the 5d field $^{-}$ and its 3-space derivative to be regular and single-valued. For all the other fields the boundary conditions are the same of the massless case and are reported in appendix B.

Zero-Mode Fluctuations

In order to describe the baryons we need to consider the time-dependent deformations of the static soliton solution. The analysis proceeds exactly as in the massless case, we will therefore skip most of the details and refer the interested reader to ref. [21].

The single-baryon states can be identified with the zero-mode fluctuations, thus an analysis of the infinitesimal deformations will be su cient for our purposes. The relevant configurations are the ones which describe a slowly-rotating solution, whose degrees of freedom can be parametrized by three collective coordinates encoded in an $SU(2)$ matrix $U(t)$.

To describe the solution we need to generalize the ansatze given in eqs. (2.53) and (2.55). The ansatz for the gauge fields is analogous to the one for the massless pion case:

$$R\ (\mathbf{x}, z; U) \ = \ U\, \overline{R}\ (\mathbf{x}, z)\, U^{\dagger} \ , \qquad \widehat{R}_0(\mathbf{x}, z; U) \ = \ \widehat{\overline{R}}_0(\mathbf{x}, z)\,, \tag{2.68}$$

and

$$R_0(\mathbf{x}, z; U) \ = \ U\, \overline{R}_0(\mathbf{x}, z; K)\, U^{\dagger} \ + \ i\, U \ {}_0 U^{\dagger} \ , \qquad \widehat{R}\ (\mathbf{x}, z; U) \ = \ \widehat{\overline{R}}\ (\mathbf{x}, z; K)\,, \tag{2.69}$$

where

$$\begin{cases} \overline{R}^a_0(\mathbf{x}, z; K) = \ {}_{(x)}(r, z) k_b \ {}^{(x)\, ab} + w(r, z)(k \ \ \widehat{x})\widehat{x}^a\,, \\ \widehat{\overline{R}}_i(\mathbf{x}, z; K) = \dfrac{(r, z)}{r}\left(k^i - (k \ \ \widehat{x})\widehat{x}^i\right) + B_1(r, z)(k \ \ \widehat{x})\widehat{x}^i + Q(r, z)\ {}^{ibc} k_b \widehat{x}_c\,, \\ \widehat{\overline{R}}_5(\mathbf{x}, z; K) = B_2(r, z)(k \ \ \widehat{x})\,. \end{cases} \tag{2.70}$$

The ansatz for the scalar field is given by

$$(\mathbf{x},\, z;\, U) \;=\; U^{\overline{\ }}(\mathbf{x},\, z)\, U \quad , \tag{2.71}$$

where $^{\overline{\ }}$ is as in eq. (2.55) with the new definitions

$$\begin{cases} \quad {}_0(r,z) = \exp\left[-i(k \quad \widehat{x}) \;\; (r,z)\right] \left(\;\; {}_2(r,z) + i(k \quad \widehat{x}) \;\; {}_2(r,z)\right) \,, \\ \quad {}_a(r,z) = \exp\left[-i(k \quad \widehat{x}) \;\; (r,z)\right] \left[\left(\;\; {}_1(r,z) + i(k \quad \widehat{x}) \;\; {}_1(r,z)\right) \widehat{x}^a - i\left((k \quad \widehat{x})\widehat{x}^a - k^a\right) \;\; (r,z)\right] . \end{cases} \tag{2.72}$$

In the above equation, the 3-vector k_a denotes the Skyrmion rotational velocity

$$K = k_a \;\; {}^a/2 = -iU \;\, dU/dt \,,$$

and the field is the same that appears in the ansatz for the gauge fields in eq. (2.70). The above ansatz can be obtained, similarly to the one for the static solution, by imposing time-inversion, parity, and cylindrical symmetry.

Plugging the ansatz in the 5d lagrangian one obtains the collective coordinates lagrangian

$$L = -M + \frac{}{2}\, k_a k^a \,, \tag{2.73}$$

where M is the Skyrmion mass and is its moment of inertia. The latter receives a contribution from the gauge Lagrangian

$$\begin{aligned} {}_G \;\; = \;\; & 16\pi M_5 \frac{1}{3} \int_0 \;\; dr \int_{z_{\rm UV}}^{z_{\rm IR}} dz \left\{ a(z) \left[-\left(D \quad \right)^2 - r^2 \left(\quad Q\right)^2 - 2Q^2 - \frac{r^2}{4} B \quad B \right.\right. \\ & \left. + r^2 \left(D \quad \right)^2 + \frac{r^2}{2} \left(\quad w\right)^2 + \left(\;\; {}_{(x)} \;\; {}_{(x)} + w^2\right) \left(1 + \;\; {}_{(x)} \;\; {}_{(x)}\right) - 4w \;\; {}_{(x)} \;\; {}_{(x)} \right] \\ & + \;\; L \left[-2 \quad D \quad\;\; {}_{(x)} \left(D \quad \right)_{(x)} + 2 \quad\;\; \left(r\, Q\right) \;\; {}_{(x)} \;\; {}^{(xy)} \left(D \quad \right)_{(y)} \right. \\ & \left.\left. - w \left(\frac{1}{2} \quad B \quad \left(\;\; {}_{(x)} \;\; {}_{(x)} - 1\right) + r\, Q \quad A \quad \right) + 2r\, Q \quad D \quad\;\; \left(\frac{s}{r}\right) \right] \right\} \end{aligned} \tag{2.74}$$

and a contribution from the scalar, which is given by

$$\begin{aligned} = \;\; & \frac{16}{3}\pi M_5 \int_0 \;\; dr \int_{z_{\rm UV}}^{z_{\rm IR}} dz \left\{ a^3(z) \left[-\frac{r^2}{4} \quad\;\; (D \quad)(D \quad) - \frac{r^2}{4} (D \quad) \;\, (D \quad) - \frac{r^2}{2} (\quad\;\;)(\quad\;\;) \right.\right. \\ & + \frac{r^2}{4} D \quad [\;\, (D \quad) \;\; - \;\; (D \quad) \;\; + \text{h.c.}] - \frac{1}{2} \quad\;\; + \frac{1}{8} (\quad\;\; - \quad\;\;)^2 - \frac{r^2}{8} (\quad\;\; - \quad\;\;)^2 \\ & \left.\left. - i \;\, (\quad\;\; - \quad\;\;) - \frac{1}{2} \;\; {}^2 (1 + \quad\;\;) \right] - r^2 a^5(z) M_{Bulk}^2 \left[\frac{1}{4} \quad\;\; + \frac{1}{2} \;\; {}^2 \right] \right\} , \end{aligned} \tag{2.75}$$

where we defined

$$= \;\; {}_1 + i \;\; {}_2 \,, \qquad\qquad D \qquad\qquad - iA \quad . \tag{2.76}$$

while the other notations are defined in appendix B.

Numerical Results

The soliton solution can not be determined analytically, however, it can be studied numerically by using the techniques described in [21]. In the massless case it was found that, due to the peculiarity of the 5d gauge action, the soliton solution is stabilized thanks to the presence of the CS term [20]. This peculiar feature disappears once we modify the action by the introduction of the bulk scalar field and, in the present model, we checked in our numerical analysis that the Skyrmion size is stable even if the CS term is not present.

From the soliton solution we can extract the electromagnetic and axial properties of the nucleons, which are encoded in a set of form factors which parametrize the matrix element of the currents on two nucleon states.

The chiral currents can be determined by computing the variation of the action with respect to the sources $\mathbf{l}$ and $\mathbf{r}$. It is simple to show that the action describing the scalar field does not contribute to the currents, which are exactly the same as in the massless pion case:

$$J_L^a = M_5\Big(a(z)L^a{}_5\Big)_{z=z_{\rm UV}} , \qquad \widehat{J}_L = M_5\Big(a(z)\widehat{L}_5\Big)_{z=z_{\rm UV}} , \tag{2.77}$$

and analogously for R.

The isoscalar and isovector form factors are defined through the relations

$$\begin{aligned}
N_f(q/2)\, J_S^0(0)\, N_i(-q/2) &= G_E^S(q^2)_{f\ i}\,, \\
N_f(q/2)\, J_S^i(0)\, N_i(-q/2) &= i\,\frac{G_M^S(q^2)}{2M_N}{}_f 2(S\quad q)^i{}_i\,, \\
N_f(q/2)\, J_V^{0a}(0)\, N_i(-q/2) &= G_E^V(q^2)_{f\ }(2I^a)_{\ i}\,, \\
N_f(q/2)\, J_V^{ia}(0)\, N_i(-q/2) &= i\,\frac{G_M^V(q^2)}{2M_N}{}_f 2(S\quad q)^i(2I^a)_{\ i}\,,
\end{aligned} \tag{2.78}$$

where the currents are given by $J_V^a = J_R^a + J_L^a$ and $J_S = 1/3(\widehat{J}_R + \widehat{J}_L)$, and we used the notation $_{i\,f}$ for the nucleon spin/isospin vectors of state (normalized to $= 1$) and the definition $(S\quad q)^i \quad {}^{ijk}S^j q^k$. From the axial current $J_A^a = J_R^a - J_L^a$, we define the axial form factors

$$N_f(q/2)\, J_A^{i\,a}(0)\, N_i(-q/2) = {}_f\left[\frac{E}{M_N}G_A(q^2)S_T^i + \left(G_A(q^2) - \frac{q^2}{4M_N^2}G_p(q^2)\right)S_L^i\right]I^a \tag{2.79}$$

$$N_f(q/2)\, J_A^{0\,a}(0)\, N_i(-q/2) = 0 \tag{2.80}$$

where $S_T \quad S - q\ S\ \ q$ and $S_L \quad q\ S\ \ q$ are the transverse and the longitudinal components of the spin operator.

	Experiment	AdS_5	Deviat.
M_N	940 MeV	1090 MeV	16%
$_S$	0.44	0.43	2%
$_V$	2.35	1.18	100%
g_A	1.25	0.58	100%
$\sqrt{r^2_{E\,S}}$	0.79 fm	0.82 fm	4%
$\sqrt{r^2_{E\,V}}$	0.93 fm	0.97 fm	4%
$\sqrt{r^2_{M\,S}}$	0.82 fm	0.84 fm	2%
$\sqrt{r^2_{M\,V}}$	0.87 fm	0.87 fm	0.5%
$\sqrt{r^2_A}$	0.68 fm	0.65 fm	5%

	Experiment	AdS_5	Deviat.
M_N	940 MeV	1104 MeV	17%
$_S$	0.44	0.43	3%
$_V$	2.35	1.15	100%
g_A	1.25	0.59	100%
$\sqrt{r^2_{E\,S}}$	0.79 fm	0.84 fm	6%
$\sqrt{r^2_{E\,V}}$	0.93 fm	1.02 fm	9%
$\sqrt{r^2_{M\,S}}$	0.82 fm	0.86 fm	5%
$\sqrt{r^2_{M\,V}}$	0.87 fm	0.86 fm	1%
$\sqrt{r^2_A}$	0.68 fm	0.68 fm	0.2%

Table 2.3: Prediction for the static nucleon observables with the parameter values fixed by the fit on the mesonic observables (RMSE fit for the left table and maximal deviation fit for the right table).

To find the explicit expressions for the form factors we need to plug the ansatze for the soliton solution into the definitions of the currents (2.77) and then perform the quantization of the soliton solution as explained in [21]. The result is the same as in the massless pion case:

$$\begin{aligned}
G_E^S &= -\frac{N_c}{6\pi\ L}\int dr\, r\, j_0(qr)\,(a(z)\ \ {}_z s)_{UV}\\
G_E^V &= \frac{4\pi M_5}{3}\int dr\, r^2\, j_0(qr)\left[a(z)\left(\ \ {}_z w - 2\,(D_z\ \ )_{(2)}\right)\right]_{UV}\\
G_M^S &= \frac{8\pi M_N M_5}{3}\int dr\, r^3\,\frac{j_1(qr)}{qr}\,(a(z)\ \ {}_z Q)_{UV}\\
G_M^V &= \frac{M_N\, N_c}{3\pi L}\int dr\, r^2\,\frac{j_1(qr)}{qr}\left(a(z)\,(D_z\ \ )_{(2)}\right)_{UV}\\
G_A &= \frac{M_N}{E}\frac{N_c}{3\pi\ L}\int dr\, r\left[a(z)\frac{j_1(qr)}{qr}\left((D_z\ \ )_{(1)} - r\,A_{zr}\right) - a(z)\,(D_z\ \ )_{(1)}\, j_0(qr)\right]_{UV}
\end{aligned} \tag{2.81}$$

where j_n are spherical Bessel functions.

By employing suitable numerical techniques, the 2d EOM [8] obtained by varying the soliton mass M and its moment of inertia can be solved, and both the static and slowly-rotating Skyrmion solution computed. The numerical predictions for the static nucleon observables are listed in table 2.3. In the analysis we used the values of the microscopic parameters obtained from the fits on the mesonic observables presented in section 2.1.4.

[8] The EOM for the 2d fields are reported in appendix B.

The numerical results for the two sets of microscopic parameters considered show very similar deviation patterns from the data. Many of the numerical predictions are very close to the experimental results, although the magnetic vector moment $_V$ and the axial coupling g_A present a deviation of order 100%. We notice, however, that the overall agreement with the data (root mean square error 45%) is still compatible with the possibility of having sizable $1/N_c$ corrections, which can not be excluded given that $N_c = 3$. [9] By comparing the present results with the ones found in the simplified model without a pion mass [21], we see that all the observables show an improved agreement with the data except for the $_V$ and g_A, whose deviations become significantly larger.

Form the qualitative point of view, we remark that an important check of the validity of the description of baryons as solitons is the behavior of the electric and magnetic vector radii, namely $r_{E\,V}$ and $r_{M\,V}$. These two quantities are expected to be divergent in the chiral limit, as explicitly verified in [21], while they should become finite once a pion mass is introduced, as we find in the present model.

2.1.6 Conclusions

We have shown that it is rather easy to construct a model of holographic QCD which describes at the same time the pion mass, the QCD anomalies and the baryons as topological solitons. After introducing an explicit minimal model we have studied its phenomenology in both the mesonic and baryonic sector and found a significant level of agreement. In extreme synthesis, our result is that the general picture on the holographic QCD models outlined in the Introduction survives unchanged to the inclusion of the pion mass.

Few unexpected results have been found, however, that is worth discussing. In Sect. 2.1.4 we saw that our model easily reproduces the mass of the $\pi(1300)$ meson, a task that was impossible to achieve in the original scenario [36]. This came because of the change in the IR boundary conditions and gives a phenomenological support to this modification, that we had instead motivated on purely theoretical grounds. It is also remarkable that the other predictions are almost unaffected so that all the valid phenomenology of the original construction is retained. The "new" observables that were absent in the original model, *i.e.* the anomalous

[9] It is interesting to notice that using a di erent approach to the quantization of the collective coordinates, as suggested in [48], one gets much better predictions for $_V$ and g_A. With this procedure, the predictions for $_V$ and g_A are rescaled by a factor 5 3, thus agreeing with the data at the 20% level, while all the other observables are unchanged. We have no reason to believe that the modified quantization procedure correctly captures the 1 N_c corrections, nevertheless, this result seems to point out that large corrections could indeed be responsible for the deviations of $_V$ and g_A.

parity couplings originating from the CS term, also show a good agreement with the observations. Our results in the baryonic sector, shown in table 2.3, are also surprising, especially if compared with the ones obtained in the chiral-symmetric case [19 21]. For all the observables except $_V$ and g_A, a significant improvement is found in the agreement with observations. The isovector radii, that have became finite due to the presence of the pion mass, are also extremely well predicted. The situation has got significantly worst, on the contrary, for $_V$ and g_A that have became a factor of 2 smaller than the observations. [10] This failure persists in both the best fit points that we have used as input parameters in table 2.3, so that it is probably a robust feature. It might signal that the model is incomplete, but it might also be attributed to anomalously large $1/N_c$ corrections.

Some final comments on the theoretical implications of our results. The microscopic origin of holographic QCD models is basically unknown, even though the holographic implementation of the chiral symmetry provides a robust (but purely technical) connection with AdS/CFT. The success of the Regge phenomenology suggests, independently of AdS/CFT, the dual of large-N_c QCD being a string model and the validity of the holographic QCD approach suggests that this string model should contain a sector that is well described by a 5d field theory similar to the one we have considered. In the case of exact chiral symmetry, the Sakai Sugimoto model [49, 50] provides a partial realization of this idea because it is equivalent to holographic QCD for what the physics of the light meson is concerned. [11] It is on the contrary different, and problematic, in the baryonic sector [19 21, 40] and its phenomenology in the sector of higher spin states (where it genuinely differs from holographic QCD and shows its stringy nature) seems not very promising [50]. The inclusion of the explicit chiral breaking considered in the present paper provides an additional piece of information. The chiral symmetry is not explicitly broken in Sakai Sugimoto, and even though it was possible to include the explicit breaking by some deformation, the resulting model could not reduce to a field-theoretical model such as the one we have considered. The reason for this is that the Left and Right global groups are localized, in Sakai Sugimoto, at two different boundaries of the 5d space and the quark mass spurion M is unavoidably a non local object which is impossible to describe in a field theoretical language. Therefore, any string model that incorporated ours, inheriting its phenomenology, would be deeply different from Sakai Sugimoto; it might be worth trying to construct one following a bottom up approach.

[10] Actually, the discrepancy is almost exactly given by a factor of 2. By looking at table 2.3 one could imagine a factor 2 mistake in the problematic predictions, we are however confident of our calculations.

[11] See [38] for a precise justification of this equivalence.

2.2 Holographic Superconductors

2.2.1 Introduction

At the beginning of the 20^{th} century it was noticed that some metals exhibit perfect diamagnetism at temperatures below some critical point T_c, what implies that the magnetic field is expelled from this material. This is known as the Meissner effect. Moreover, it was shown that these metals also present a null electrical resistivity below T_c and therefore the Electric current flows inside the material without opposition. For this reason these materials were called Superconductors.

The first phenomenologically successful description of superconductivity came out from the London brothers in 1935 [24]. Assuming the simple relation $J_i \quad A_i$ and using the Maxwell equations they were able to describe both perfect diamagnetism and zero electrical resistivity. Nevertheless, the transition between normal and superconducting phases was not clear in this approach.

In 1959 Ginzburg and Landau went one step further and described superconductivity as a second order phase transition whose order parameter was a scalar field associated with the density of superconducting particles $(x)^2 = n_s$ [25]. The free energy at temperatures, $T \simeq T_c$ was assumed to take the form

$$F = \int dx^4 \left(\ (T - T_c) \quad ^2 + \quad ^4 \right), \tag{2.82}$$

where and are positive constants. At temperatures $T < T_c$ the scalar field develops a vacuum expectation value (vev) breaking therefore the U(1) symmetry of the system. This is exactly analogous to the Higgs mechanism of spontaneous symmetry breaking.

In principle more terms respecting the U(1) global invariance could be added to the free energy, is for this reason that the Ginzburg-Landau (GL) equation is only valid at $T \simeq T_c$, where the scalar field still has a small value.

We can couple this scalar to a dynamical EM field in such a way as gauging the global U(1) symmetry

$$F = \frac{1}{T} \int d^4x \left[\frac{1}{4e^2} \mathcal{F} \quad + \ D \quad ^2 + V_{GL}(\ ) \right], \tag{2.83}$$

where V_{GL} is the potential for the scalar field of the form of the one given in Eq. (2.82), e the coupling of the gauge and scalar fields, $D \ = \quad - ia$ and $F \ = \ _i a_j - \ _j a_i$ the usual covariant derivative and field strength for the EM field. At temperatures below the critical temperature, $T < T_c$, the scalar field gets a

vacuum expectation value (vev) giving then mass to the EM field. Therefore, inside the superconductor, where $n_s = 0$, the EM field gets a mass and its propagation is therefore suppressed, describing then the Meissner effect.

As explained above, the successful description of superconductivity given by Ginzburg and Landau in terms of a condensed scalar field is only useful at $T \simeq T_c$ making this theory only valid in a narrow region below the critical temperature. Luckily, a deeper insight on this phenomenon came out in 1957 with the advent of the BCS theory due to Bardeen, Cooper and Schrieffer [26]. They showed that interactions with phonons can cause pairs of electrons of opposite spin to bind and form a charged boson called Copper pair. The BCS theory explains all phenomena related with superconductivity in terms of the condensation of Cooper pairs for low T_c superconductors, *i.e.* metals in wich the transition from the normal to the superconducting phases happens at low temperatures, T_c 30 K. Nevertheless, in metals with a high T_c the pairing mechanism is not well understood, since it involves strong coupling. Therefore, high T_c superconductors seem a suitable ground for applying the Gravity/Gauge correspondence.

2.2.2 E ective theories of super uids and superconductors

We are interested in the effective theory for time-independent configurations of a U(1) gauge field $a = (a_0, a_i)$, where $i, j = 1, ..., d-1$, and a scalar field $_{\rm cl}$ whose non-zero value will be responsible for the U(1) breaking. The effective action at finite temperature T for a_i and the order parameter $_{\rm cl}$, obtained after integrating out all the other fields of the theory, depends on an effective Lagrange density constructed from gauge-invariant operators:

$$= \int d^{d-1}x\, \mathcal{L}_{\rm e} \quad , \qquad \mathcal{L}_{\rm e} = \mathcal{L}_{\rm e}\left(\mathcal{F}_{ij}^2,\ D_i \ {}_{\rm cl}{}^2,\ {}_{\rm cl}\,, ...\right), \tag{2.84}$$

where $D_j = {}_j - ia_j$ and $= 1/T$. Eq. (2.84) is defined in some renormalization scheme. We will be assuming that this theory depends only on two mass-scales, (that later we will associate with a chemical potential) and the temperature T.

The generic effective theory given by Eq. (2.84) simplifies in two limits. In the limit of small fields (as compared to and T), this theory approximates to the GL theory

$$_{\rm GL} = \int d^{d-1}x \left\{ \frac{1}{4e_0^2}\mathcal{F}_{ij}^2 + \ D_i \ {}_{\rm GL}{}^2 + V_{\rm GL}(\ {}_{\rm GL}\ ) \right\}. \tag{2.85}$$

The GL field $_{\rm GL}$ is defined to be canonically normalized, $_{\rm GL} = \overline{h_0}\ {}_{\rm cl}$, where h_0 is a positive constant, and

$$V_{\rm GL} = -\frac{1}{2\ {}^2_{\rm GL}}\ {}_{\rm GL}{}^2 + b_{\rm GL}\ {}_{\rm GL}{}^4. \tag{2.86}$$

This approximation becomes reliable, for example, close to the critical temperature $T \quad T_c(\ )$ where the "condensate" $_{\rm cl}$ has a small value. The other useful limit corresponds to slowly varying fields, which implies that $D_i \ _{\rm cl}$ and $\mathcal{F}_{ij}$ are small and

$$\simeq \quad \int d^{d-1}x\, h(\ _{\rm cl}\,)\Big\{\frac{1}{4e^2(\ _{\rm cl}\,)}\mathcal{F}_{ij}^2 + \ D_i \ _{\rm cl}\,^2 + W(\ _{\rm cl}\,)\Big\}\,, \tag{2.87}$$

where h, W and e are generic functions of $_{\rm cl}\,^2$. In the limit of small fields, we obtain the GL theory: $h(\ _{\rm cl}\,) \quad h(0) = h_0$, $W(\ _{\rm cl}\,) \quad V_{\rm GL}(\ _{\rm GL}\,)/h_0$ and $e^2(\ _{\rm cl}\,) \quad e^2(0) = h_0 e_0^2$. When Eq. (2.85) and/or Eq. (2.87) are applicable they can be used to extract model independent features of superconductors and superfluids.

Consider first the case where we are at large temperatures $T > T_c(\ )$; here the condensate $_{\rm cl}$ is zero, corresponding to the "normal" phase. By decreasing the temperature, $T < T_c(\ )$ at zero magnetic field, the modulus of the scalar field $_{\rm cl} = \ _{\rm cl}$ will get a nonzero constant value $\ $. For this homogeneous configuration the effective action in Eq. (2.87) is obviously a good approximation of the theory [12], and the value of $\ $ is determined by the minimum of the potential $V = hW$:

$$\frac{V}{\ _{\rm cl}}(\ \ ) = 0\ . \tag{2.88}$$

This configuration corresponds to the superfluid/superconductor phase. Two important parameters describing these systems are $\ $ and $\ $, defined as

$$\frac{1}{\ ^2} = \frac{1}{2h(\ \ )}\frac{^2V}{^2_{\rm cl}}(\ \ ) > 0\,, \qquad = \frac{1}{\overline{2}e(\ \ )}\,. \tag{2.89}$$

These quantities exactly correspond to the inverse mass of the scalar $_{\rm cl}$ and a_i respectively.

In this work we will be considering time-independent vortex configurations with cylindrical symmetry as the main example of our theoretical framework. We define $(r, \ )$ as the polar coordinates restricted to $0 \quad r \quad R$, $0 \quad < 2\pi$. We will always consider the case $\quad R$ and, in the superconductor case, also $\quad R$. We take the Ansatz

$$a \ = a\ (r)\ , \qquad _{\rm cl} = e^{in} \ _{\rm cl}(r)\,, \tag{2.90}$$

where n is an integer, and all other gauge components are set to zero. For $n = 0$, the fields $a\ (r)$ and $_{\rm cl}(r)$, satisfying the equations of motion from the Lagrangian

[12] Notice however that, generically, this is not the case for the GL theory in Eq. (2.85).

in (2.84), describe a straight vortex line centered at $r = 0$. If we insert the Ansatz (2.90) into the action in (2.87) we obtain

$$\simeq 2\pi V^{d-3} \int_0^R dr\, r\, h(\ _{\rm cl}) \left\{ \frac{1}{2e^2(\ _{\rm cl}) r^2} (\ _r a\ )^2 + (\ _r\ _{\rm cl})^2 + \frac{1}{r^2}(n - a\ )^2\ _{\rm cl}^2 + W(\ _{\rm cl}) \right\}, \tag{2.91}$$

where V^{d-3} is the volume of the space orthogonal to the plane $(r,\ )$. Here the current is given by [13]

$$J\ = -\frac{1}{a}\frac{}{} = 2h(\ _{\rm cl})(n - a\ )\ _{\rm cl}^2 + r\ _r \left(\frac{h(\ _{\rm cl})}{e^2(\ _{\rm cl}) r}\ _r a \right). \tag{2.92}$$

In the vortex case $(n = 0)$ $_{\rm cl}$ goes to far away from the vortex center; this corresponds to the physical fact that a vortex line destroys superfluidity/superconductivity only in a region close to its center. The details of the vortex configurations depend on whether the field a is dynamical as in the superconductor case, or just a non-dynamical background as in a superfluid system. We consider the two cases in turn.

Super uid vortex

For superfluids the modulus and phase of $_{\rm cl}$ are respectively associated with the density n_s and velocity v_i of the superfluid. In the limit of slowly varying fields, Eq. (2.87), we define them as [14]

$$n_s(\ _{\rm cl}\ ) = 2\ _{\rm cl}{}^2 h(\ _{\rm cl}\ ), \quad v_i = \ _i{\rm Arg}[\ _{\rm cl}]\,. \tag{2.93}$$

The field a is not dynamical; it just represents an external angular velocity performed on the superfluid. This is implemented by working in a rotating frame with a constant angular velocity $= a\ /r^2$. In going from the static to the rotating frame the angular velocity of the superfluid is changed accordingly: v $v - r^2$. The current is then given by $J\ = n_s(v\ - \ r^2)$.

Superfluid dynamics coincides with those of a superconductor in the limit in which the EM field is frozen to certain values. This is achieved by taking the limit e 0 while keeping the external magnetic field $B = \ _r a\ /r$ constant. In this limit the correspondence between the superfluid and the superconductor systems is given by

$$B/2\ , \quad L \qquad 2M\,, \tag{2.94}$$

[13] Notice that we have defined the current to include the kinetic term of the gauge field. This is done in order to facilitate our treatment for both, dynamical and non-dynamical gauge fields.

[14] Right dimensions are obtained by putting appropriate powers of the boson mass causing the super uidity.

where L is the angular momentum and M the magnetization of the system in the direction perpendicular to the $(r, \ )$ plane. In the rest of this section we will use the superconductor notation.

Vortices correspond to configurations with $n = 0$ where $_{\rm cl}$ varies from zero (at $r = 0$) to at large r. The exact solution depends on the specific effective action and therefore it is very model dependent. Nevertheless, we can obtain the behavior of $_{\rm cl}$ in the limit $r \ 0$ and for large r. Indeed, for $r \ 0$, the condensate goes to zero and the GL action can be applied to obtain

$$_{\rm cl} \ r^{\ n} \ . \tag{2.95}$$

For large r, we can use Eq. (2.91) to obtain, in the absence of rotation ($B = 0$),

$$_{\rm cl} \simeq \ \left[1 - n^2 \frac{^2}{r^2}\left(1 + \frac{h}{2h(\ )} \frac{}{_{\rm cl}(\ )}\right)\right] , \tag{2.96}$$

showing that $\sim$ gives the size of the vortex core radius. For $B = 0$ the free energy per unit of volume V^{d-3}, F_n, is dominated by the third term of Eq. (2.91):

$$F_n - F_0 \simeq 2\pi \int_0^R \frac{dr}{r} h(\ _{\rm cl})\, n^2 \ ^2_{\rm cl} \simeq \pi n_s(\ )\, n^2 \int^R \frac{dr}{r} = \pi n_s(\ )\, n^2 \ln(R/\ ) \ , \tag{2.97}$$

that depends logarithmically on the size of the superfluid sample R. This shows that superfluid vortices are not finite-energy configurations in the limit R . For $B = 0$, we have to consider the free energy as a function of the angular velocity, obtaining [15]

$$F_n(B) = F_n(0) - \int_0^B M_n(B) dB \, , \tag{2.98}$$

where $M_n(B)$ is the magnetization (angular momentum from Eq. (2.94)) of the n-vortex configuration:

$$M_n = \pi \int dr \, rJ \ . \tag{2.99}$$

The value of M_n is approximately given by

$$M_n \simeq \pi n_s(\ ) \int^R dr r \left(n - \frac{r^2}{2} B\right) \simeq \pi n_s(\ ) \left(\frac{nR^2}{2} - \frac{R^4}{8} B\right) , \tag{2.100}$$

that leads to

$$F_n(B) \simeq F_0(B) + \pi n_s(\ ) \left(n^2 \ln(R/\ ) - \frac{1}{2} n R^2 B\right) . \tag{2.101}$$

[15] In the super uid case, this is the correct expression for the energy calculated in the co-rotating system with respect to the container.

From this formula we can easily calculate the critical angular velocity B_{c1} above which the vortex configuration is energetically favorable. This is given by the B field at which $F_1 = F_0$:

$$B_{c1} \simeq \frac{2}{R^2} \ln (R/\ ) \ . \tag{2.102}$$

We observe that B_{c1} 0 when the size of the sample goes to infinity, that is R .

By increasing B, more and more vortices are formed up to a critical value B_{c2} at which the normal phase is favorable. In the limit B B_{c2} the condensate goes to zero, and the GL theory can be applied. One obtains, with a standard textbook derivation,

$$B_{c2} = \frac{1}{2\ ^2_{\rm GL}} \ . \tag{2.103}$$

Superconductor vortex

For superconductors, a_i, and correspondingly the magnetic field B, are dynamical fields [16]. Superconductor vortex configurations are therefore described by two fields, $_{\rm cl}$ and a . The value of a varies from zero (at $r = 0$) to n at infinity, canceling the logarithmic divergence in Eq. (2.97) and making the vortex energy finite in the limit R .

Like in the superfluid case, we can obtain the behavior of the fields at small and large r in a model independent way. At small r, the condensate drops to zero and the GL action can be used; in this limit one can derive

$$_{\rm cl} \quad r^{\,n} \ , \quad a \quad r^2 \, . \tag{2.104}$$

At large r the situation is more complicated. If one uses Eq. (2.91) it is possible to show that the fields have the following large r behavior

$$_{\rm cl} \simeq \quad + \frac{1}{\ r} e^{-r} \ ' \ , \quad a \ \simeq n + a_1 \ \ \bar{r} e^{-r} \ ' \ , \tag{2.105}$$

with = , = and $_1$ and a_1 being constants. Nevertheless, Eq. (2.105) shows that higher derivatives are not negligible with respect to the first and second derivatives that we included in Eq. (2.91). Indeed, we have

$$\frac{^n_r a}{\ ^n} \sim \frac{1}{(\ \ )^{n-1}} \frac{_r a}{\ } \sim \frac{_r a}{\ } \, , \tag{2.106}$$

[16] In this case we call the dynamical magnetic field B, while we keep H for the external magnetic field.

where we have assumed, based on dimensional grounds, that the scale suppresses the higher-dimensional operators, and that is of order 1/ . A similar situation happens for $_{\rm cl}$. We are therefore led to the conclusion that we cannot neglect higher-derivative terms to describe the large r behavior of the fields. Including them, the equations of motion can (formally) be written as

$$\mathcal{M}(\Box)\ _{\rm cl} \simeq \frac{1}{2}(\ _{\rm cl} - \ ) \ , \quad \mathcal{N}(\Box)a\ \simeq \frac{1}{2}(a\ - n) \ , \tag{2.107}$$

where $\mathcal{M}$ and $\mathcal{N}$ are unknown functions and the box operator acts on $_{\rm cl}$ and a as

$$\Box\ _{\rm cl} = \frac{1}{r}\ _r(r\ _r\ _{\rm cl}) \ , \quad \Box a\ = r\ _r\left(\frac{1}{r}\ _r a\ \right) . \tag{2.108}$$

Fortunately, the solutions to the equations above are also of the form of Eq. (2.105) but with and generically different from and . In other words, the effect of the higher-derivative terms is just to change the values of and . From this large r behavior we can see that the radius size of the vortex core and the radius size of the magnetic tube passing through the vortex (the penetration length) are, respectively, characterized by and .

To calculate the external magnetic field H at which the vortex configuration is energetically favorable we must obtain the Gibbs free energy. This is given in terms of the free energy F by

$$G[J_{ext}] = F - \int d^{d-1}x\, a_i J^i_{ext} \, , \tag{2.109}$$

where J^i_{ext} is an external current coupled to the gauge field a_i. We can relate J_{ext} to the external magnetic field H that it produces, through [17]

$$H = e_0^2 J_{ext} \, . \tag{2.110}$$

Then we end up with the following Gibbs free energy per unit of volume V^{d-3} of the vortex configuration

$$G_n[H] = F_n - \frac{1}{e_0^2}\int rdrd\ \ BH = F_n - \frac{2\pi n}{e_0^2}H \, , \tag{2.111}$$

where we have used the magnetic flux condition $\int rdrd\ \ B = 2\pi n$ and assumed that H is constant. The critical H_{c1} is defined as the value of H at which $G_1 = G_0$ that corresponds to

$$H_{c1} = \frac{e_0^2}{2\pi}(F_1 - F_0) \, . \tag{2.112}$$

[17] In this Maxwell equation of the external field we use e_0, defined as the electric charge in the normal phase ($_{\rm cl} = 0$), to guarantee that when T T_c, the magnetic field B approaches H.

The exact value of $F_1 - F_0$ depends strongly on the model and therefore H_{c1} can only be calculated once the model is specified.

The minimum value of H for which the energetically favorable phase is the normal phase is also, as in the superfluid case, $H_{c2} = 1/(2\ ^2_{\rm GL})$. The superconductors that have energetically favorable vortex solutions, that is $H_{c1} < H_{c2}$, are called Type II superconductors, while the others are called Type I. When the external field is slightly smaller than H_{c2} the condensate has a small value and the GL theory can be applied to predict that Type II superconductors present a triangular lattice of vortices [60]. Superfluids can be considered as deep Type II superconductors and therefore they also present a triangular lattice of vortices. We will show that holographic superconductors are of Type II.

2.2.3 Holographic approach to Superconductivity and Super uidity

As we have seen in the previous section the temperature plays a central role in a superconducting system. Nevertheless we have said nothing about temperature in the framework of AdS/CFT correspondence so far. Therefore, the first task is to introduce its analog in the gravity side. It was found that the notion of temperature can be introduced through stationary black-holes in ED. Due to its Hawking radiation, black holes have a temperature T related to its surface gravity via $T = /2\pi$: in the framework of the gravity/gauge correspondence we associate the hawking temperature of a given black hole to the temperature in the holographic theory. Since this duality requires an asymptotically AdS space at the UV we will place the black hole in a background geometry that will approach AdS at the UV brane.

Another important feature is that we must be able to reproduce the phase transition of the material from the normal to the superconducting phase around some critical temperature T_c. This is done by placing a field in the bulk of the AdS space coupled to the black hole, what is called black hole *hair*. This field will be associated to some operator $\mathcal{O}$ in the dual CFT that will play the role of the condensate and therefore this operator will be the analog of the scalar field in the GL theory. In order to reproduce the phase transition we must require an AdS black hole that is hired at low temperatures but has no hire at high temperatures. This can actually be accomplished by placing a charged black hole in the AdS background.

Taking these considerations into account we can write a general Lagrangian in

d dimensions as an ED analog of a superconducting system in $d-1$ dimensions

$$S = \int d^d x \quad \overline{-g}\Big\{ \frac{R-\Lambda}{16\pi G_N} - \frac{1}{g^2}\left[\frac{1}{4}F \quad F \quad - \; D \quad ^2\right]\Big\}. \tag{2.113}$$

We have considered an Einstein-Hilbert action with bulk cosmological constant $\Lambda = -3/L^2$, coupled to a U(1) gauge field and a charged scalar. F and D are the usual field strength and covariant derivative for the U(1) gauge field A and , $= (0, 1...d)$.

For simplicity we will always work in the limit in which $G_N \quad 0$ and $g \quad 0$ taken in such a way as to decouple the gravity from the matter actions, *i.e.* gravitational effects due to the backreaction of the matter fields A and with the background metric can be neglected, this is called the probe limit. The decoupling of matter and gravitational effects simplifies very much the problem and, in addition, still describes the physics we are interested in, since non linear interactions between the scalar and the gauge fields are retained in this limit.

In the probe limit the black hole solution for the metric in a d dimensional AdS space is,

$$ds^2 = \frac{L^2}{z^2}[-f(z)dt^2 + dy^2] + \frac{L^2}{z^2 f(z)}dz^2, \tag{2.114}$$

where z is the holographic direction, y stands for the $d-1$ dimensional flat metric and

$$f(z) = 1 - \left(\frac{z}{z_h}\right)^d \tag{2.115}$$

being z_h the position of the black hole horizon, which is related with the temperature of the dual FT through

$$T = \frac{d}{4\pi z_h} \tag{2.116}$$

So far we have described a d dimensional gravitational theory with a local U(1) gauge invariance under which is charged and A is the associated gauge field. The holographic theory will look like a CFT at a finite temperature $T = d/4\pi z_h$ with an external gauge field $a \quad = A \quad _{z_{UV}}$ and an operator $\mathcal{O} = \quad _{z_{UV}}$ that will condense below some critical temperature T_c thus breaking the U(1) invariance of the CFT. This picture resembles the previously mentioned GL theory. This kind of theories have been extensively studied in the literature and shown to describe the main properties of superconductors [27]. Moreover, in the limit of small fields, *i.e.* at temperatures $T \sim T_c$, GL theory is recovered. Nevertheless in all these studies a non-dynamical gauge field was considered in the dual CFT, what means that, strictly speaking, the dual theory can not be interpreted as

a superconductor system but as a superfluid, since a dynamical gauge field is needed in order to describe its interactions with the superconducting system and see phenomena associated with it such as the Meissner effect. In the next Section we explore the possibility of giving dynamics to the gauge field in the ED boundary and its consequences on the dual CFT.

As discussed in Sec 2.2.1 it is possible to construct holographic models of superconductivity [51]. Their properties have been widely studied in the literature and found to be in good agreement with properties of real superconductors [27]. Nevertheless, the absence of a dynamical gauge field in these models makes impossible to study some properties of superconductivity like the Meissner effect and besides, strictly speaking, these models just describe either a superfluid [52] or a superconductor in the gauge-less limit.

The reason for the absence of a dynamical gauge field in previously studied holographic superconductors is the chosen AdS-boundary condition for the U(1) gauge field. In most of these studies the gauge field was chosen to be frozen at the AdS-boundary by imposing a Dirichlet boundary condition. One can make, however, the gauge field dynamical if one instead imposes a Neumann-type boundary condition at the AdS-boundary. In this article we will make use of this option to study the role of dynamical gauge fields in holographic superconductors [18].

In a $3+1$ dimensional AdS space it is known that we can impose either a Dirichlet or a Neumann AdS-boundary condition to quantize a gauge theory, being both related by an S-duality [53]. In the Neumann case, one finds a massless gauge field in the spectrum that, by means of the AdS/CFT correspondence, can be considered to arise from a $2+1$ dimensional CFT. It is therefore an emergent phenomenon. In $4+1$ dimensions, however, a Neumann AdS-boundary condition for the gauge field is not well-defined since it leads to a non-finite Hamiltonian. This will require, as we will show, to regularize the theory and absorb the divergencies in local counterterms. In this case, the gauge field will not be an emergent phenomenon but just an external dynamical gauge field coupled to a $3+1$ CFT [13].

An alternative way to understand the distinction between a gauge field in a $2+1$ and $3+1$ CFT is to look at the zero mode of the Kaluza-Klein expansion of the gauge field in the holographic superconductor model at temperatures T bigger than the critical temperature T_c. For a stationary vector potential a_i we find, after integrating over the extra dimension, a kinetic term given by $\int d^d x \mathcal{F}_{ij}^2/(4e_0^2)$,

[18] Neumann boundary conditions have been previously considered in holographic superconductors to study systems at fixed charge density. In these cases, however, the studied systems are homogeneous and therefore the dynamical electric field vanishes.

where $\mathcal{F}_{ij} = \ _i a_j - \ _j a_i$ and

$$\frac{1}{e_0^2} = \frac{3}{4\pi g^2 T} \quad \text{for } d = 2+1\,, \qquad \frac{1}{e_0^2} = -\frac{L}{g^2}\ln\left(z\pi T\right)_{\ z=0} \quad \text{for } d = 3+1\,. \tag{2.117}$$

Here g is the gauge coupling in the AdS model and L is the AdS radius. In $2+1$ dimensions this massless gauge boson mode has a finite norm and therefore remains in the spectrum, while for $d = 3+1$ this is a non-normalizable mode and disappears from the set of dynamical degrees of freedom. To keep this mode in $3+1$ dimensions we must then make its norm finite, for example by adding local counterterms.

The impact of a dynamical gauge field in superconductors is expected to be important in inhomogeneous configurations. For this reason we will concentrate here on the vortex configurations of the holographic models. We will explicitly analyze the cases $d = 2+1$ and $d = 3+1$, introducing, when studying the $d = 3+1$ holographic superconductor, local counterterms to render the norm of a_i finite. This will allow us to explicitly see that the dynamical magnetic field B plays an important role in reproducing some of the known features of superconductor vortices, such as the exponential damping of B inside the superconductor. We will also show that the dynamical gauge field changes the vortex configurations of the holographic models, making the energy and, correspondingly, the first critical magnetic field H_{c1} independent of the sample size, as expected from a true Abrikosov vortex. The properties of the new configurations are qualitatively similar to those arising from a Ginzburg-Landau (GL) theory [25], although we find important quantitative differences in the size of the vortex core, the profile of B flowing through the vortex and H_{c1}.

The effect of an external magnetic field on holographic superconductors has been considered in [54, 55] and vortex solutions have been studied before for $d = 2+1$ in Refs. [56, 57]. In all these cases there was no dynamical electromagnetic (EM) field, and therefore the vortices were not true Abrikosov configurations but just superfluid vortices. Only Ref. [58] showed, for $d = 2+1$, a non trivial profile for the magnetic field of the form of a vortex magnetic tube; it is however unclear the origin of this magnetic field and its relation with Abrikosov configurations.

The organization of this chapter is as follows. In Section 2 we describe, similarly in spirit to Ref. [59], effective field theories from which we can obtain model-independent properties of superconductors and superfluids, and their vortex configurations. This will also help us to make contact with the GL predictions [19]. In Section 3 we present the holographic model and explain how to introduce dynamical gauge fields. We then focus on the holographic superfluid and superconductor

[19] What we mean with GL theory in the case of super uids is the limit of frozen magnetic fields in the GL theory for superconductors.

(Abrikosov) vortex in $d = 2 + 1$ and $d = 3 + 1$ dimensions, comparing them with those of the GL theory. We calculate the energy of these configurations to find the critical magnetic fields H_{c1} and H_{c2} and show that the holographic superconductors are always of Type II. In Section 4 we present a summary of the results and other concluding remarks.

The holographic theory that we want to study is defined [51, 61] by a charged scalar coupled to a U(1) gauge field A in $d+1$ dimensions (, $= 0, 1, ..., d$) and an action given by

$$S = \int d^{d+1}x \quad \overline{-G}\left\{\frac{1}{16\pi G_N}(R - \Lambda) + \frac{1}{g^2}\mathcal{L}\right\} , \quad \text{with} \quad \mathcal{L} = -\frac{1}{4}\mathcal{F}^2 \quad - \frac{1}{L^2} D \quad ^2 . \tag{2.118}$$

G_N is the gravitational Newton constant and the cosmological constant Λ defines the asymptotic AdS radius L via the relation $\Lambda = -d(d-1)/L^2$; moreover we introduced $\mathcal{F} = A - A$ and $D = - iA$. For simplicity, we have not added any potential for the scalar. We will later discuss the implications of including these terms. We will work in the probe limit, *i.e.* $G_N \quad 0$ and $g \quad 0$ taken such that the gravitational effect of $\mathcal{L}/g^2$ can be neglected. In this limit the metric is given by an AdS-Schwarzschild black hole (BH):

$$ds^2 = \frac{L^2}{z^2}\left[-f(z)dt^2 + dy^2\right] + \frac{L^2}{z^2 f(z)}dz^2 , \quad f(z) = 1 - \left(\frac{z}{z_h}\right)^d , \tag{2.119}$$

where t is time, z is the holographic direction such that the AdS-boundary occurs at $z = 0$, while the BH horizon is at $z = z_h$ and dy^2 stands for the $d-1$ dimensional flat metric. Since we are interested in the theory at finite temperature, we will perform the Euclidean continuation with compact time $it \quad [0, 1/T]$ where $T = d/(4\pi z_h)$.

The AdS/CFT correspondence and dynamical gauge elds

This $d+1$ dimensional theory has a dual interpretation in terms of a d dimensional CFT at nonzero temperature. The AdS/CFT dictionary relates the properties of the AdS gravitational theory with those of the CFT. In particular, the fields A and evaluated on the AdS-boundary correspond to fields external to the CFT:

$$a \ = A \ _{z=0} , \quad s = \quad _{z=0} . \tag{2.120}$$

They are coupled to CFT operators through the interaction terms $a \ J \ + s\mathcal{O}$. The operator J corresponds to the U(1) current of the CFT theory, while $\mathcal{O}$ is a CFT operator charged under the U(1) with $\text{Dim}[\mathcal{O}] = 3(4)$ for $d = 3(4)$. Having chosen a nonzero mass for the scalar in Eq. (2.118), would have corresponded

to take another dimensionality for $\mathcal{O}$. We do not expect however any important qualitative difference for other choices of the mass. The dual CFT theory, if it exists, is supposed to be strongly coupled and the limit $g \to 0$ in the AdS theory corresponds to be working at the planar level in the CFT.

Integrating over the CFT fields, one can obtain the free energy $F[a, s]$ from which the vacuum expectation values (VEV) of the CFT operators can be extracted. In the gravity side, $F[a, s]$ is obtained from the $d+1$ dimensional AdS Euclidean action $S_E[a, s]$ evaluated with all bulk fields on-shell restricted to Eq. (2.120):

$$F[a, s] = T\, S_E[a, s]\,, \tag{2.121}$$

from which we obtain the VEVs of the currents

$$J = \frac{L^{d-3}}{g^2} z^{3-d} \mathcal{F}_z \Big|_{z=0}\,, \quad \mathcal{O} = \frac{L^{d-3}}{g^2} z^{1-d} D_z \Big|_{z=0}\,. \tag{2.122}$$

The matching with the effective theory of Section 2 is straightforward: the gauge field a_i of Eq. (2.120) is identified with that in Eq. (2.84), while J_i and $\mathcal{O}$ of Eq. (2.122) are identified respectively with $-\partial^{-1}/\partial a^i$ and $\langle \mathcal{O} \rangle_{\rm cl}$ when renormalized in the same scheme.

In the AdS/CFT correspondence, the external fields in Eq. (2.121) are considered to be frozen background fields. This is suited for holographic superfluids, but not for superconductors that require the presence of dynamical gauge fields coupled to the CFT. It is easy however to promote the external a field to a dynamical field. This corresponds to integrating over it in the path integral:

$$G[s, J_{ext}] = -T \ln \int Da\, e^{-F[a_\mu, s] + \int d^d x \left[-\frac{1}{4e_b^2} \mathcal{F}_{\mu\nu}^2 + a_\mu J_{ext}^\mu \right]}\,, \tag{2.123}$$

where, for generality, we have added to $F[a, s]$ a "bare" kinetic term for a (e_b denotes the bare electric charge), and have coupled it to a background external current J_{ext} to define a Gibbs energy. Working in the semiclassical approximation[20], Eq. (2.123) leads to the Maxwell equation for the gauge field a :

$$J + \frac{1}{e_b^2} \partial \mathcal{F} + J_{ext} = 0\,, \tag{2.124}$$

where we have used that $J = -\partial F/\partial a$. Let us see how the above procedure can be implemented in the gravity side. Using Eq. (2.122), we can write Eq. (2.124) as the following AdS-boundary condition:

$$\frac{L^{d-3}}{g^2} z^{3-d} \mathcal{F}_z \Big|_{z=0} + \frac{1}{e_b^2} \partial \mathcal{F} \Big|_{z=0} + J_{ext} = 0\,. \tag{2.125}$$

[20]The semiclassical approximation is valid in the limit $g \to 0$ and $e_b \to 0$.

This is a boundary condition of Neumann type that, in order to be consistent with the variational principle, requires the AdS model to include the following extra terms on the AdS-boundary:

$$\int d^d x \left[-\frac{1}{4e_b^2}\mathcal{F}^2 \ + A \ J_{ext} \right]_{z=0} . \tag{2.126}$$

Therefore the Gibbs free energy is given by the AdS Euclidean action S_E including the additional terms Eq. (2.126) evaluated on-shell with the bulk fields restricted to the AdS-boundary condition Eq. (2.125).

In the particular case of $d = 2+1$, and in the limit where e_b/g (not adding a kinetic term for the gauge field on the AdS-boundary), one can show that the theory defined by Eq. (2.123) preserves conformal symmetry. In this case the original CFT and the a can be considered as part of a new CFT. Another way to understand this result is given in Ref. [53]. There it was shown that there are two ways to quantize a gauge field in the four dimensional AdS. We can either impose a Dirichlet or a Neumann boundary condition at $z = 0$. Each option is associated with a different CFT, S-dual to each other, with different global U(1). While in the first option (Dirichlet boundary condition) the gauge field a is a background field, in the second one (Neumann boundary condition) the gauge field is truly dynamical [53]. In this latter case the gauge field arises from the CFT as a composite state, as shows the fact that its kinetic term is induced by the AdS bulk dynamics. In other words, this local U(1) appears as an emerging phenomenon. As emphasized in Ref. [53], this CFT, which includes a dynamical gauge field, has also a global U(1) with an associated conserved current given by $J = a$, and should not be confused with the emerging local U(1). Here we also observe that the emergence of the dynamical U(1) can be understood without using conformal invariance. Even for a warped space different from AdS, the massless zero-mode of a gauge field in $3 + 1$ dimensions has finite norm, corresponding then to a composite state in the dual $d = 2 + 1$ theory. This is related to the fact that the gauge interaction in $d = 2 + 1$ is a relevant operator and therefore is dominated by IR physics. It is thus possible to send e_b/g to infinity in this case.

For $d = 3 + 1$, the situation is different. The current J contains a logarithmically divergent piece given by (in the gauge $A_z = 0$)

$$\frac{1}{z} \ {}_zA \ \Big|_{z=0} = - \ \mathcal{F} \ \ln z \Big|_{z=0} + \ldots . \tag{2.127}$$

The appearance of the logarithmic divergence was already expected from the calculation of the kinetic term of a_i in Eq. (2.117). This can also be understood by looking at the dual CFT interpretation of the gravitational theory. Indeed, at

short distances (smaller than $1/T$) this dual theory is a $3+1$ dimensional relativistic theory charged under a U(1). At the quantum level an external a gauging this U(1) receives corrections to its self-energy that in momentum space go as

$$(p^2) \simeq p^2 \ln\left(p^2/\Lambda_b^2\right) , \tag{2.128}$$

where p^2 is the 4-dimensional momentum of the gauge field and Λ_b is a momentum cut-off that regularizes a logarithmic divergence. Therefore a is a state of infinite norm. If our intention is to keep the external gauge field in the theory we must renormalize it. A possible way to do so is to place a UV-brane at finite $z > 0$ as in Randall-Sundrum models [9]. Alternatively, we can absorb the divergence in the local counterterm of Eq. (2.126), i.e., defining the bare coupling e_b as

$$\frac{1}{e_b^2} = \frac{1}{e_0^2} + \frac{L}{g^2} \ln z \, _{z=0} + finite \ terms \, , \tag{2.129}$$

where e_0 denotes here and thereafter our renormalized (physical) electric charge at the normal phase ($_{\rm cl} = 0$). Contrary to the $d = 2+1$ case, the presence of the gauge field a breaks conformal invariance; therefore the gauge field cannot be considered an emerging phenomenon but just a new external state coupled to the CFT [13]. The same is true for any $d > 4$.

We are now ready to study models of holographic superconductors. We are interested in vortex configurations where, as we said, the effects of dynamical gauge fields are important. We will however present first the holographic superfluid vortex configurations for both $d = 2+1$ and $d = 3+1$. This will be useful to clarify previous results in the literature [56], showing that these holographic vortices fulfill the expectations of Section 2 for configurations without dynamical gauge fields. Then, we will present our main result: the Abrikosov superconducting vortex.

The vortex Ansatz

For both the superfluid and the superconductor we will demand

$$s = 0 \ , \quad a_0 = \quad , \tag{2.130}$$

where is a constant. We fix $s = 0$ since we are only interested in the case in which the U(1) symmetry is broken dynamically by the VEV of $\mathcal{O}$. The constant plays the role of a chemical potential. As shown in Ref. [51, 61], a nonzero is necessary in order to induce, at temperatures smaller than some critical temperature $T_c(\ )$, a nonzero value for $\mathcal{O}$ and to have the system in a superfluid/superconductor phase. This critical temperature is given by [51, 61]

$$T_c \simeq 0.03(0.05) \qquad \text{for } \ d = 3(4) \, . \tag{2.131}$$

Notice that $= 0$ breaks the conformal symmetry of the system and, together with T, set the scales of the model.

To obtain vortex solutions we take the Ansatz [56, 58]

$$= (z,r)e^{in} \quad , \quad A_0 = A_0(z,r) \; , \quad A \; = A \; (z,r) \, , \tag{2.132}$$

and the other components of A set equal to zero. As in the previous section, n is an integer and a vortex corresponds to $n = 0$. We will be working in polar coordinates ($dy^2 = dr^2 + r^2 d \; ^2$) for $d = 2 + 1$ and in cylindrical coordinates ($dy^2 = dr^2 + r^2 d \; ^2 + dy_3^2$) for $d = 3 + 1$. The equations of motion for the Ansatz (2.132) are given by

$$\begin{aligned} z^{d-1} \; _z \left(\frac{f}{z^{d-1}} \; _z \right) + \frac{1}{r} \; _r (r \; _r \;) + \left(\frac{A_0^2}{f} - \frac{(A \; - n)^2}{r^2} \right) \quad &= \; 0 \, , \\ z^{d-3} \; _z \left(\frac{f}{z^{d-3}} \; _z A \; \right) + r \; _r \left(\frac{1}{r} \; _r A \; \right) - \frac{2 \, (A \; - n)}{z^2} \quad ^2 \; &= \; 0 \, , \\ z^{d-3} \; _z \left(\frac{_z A_0}{z^{d-3}} \right) + \frac{1}{rf} \; _r \, (r \; _r A_0) - \frac{2 \, A_0}{z^2 \, f} \quad ^2 \; &= \; 0 \, . \end{aligned} \tag{2.133}$$

We will impose regularity to our solutions. This requires at $z = z_h$:

$$\begin{aligned} - \frac{d}{z_h} \; _z \; + \frac{1}{r} \; _r (r \; _r \;) - \frac{(A \; - n)^2}{r^2} \quad &= \; 0 \, , \\ - \frac{d}{z_h} \; _z A \; + r \; _r \left(\frac{1}{r} \; _r A \; \right) - \frac{2 \, (A \; - n)}{z_h^2} \quad ^2 \; &= \; 0 \, , \\ A_0 \; &= \; 0 \, , \end{aligned} \tag{2.134}$$

while at $r = 0$ we must have

$$\begin{aligned} _r A_0 \; &= \; 0 \; , \quad A \; = 0 \, , \\ _r \quad &= \; 0 \; \text{ for } n = 0 \; , \qquad = 0 \; \text{ for } n = 0 \, . \end{aligned} \tag{2.135}$$

For a superfluid, as we explained before, the energy of the vortices is sensitive to the size of the sample R. We will therefore limit $r \quad R$, where R, as we commented before, is taken much bigger than the vortex radius.

Holographic super uid vortices

For a vortex superfluid configuration a is fixed:

$$a \; = A \; _{z=0} = \frac{1}{2} B r^2 \, , \tag{2.136}$$

where the constant B represents the external rotation (or, equivalently, the external magnetic field for a superconductor in a situation in which the magnetic field can be considered frozen). This corresponds to a Dirichlet boundary condition at $z = 0$.

Also we impose the following boundary conditions at $r = R$:

$$_r \quad = 0 \ , \qquad _r A_0 = 0 \ , \quad A \ = \frac{1}{2} B R^2 \, . \tag{2.137}$$

These conditions are consistent with the variational principle which is used to derive the equations of motion from the action. The first two conditions represent the physical requirement that, far away from the vortex center, the solution should reduce to the superconducting/superfluid phase, which is independent of r, while the third one is a simple option compatible with (2.136).

We have solved numerically Eqs. (2.133) with the boundary conditions Eqs. (2.134), (2.135), (2.130), (2.136) and (2.137) by using the COMSOL 3.4 package [62]. In Fig. 2.6 we present the order parameter and the current as functions of r for the $n = 1$ vortex solution obtained from such numerical analysis. Our solutions have the right behavior at $r \quad 0$ and $r \qquad$ as predicted in Eqs. (2.95) and (2.96) respectively. We notice however that, unexpectedly, the order parameter $\mathcal{O}$ develops a small bump at around $r \sim 12/ \ $, especially for the $d = 2 + 1$ case.

It is interesting to know whether our results deviate from those of the simple GL theory. For this purpose, we must first specify the input parameters, $_{\rm GL}$ and $b_{\rm GL}$, of the GL model. We fit these two parameters from two predictions of the holographic model: B_{c2} and J at large r. The value of B_{c2} is determined in the holographic model as the value of B at which $\mathcal{O}$ reduces to zero everywhere in space. With this value and Eq. (2.103) we can obtain $_{\rm GL}$. From the value of J at large r as given in Fig. 1 we match with the corresponding current in the GL model, which, for $B = 0$, reads $J^{\rm GL}(r \qquad) = 2n \quad _{\rm GL}(r \qquad)^{\,2}$; this allows to obtain $b_{\rm GL}$. We find

$$_{\rm GL} \simeq 1.1 \ (0.9) \ ^{-1} \ , \quad b_{\rm GL} \simeq 3.3 \quad (12.4) \, , \tag{2.138}$$

for $d = 3$ (4) at $T/T_c = 0.3$. Once $_{\rm GL}$ and $b_{\rm GL}$ are determined, we can obtain the prediction of the GL model for the condensate and the current as functions of r in the $n = 1$ vortex configuration. We show these in Fig. 2.6. We can appreciate that the holographic vortex differs significantly from that of the GL theory. In particular, the radius size of the vortex core in the holographic model is considerably bigger than that in the GL theory, namely $> \ _{\rm GL}$. For $T \simeq T_c$, however, the holographic model, like any other model of superfluidity, should reduce to the GL theory. We have checked numerically that the holographic prediction for $\mathcal{O}$ and J approaches that of the GL theory when the temperature is very close to T_c.

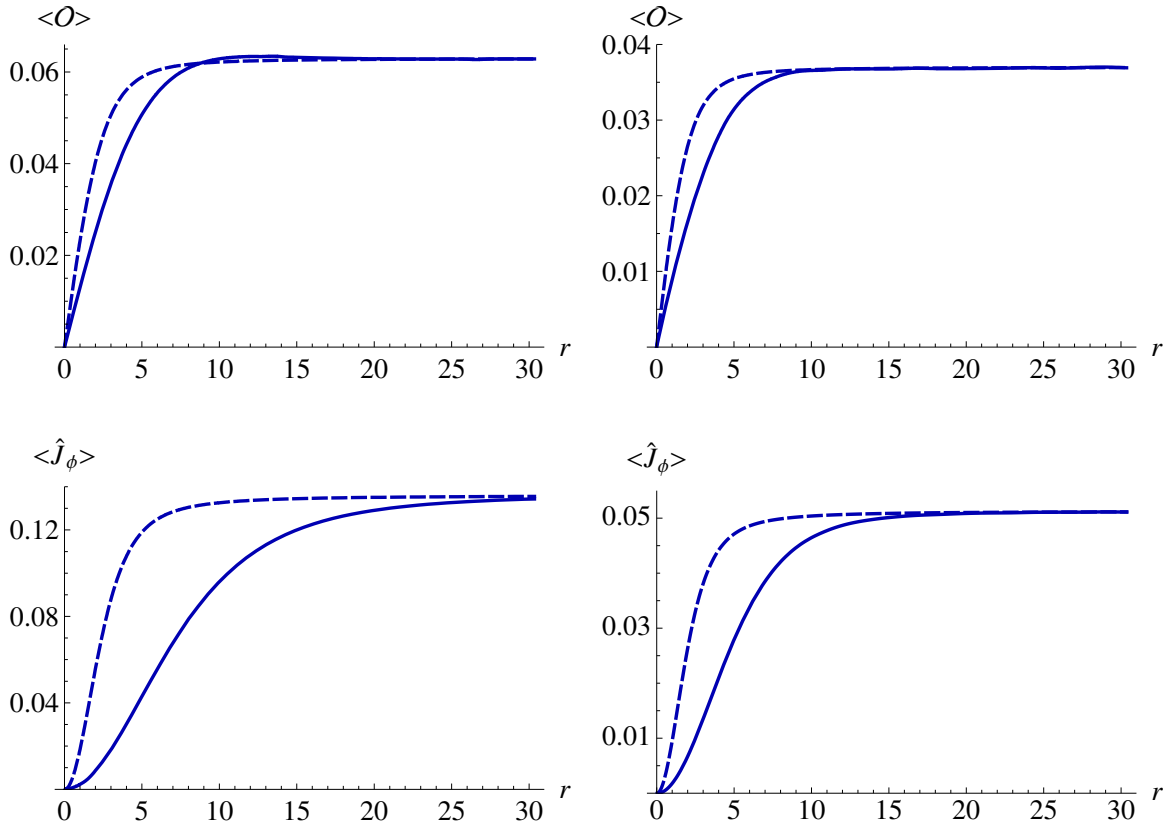

Figure 2.6: The modulus of $\mathcal{O}$ and J (up to a factor $L^{d-3}\ g^2$) as functions of r from the holographic model in the $n = 1$ super uid vortex solution for $d = 2 + 1$ (solid lines on the left) and $d = 3+1$ (solid lines on the right). In this plot we chose $T\ T_c = 0.3$ and $B = 0$. The dashed lines are the corresponding profiles in the GL model. Presented in units of $= 1$.

Next, we calculate the vortex free energy F_n of the d dimensional superfluid. It is then possible to verify that B_{c1} behaves as predicted by the effective theory approach, Eq. (2.102), and also that F_n follows, to a very good approximation, Eq. (2.101). Similarly, the results from the effective theory of Section 2, can explain the results obtained in Ref. [56]. Indeed, taking the value of $n_s(\ \ ) = 0.28\ \ ^-$ as in Ref. [56], we obtain, from Eqs. (2.100) and (2.101),

$$M_n \simeq 0.4nR^2\ \ ^- - 0.1R^4\ \ ^-B\ , \quad \frac{F_1 - F_0}{^-} = 0.9\ln(R/\ ) - 0.4R^2B\,, \qquad (2.139)$$

that agrees [21], as well as B_{c1} in Eq. (2.102), with the numerical values obtained in Ref. [56].

[21] Here we point out a missprint in the value of $_n$ given in Eq. (24) of Ref. [56]: the correct one is $_n \simeq 0.1(0.2)R^4\ \ ^-$.

The value of B_{c2} as a function of T, that, as explained before, coincides with that of a superconductor ($B_{c2} = H_{c2}$), will be presented in Section 2.2.3. As discussed in Section 2.2.2, any superfluid can be considered as a deep Type II superconductor and therefore, when B is slightly smaller than B_{c2}, presents a triangular vortex lattice. This property has been checked in Ref. [63] for a holographic superfluid for $d = 2 + 1$. Here we stress that the same remains valid also for bigger values of d as it uniquely comes from the fact that, when the condensate is small, the theory is well approximated by a GL theory. In the next section we will show that our holographic superconductor is a Type II superconductor and therefore is also characterized by a triangular lattice of vortices for H slightly smaller than H_{c2}.

Holographic superconductor vortices

To model an Abrikosov vortex we consider stationary configurations that do not possess a dynamical electric field but only a dynamical magnetic field. Therefore at $z = 0$ we will impose the boundary condition Eq. (2.130) for A_0 and Eq. (2.125) for A_i that, in polar coordinates, reads

$$\frac{L^{d-3}}{g^2} z^{3-d} \; {}_z A \; \Big|_{z=0} + \frac{1}{e_b^2} r \; {}_r \left(\frac{1}{r} \; {}_r A \; \right) \Big|_{z=0} = 0 \,, \tag{2.140}$$

where we have taken $J_{ext} = 0$. At $r = R$ we impose that

$$ {}_r \quad = 0 \,, \qquad {}_r A_0 = 0 \,, \quad A \; = n \,. \tag{2.141}$$

From the set of equations (2.133) and boundary conditions Eqs. (2.134), (2.135), (2.130), (2.140) and (2.141), we can numerically obtain the superconductor vortex configurations. The profile for the condensate $\mathcal{O}$ and the magnetic field $B(r) = {}_r A \; {}_{z=0}/r$ are given as functions of r in Fig. 2.7. We have chosen $T/T_c = 0.3$ and e_b/g for $d = 2 + 1$, while, for $d = 3 + 1$, we have taken e_b to satisfy $e_0^{-2}(T = T_c) \simeq 1.7 L/g^2$. We observed that the fields have the expected behavior at small and large r given by Eqs. (2.104) and (2.105) respectively. Indeed, the vortex profile at large r has changed from the behavior of Eq. (2.96) to that of Eq. (2.105) as expected in an Abrikosov vortex with dynamical EM fields. Similar to the superfluid case, however, the order parameter $\mathcal{O}$ shows an unexpected slight increase at around $r \sim 12/$. In Fig. 2.8 we show and , defined respectively in Eqs. (2.89) and (2.105), as functions of the temperature. For T T_c both quantities diverge as expected, since in this limit we have 0 and therefore . As T 0, however, we observe that and differ considerably, with increasing its value at $T/T_c \simeq 0.3 - 0.4$. A priori, this would

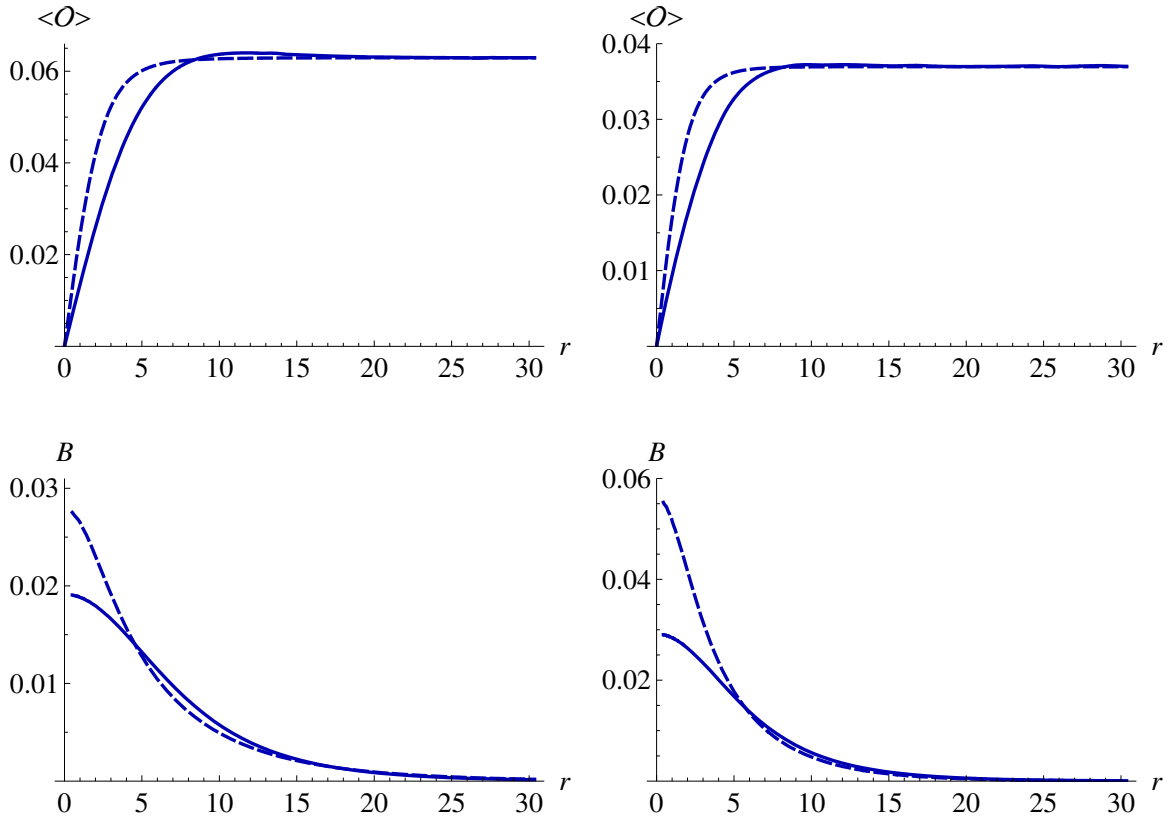

Figure 2.7: The modulus of $\mathcal{O}$ (up to a factor $L^{d-3}\ g^2$) and B as functions of r from our holographic model in the $n = 1$ superconductor vortex solution for $d = 2 + 1$ (solid lines on the left) and $d = 3 + 1$ (solid lines on the right). The dashed lines are the corresponding profiles in the GL theory. Presented in units of $\quad = 1$.

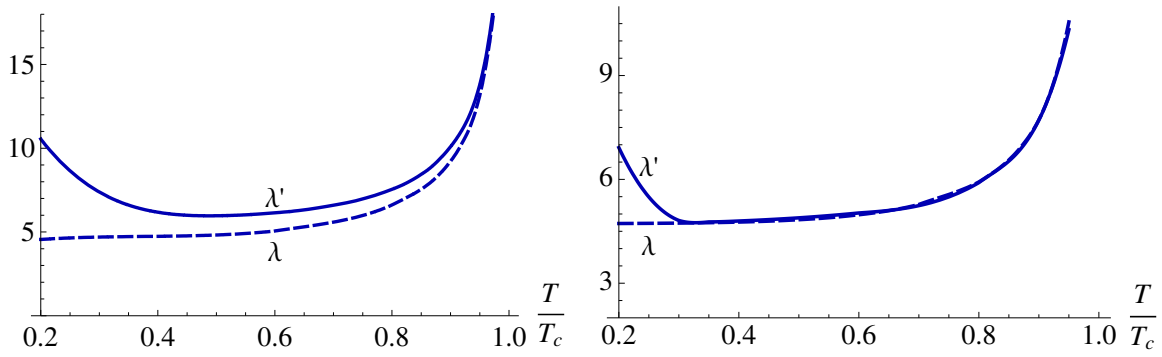

Figure 2.8: and ′ as functions of T from our holographic model for $d = 2 + 1$ (on the left) and $d = 3 + 1$ (on the right). Presented in units of $= 1$.

indicate that the magnetic flux tube becomes broader as T goes to zero, since the penetration length grows. Nevertheless, we find that the situation is more complex; as T 0 the magnetic flux develops two cores, one of size $\sim 1/$ while the other $\sim$. This unexpected behavior deserves further studies.

In Fig. 2.7 we also provide the corresponding curves in the GL theory; the parameters $_{\rm GL}$ and $b_{\rm GL}$ in the GL potential are fixed as in the superfluid case, Eq. (2.138), while the electric charge e_0 appearing in the GL action is determined by using the second definition in Eq. (2.89) applied to the GL case, that is $_{\rm GL} = 1/(\ \overline{2}e_0\ _{\rm GL}(r\ \ )\ )$, and by requiring $_{\rm GL}$ to be equal to the value of of the holographic superconductor. Again, as in the superfluid case, we observe that the radius size of the vortex core is bigger in the holographic model than in the GL theory. As expected, we find these differences disappear as T T_c.

The free energy per unit of volume V^{d-3} of the vortex configuration is, after taking into account the kinetic term in Eq. (2.123), given by

$$F_n = \frac{T}{V^{d-3}} S_E + 2\pi \int dr r \frac{1}{2e_b^2} \frac{(\ _r a\ )^2}{r^2}\,, \tag{2.142}$$

where S_E is calculated with the appropriated boundary conditions already stated. Contrary to the superfluid case, we have checked that $F_1 - F_0$ is finite for R thanks to the presence of the gauge field.

To calculate the critical magnetic field H_{c1} we follow Eq. (2.112). We find that $H_{c1} < H_{c2}$ for any real value of e_0. This implies that for these holographic superconductors there is always a range of values of H for which vortex solutions are energetically favorable; the superconductors are always of Type II. In Fig. 2.9 we show H_{c1} and H_{c2} as functions of the temperature for the same values of e_b as in Fig. 2.7. Notice that H_{c1} approaches zero as T 0. This is due to our

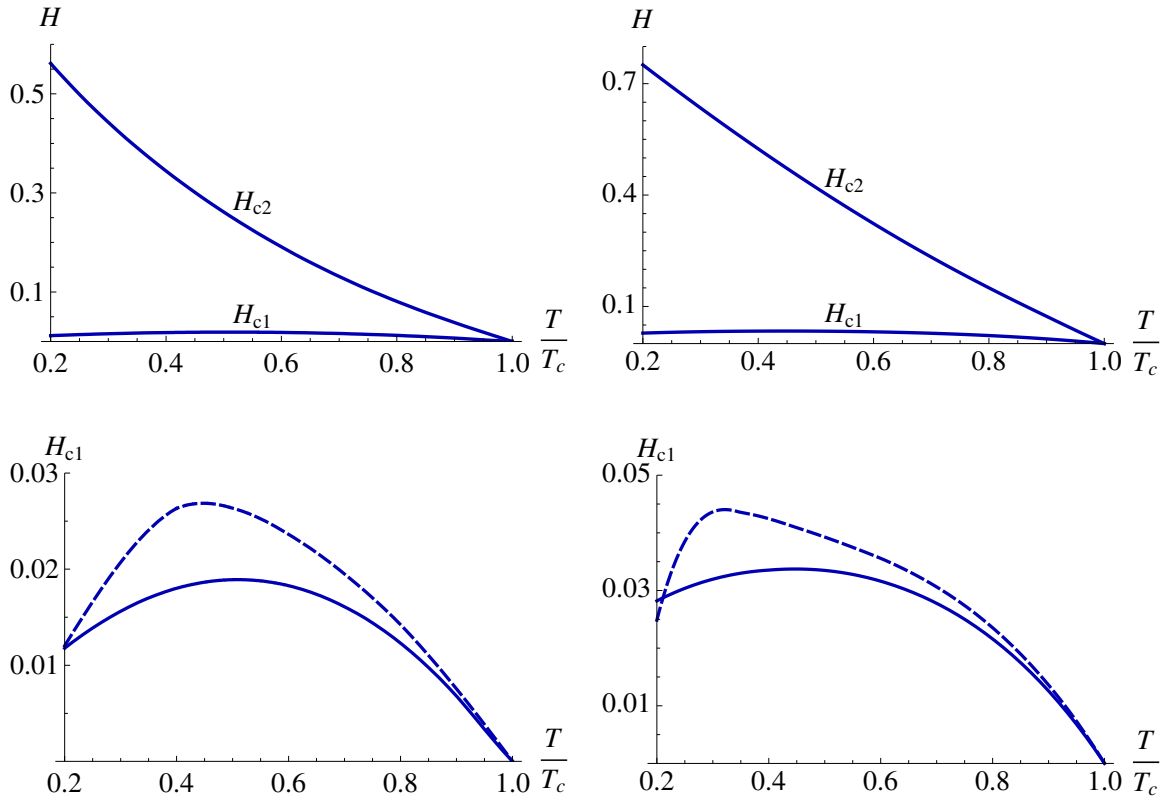

Figure 2.9: H_{c1} and H_{c2} as functions of T from our holographic model for $d = 2+1$ (solid lines on the left) and $d = 3+1$ (solid lines on the right). The dashed lines are the corresponding predictions for H_{c1} from the GL theory. Presented in units of $= 1$.

normalization of H in Eq. (2.110) that makes H_{c1} e_0^2, which goes to zero as T 0. We can, however, derive H_{c2}/H_{c1} as T 0 independently of such normalization. This is a generic prediction of superconducting CFT. Finally, we compare our results with those arising from the GL theory of superconductors. We observe that H_{c1} deviates from the GL prediction for temperatures smaller than T_c.

From the discussion given in Section 2.2.2, and the fact that our superconductors are of Type II, we know that the energetically favorable configuration when H is slightly smaller than H_{c2} is a triangular lattice of vortices.

2.2.4 Conclusions

We have shown how to introduce a dynamical gauge field in holographic superconductors to study vortex configurations. In $d = 2+1$ this gauge field is part of the

CFT spectrum and therefore can be considered to be an emergent phenomenon, instead of an external field. We have shown that vortex configurations, in the presence of this gauge field, follow the expected properties of finite-energy Abrikosov vortices where the magnetic field drops exponentially at distances larger than the vortex core. We have calculated the energy of the vortices and the critical magnetic fields H_{c1} and H_{c2} that determine the intermediate (Shubnikov) phase. In all cases we have found that $H_{c1} < H_{c2}$ indicating that holographic superconductors are of Type II. For comparison, we have also calculated the vortex configurations in the absence of dynamical fields, corresponding to superfluid vortices, and described their properties.

The vortex configurations found here differ considerably from those arising from a GL theory. In particular, the vortex size comes out to be larger, H_{c1} has a different T dependence, and, more importantly, the penetration length of the magnetic field differs significantly as $T \quad 0$.

We have extended the study to $d = 3 + 1$ where a dynamical gauge field has to be introduced by a proper renormalization of the AdS-boundary terms. In this case, the gauge field does not respect conformal symmetry and is external to the CFT. In spite of this, the vortex properties are found to be very similar to the $d = 2 + 1$ case.

Although we have focused on vortex solutions, the method described here to introduce a dynamical gauge field is general and can be used in other situations. For example, one could study the behavior of the EM field near the surface of a finite size superconductor or in the junction between two superconducting samples in the presence of the Josephson effect [64]. Moreover, it would be interesting to extend the present analysis to 3+1 dimensional gauge fields sourced by a 2+1 dimensional CFT; this would allow to study interactions between the EM field and layered superconductors. Our studies can also be extended to p-wave holographic superconductors [65] and to holographic models that are dual to non-relativistic scale-invariant theories [66].

Chapter 3

Quark Compositeness

3.1 Introduction

There are strong motivations to search for an underlying structure in some of the SM particles mainly related to the large hierarchy between the two natural scales in the SM: the EW and the Planck scales. Naturalness problems on the Higgs mass due to this hierarchy can be addressed if the Higgs itself arise as a composite particle of some strongly interacting sector. Moreover the heaviness of the Top quark, the heaviest particle in the SM spectrum, also suggests that it could have a composite nature, at least partially. Up to this point we could wonder if not just the Higgs and the Top but the whole plethora of SM particles could be composite.

The main purpose of this chapter is to look for the feasibility of the compositeness of the different SM particles. We will specifically focus on quark compositeness since, as we will see, this is the most poorly tested direction within the SM by experiments previous to the LHC. We will also see that we can study the quark sector through the analysis of dijet events at the LHC.

The dijet analysis will serve us to analyze not only the feasibility of explicit extra dimensional models of quark compositeness but different BSM models and even to constrain the Oblique parameters Y, W and Z, obtaining for the latter the best bound up to date. Moreover, we will see that the range of applicability of the dijet analysis is so broad that it will comprise any model in which quarks are coupled to heavy resonances with mass above 2 TeV.

This chapter is organized as follows. We will start showing how well the different sectors of the SM have been tested in the pre-LHC era, and which type of deformations from the SM, parametrized by dimension-six operators, can be

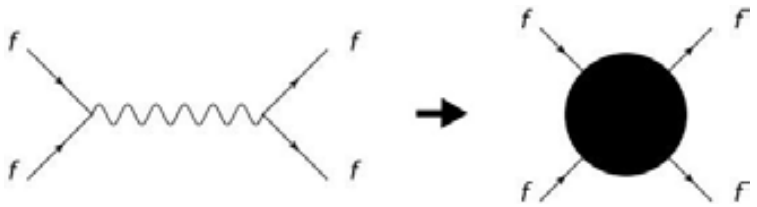

Figure 3.1: Low energy picture of a heavy particle exchange in the limit of $s\Lambda_{CH}$

much better bounded by the LHC. In section 3.3 we present the calculation of the dijet angular distributions and the F parameter that seems to be very well suited to obtain limits on four-quark interactions. By using the LHC data we will obtain bounds on all possible new four-quark interactions (see also Ref. [75]), and translate these bounds into limits on the scale of compositeness of the quarks, on possible new gauge sectors, on the scale of compositeness of the SM gauge bosons, and finally on new physics scenarios responsible for explaining the present experimental discrepancy in the forward-backward asymmetry A_{FB} of the top [76, 77].

3.2 Tests of the SM sectors before LHC

Explicit realizations of Composite Higgs models are indeed di cult since they involve strong dynamics and therefore a perturbative expansion is not possible. However, its resemblance with QCD suggests that we can find extra dimensional analogs for this class of theories in an analogous way as proposed for the case of large-N_c QCD in Sec 2.1.2. This has actually been done in the literature, where explicit 5D theories involving certain symmetry breaking patterns has been used to describe calculable models of composite pNGB Higgs [32]. They predict the existence of heavier resonances and deviations from SM couplings that can be proved at colliders. Nevertheless it is not always necessary to go to the full ED theory in order to study the predictions of CHM. A simple parametrization of NP effects due to the strong sector responsible for Electroweak Symmetry Breaking (EWSB) is possible when the mass of the resonances M are larger than the energies involved in collider experiments. In this case NP effects can be parametrized through the addition of operators of dimension bigger than four. To illustrate this let us consider the 2 2 scattering between fermions f in the SM. If a coupling between the SM fermions and the heavy gauge resonances of the composite sector g exist this 2 2 fermion scattering can receive corrections from the exchange of heavy resonances. In the amplitude these corrections will be of the form,

$$\mathcal{M}_{res} \sim g^2 u(p_1) \quad v(p_2) \frac{g}{s - M^2} v(p_3) \quad u(p_4)\,, \tag{3.1}$$

where M is the mass of the heavy gauge resonance mediating this scattering. If we consider the limit in which $s \quad M^2$ we can neglect the s invariant in the denominator of the gauge boson propagator. In this limit we get

$$\mathcal{M}_{4f} \sim -\frac{g^2}{M^2} u(p_1) \quad v(p_2) v(p_3) \quad u(p_4) \,. \tag{3.2}$$

This looks exactly like the contribution of a higher dimensional operator involving four fermion fields multiplied by some factor, that in this particular case is $\sim -g^2/M^2$. Actually these proportionality factors can be exactly computed by integrating out the heavy resonances. Therefore, at low energies compared to M we can effectively parametrize the NP effects associated to a heavy resonance exchange as a higher dimensional operator in the following way,

$$\mathcal{M}_{res} \sim -\frac{g^2}{M^2} \mathcal{M}_{4f} \,. \tag{3.3}$$

This is schematically represented in Fig. 3.1. This argument suggests that, in the limit $s \quad M^2$, we can encode de deviation of SM predicitions from NP effects with a set of higher dimensional operators consistent with $\mathcal{G}_{\mathcal{SM}}$ and involving SM particles[1]

$$\mathcal{L}_{d>4} = \frac{c_i}{\Lambda^2_{CH}} \mathcal{O}_i^{d=6} + \dots \,, \tag{3.4}$$

where the c_i coe cients are constants associated to each operator $\mathcal{O}_i$.

In Chap. 3 we will explore the effects of such higher dimensional operators when arising from different completions of the SM and specifically we will focus on their effects when these operators are generated from a strong sector based on explicit 5D realizations of the Composite Higgs Model once the heavy resonances have been integrated out. This will allow us to derive bounds on this kind of models when comparing the deviations from the SM due to the presence of these operators with present experimental data.

Let us consider a new sector beyond the SM (BSM) whose physical scale, generically referred by Λ (that, for example, can be associated with the mass of the new states), is assumed to be much larger than the momenta p at which we are probing the SM, $\Lambda \gg p$. We can then parametrize the deviations from the SM by higher dimensional operators added to the SM Lagrangian [33]:

$$\mathcal{L}_{eff} = \mathcal{L}_{SM} + \frac{c_i}{\Lambda^2} \mathcal{O}_i^{d=6} + \quad , \tag{3.5}$$

[1] We just consider operators with dimension 6 or bigger since it can be seen that the only dimension 5 operator consistent with the SM symmetry group gives rise to a Majorana mass term for the neutrino [33]. It is not the aim of this thesis to discuss such physics and therefore we will neglect this operator.

where we only keep the dominant contributions corresponding to operators of dimension six, assuming lepton and baryon number conservation. Among these operators it is important to distinguish between two classes:

1. Operators involving extra powers of SM fields:

$$(q_L \quad q_L)^2 \ , \quad (q_L \quad q_L)(H \ D \ H) \ , \ ... \tag{3.6}$$

2. Operators involving extra (covariant) derivatives:

$$q_L \quad q_L D \ F \quad , \quad q_L u_R D \ D \ H \ , \ ... \tag{3.7}$$

The coe cients c_i in front of the first class of operators are parametrically proportional to the square of a coupling of the SM fields to the BSM sector, and then they can be as large as $c_i \quad 16\pi^2$. On the other hand, the coe cients c_i of the second class of operators should not contain couplings and are expected to be of order one $c_i \quad O(1)$. This distinction is important when considering strongly-coupled BSM with part of the SM fields arising as composite states of this new sector. In this case Λ corresponds to the mass of the heavy resonances of the new strong sector whose couplings, referred as g , can be as large as $\sim 4\pi$. Hence operators of the first class with $c_i \sim g^2$ give generically more significant modifications to SM physics than those of the second class [72, 73, 78].

At present we have important constraints on c_i/Λ^2 coming from precision measurements of SM observables. Let us start considering those involving SM fermions. In the Appendix we give the full list of independent operators involving quarks. Neglecting fermion masses (chiral limit), we have that the impact of the dimension-six operators on SM physical processes can generically be parametrized by two new types of interactions:

$$\frac{}{\Lambda^2}(\qquad)^2 + \quad \frac{v^2}{\Lambda^2}A \qquad , \tag{3.8}$$

where we denote collectively by $A \ = W \ , Z \ , ...$ the SM gauge bosons, by $=$ $u_L, u_R, ...$ the SM fermions of a given chirality, $v \simeq 246$ GeV is the Higgs vacuum expectation value (VEV), and and measure the strength of the interactions. Since both types of interactions in Eq. (3.8) can arise from operators of the first class (Eq. (3.6)), one has $0 <$, $16\pi^2$. The first term of Eq. (3.8) gives contributions to four-fermion processes that scale as p^2/Λ^2 where p characterizes the momenta of the process. The second term corresponds to deviations from the SM gauge interactions at zero-momentum, and therefore these can only arise for the W and Z gauge boson and must be proportional to the Higgs VEV.

In principle, very stringent constraints on new interactions of the type of Eq. (3.8) arise from flavor physics [79]. It is not our purpose here to discuss them; they are very model dependent and can be avoided if a flavor symmetry is imposed in the BSM sector. For example we can assume a flavor symmetry for the three left-handed quarks q_L, the three right-handed down-quarks d_R, and the two lightest right-handed up-quarks u_R, given by

$$G_F \quad U(3)_q \quad U(3)_d \quad U(2)_u \,, \tag{3.9}$$

and similarly for the lepton sector. Due to the absence of important constraints on the flavor physics for the right-handed top t_R, we can consider it a singlet of the flavor symmetry. This allows us to treat the t_R independently of the other quarks; its physical implications, some of them already studied in Ref. [78], are left for a future publication. Yukawa couplings break the G_F symmetry, but it can be shown, by using a spurion's power counting, that flavor constraints on dimension-six operators can be easily satisfied for Λ slightly above the electroweak scale [79]. From now on, we will consider BSM that, up to Yukawa couplings, fulfill the flavor symmetry G_F.

At LEP the properties of the leptons $= l_L, l_R$ were very well measured, putting bounds at the per-mille level on deviations from the SM predictions either arising from vertex corrections or new four-lepton contact interactions. From [28], one gets $\Lambda/(\sqrt{\ _{l_{L,R}}}), \Lambda/(\sqrt{\ _{l_{L,R}}})$ $3-4$ TeV. This implies, for example, that the scale of compositeness of the leptons is larger than $40-50$ TeV for $_{l_{L,R}} \sim g^2 \sim 16\pi^2$. Thus, the leptonic sector has been very well tested at LEP and recent LHC data, having only quarks in the initial state, cannot provide better bounds.

For the left-handed quark sector $= q_L$, there are very strong constraints on interactions of the second type of Eq. (3.8). The most important ones arise from Kaon and -decays [28] which have allowed to measure very precisely quark-lepton universality of the W interactions. This leads to bounds on deviations from the W coupling to left-handed quarks as strong as those for leptons, $\Lambda/(\sqrt{\ _{q_L}})$ $3-4$ TeV, which we do not expect to be improved substantially at the LHC. Similar limits are obtained from measurements at LEP of the Z decay to hadrons [28]. Bounds on four-q_L interactions are weaker, with the main constraint coming from Tevatron and giving $\Lambda/(\sqrt{\ _{q_L}})$ 1 TeV [28]. Clearly, the LHC can increase these bounds considerably as we will show later. While theories of composite Higgs and composite q_L, where one expects large $_{q_L}$ and $_{q_L}$ coe cients (since $_{q_L} \sim \ _{q_L} \sim g^2$ $16\pi^2$) [72, 73, 78], are very constrained by present experimental data, theories with only q_L composite (and elementary Higgs, as those for example in Ref. [74]) where only $_{q_L}$ is expected to grow with g^2, are not so constrained. LHC dijets can then, as we will see, probe these scenarios at an unprecedented level.

Regarding right-handed quarks u_R and d_R, their couplings to gauge bosons are still poorly measured, due to their small coupling to W and Z. For example, one of the best bounds, arising from LEP, are on the Z coupling to b_R which reads $0 \quad g_{b_R}/g_{b_R} \quad 0.2$ [80]. Furthermore these vertices can be protected by symmetries of the BSM sector [32]. The strongest constraints on $_{u_R\, d_R}$ are again coming from Tevatron and, as for the left-handed case, LHC can improve them significantly. Similar conclusions have been recently reached in Ref. [81].

For completeness, we comment on chirality-flip processes that are sensitive to fermion masses. For $m \;\; = Y\, v = 0$, two new types of interactions can be added to Eq. (3.8):

$$\frac{m}{\Lambda^2} F \qquad\qquad + \quad \frac{Y^2}{\Lambda^2} (\quad)^2 \,, \tag{3.10}$$

where and are coe cients of order one. Concerning the first one, Re[ ] and Im[ ] give a contribution to the magnetic and electric dipole moment respectively. Only electric dipole moments give important constraints on BSM sectors, but they can be avoided by demanding CP-invariance in the BSM. Moreover, in most of the BSM they arise at the one-loop level. The second interaction in Eq. (3.10) corresponds to new four-fermion interactions, but suppressed with respect to those of Eq. (3.8) by Yukawa couplings, hence we will not consider them in this work.

Let us also mention that bounds on the interactions Eq. (3.8) can also constrain BSM contributions to the self-energies of the SM gauge bosons. These effects can be parametrized by five quantities $\widehat{S}$, $\widehat{T}$, W, Y and Z [82]. The first two, $\widehat{S}$, $\widehat{T}$, are proportional to v^2/Λ^2 and find their best bound from LEP and Tevatron data. The W and Y parameters, that measure the compositeness of the W , Z and photons, are also bounded by LEP data at the per-mille level, but since these effects grow with the momenta as p^2/Λ^2, we can expect LHC to improve the bounds. Also at the LHC the best bound on the Z-parameter, that measures the compositeness of the gluon, can be obtained.

We then conclude that BSM physics generating four-quark interactions are not severely constrained by the pre-LHC data. Especially interesting BSM scenarios that contribute to this type of interactions are theories of composite quarks, either composite u_R and d_R (and Higgs), composite q_L (if the Higgs is elementary), or composite gluons. Below we will show how dijets at the LHC constrain these scenarios.

3.3 Testing Quark Compositeness at the LHC

The study at the LHC of the angular distributions of dijets in the process $pp \quad jj$ has been shown to be a powerful tool to constrain the size of four-quark contact interactions [68 71]. Here we will follow these analyses to put constraints on all possible four-quark interactions. Out of the complete list of dimension-six operators in D.1.1, only those involving the first family of quarks, up and down, are relevant for our analysis. The reason is the following. In $pp \quad jj$ the dominant contributions at high dijet invariant-mass m_{jj} arise from valence-quarks initial states, *i.e.* , uu, dd, du, being uu or uc initial state processes very suppressed. For example, in the SM we have

$$\left(\frac{(uu \quad uu)}{(uu \quad uu)}\right)_{SM}^{m_{jj}>2\,\mathrm{TeV}} \simeq 0.04\ , \qquad \left(\frac{(uc \quad uc)}{(uu \quad uu)}\right)_{SM}^{m_{jj}>2\,\mathrm{TeV}} \simeq 0.01\,. \tag{3.11}$$

Furthermore, processes with other families in the final states but having u, d in the initial state, such as $uu \quad ss, cc$, do not arise from the four-quark operators of D.1.1 due to the flavor symmetry G_F. We are then led to consider partonic processes involving only first family quarks, $uu \quad uu$, $dd \quad dd$ and $ud \quad ud$, that allow us to reduce the set of operators of Eq. (D.1) to

$$\begin{aligned}
\mathcal{O}_{uu}^{(1)} &= (u_R \quad u_R)(u_R \quad u_R) \\
\mathcal{O}_{dd}^{(1)} &= (d_R \quad d_R)(d_R \quad d_R) \\
\mathcal{O}_{ud}^{(1)} &= (u_R \quad u_R)(d_R \quad d_R) \\
\mathcal{O}_{ud}^{(8)} &= (u_R \quad T^A u_R)(d_R \quad T^A d_R) \\
\mathcal{O}_{qq}^{(1)} &= (q_L \quad q_L)(q_L \quad q_L) \\
\mathcal{O}_{qq}^{(8)} &= (q_L \quad T^A q_L)(q_L \quad T^A q_L) \\
\mathcal{O}_{qu}^{(1)} &= (q_L \quad q_L)(u_R \quad u_R) \\
\mathcal{O}_{qu}^{(8)} &= (q_L \quad T^A q_L)(u_R \quad T^A u_R) \\
\mathcal{O}_{qd}^{(1)} &= (q_L \quad q_L)(d_R \quad d_R) \\
\mathcal{O}_{qd}^{(8)} &= (q_L \quad T^A q_L)(d_R \quad T^A d_R)
\end{aligned} \tag{3.12}$$

where here we do not sum over flavor indices and from now on $q_L = (u_L, d_L)$. Apart from Eq. (3.12), there are other dimension-six operators (see the lists of D.1.2, D.2 and D.3) that can contribute to dijets. Nevertheless, these other operators are either suppressed by v^2/p^2 or Yukawa couplings with respect to those of Eq. (3.12), or can be rewritten, by use of equations of motion, as four-quark operators plus other operators not relevant for dijet physics. Therefore Eq. (3.12) exhausts the list of all leading operators contributing to dijets.

At the partonic level the SM differential cross section of $pp \to jj$ is dominated by QCD interactions [83]:

$$\begin{aligned}
\frac{s^2}{\pi}\frac{d}{dt}(q_iq_i \to q_iq_i)_{SM} &= \frac{4}{9}\frac{s^2+u^2}{t^2} + \frac{4}{9}\frac{s^2+t^2}{u^2} - \frac{8}{27}\frac{s^2}{tu}, \qquad (q_i = u,d)\\
\frac{s^2}{\pi}\frac{d}{dt}(ud \to ud)_{SM} &= \frac{4}{9}\frac{s^2+u^2}{t^2},\\
\frac{s^2}{\pi}\frac{d}{dt}(gq_i \to gq_i)_{SM} &= (s^2+u^2)\left(\frac{1}{t^2} - \frac{4}{9}\frac{1}{su}\right),\\
\frac{s^2}{\pi}\frac{d}{dt}(gg \to gg)_{SM} &= \frac{9}{2}\left(3 - \frac{tu}{s^2} - \frac{su}{t^2} - \frac{st}{u^2}\right),\\
\frac{s^2}{\pi}\frac{d}{dt}(gg \to q_iq_i)_{SM} &= \frac{3}{8}(t^2+u^2)\left(\frac{4}{9}\frac{1}{tu} - \frac{1}{s^2}\right),
\end{aligned} \tag{3.13}$$

where s, t and u are the partonic Mandelstam variables, and we are working in the massless quark limit. Contributions from the operators of Eq. (3.12) give

$$\begin{aligned}
\frac{d}{dt}(q_iq_i \to q_iq_i)_{BSM} &= -\frac{8}{27}\frac{s}{\Lambda^2}\left[A_1^{q_i}\frac{s}{tu} - A_2^{q_i}\left(\frac{u^2}{t}+\frac{t^2}{u}\right)\frac{1}{s^2}\right] + \frac{4}{27\pi\Lambda^4}\left[B_1^{q_i} + B_2^{q_i}\,\frac{u^2+t^2}{s^2}\right],\\
\frac{d}{dt}(ud \to ud)_{BSM} &= \frac{2}{9}\frac{s}{\Lambda^2}\left[A_3\frac{1}{t} + A_4\frac{u^2}{s^2t}\right] + \frac{1}{36\pi\Lambda^4}\left[B_3 + B_4\,\frac{u^2}{s^2}\right],
\end{aligned} \tag{3.14}$$

where

$$\begin{aligned}
A_1^{u\,d} &= \frac{1}{2}c_{qq}^{(8)} + \frac{3}{2}(c_{uu\,dd}^{(1)} + c_{qq}^{(1)}),\\
A_2^{u\,d} &= \frac{3}{4}c_{qu\,qd}^{(8)},\\
A_3 &= \frac{1}{2}(2c_{qq}^{(8)} + c_{ud}^{(8)}),\\
A_4 &= \frac{1}{2}(c_{qu}^{(8)} + c_{qd}^{(8)}),\\
B_1^{u\,d} &= (A_1^{u\,d})^2 + \frac{1}{16}\left[c_{qq}^{(8)} + 3(c_{qq}^{(1)} - c_{uu\,dd}^{(1)})\right]^2,\\
B_2^{u\,d} &= \frac{3}{16}(c_{qu\,qd}^{(8)})^2 + \frac{27}{32}(c_{qu\,qd}^{(1)})^2,\\
B_3 &= A_3^2 + \frac{1}{4}(2c_{qq}^{(8)} - c_{ud}^{(8)})^2 + \frac{9}{8}(2c_{qq}^{(1)} + c_{ud}^{(1)})^2 + \frac{9}{8}(2c_{qq}^{(1)} - c_{ud}^{(1)})^2,\\
B_4 &= A_4^2 + \frac{1}{4}(c_{qu}^{(8)} - c_{qd}^{(8)})^2 + \frac{9}{8}(c_{qu}^{(1)} + c_{qd}^{(1)})^2 + \frac{9}{8}(c_{qu}^{(1)} - c_{qd}^{(1)})^2,
\end{aligned} \tag{3.15}$$

being the coe cients c_i defined according to Eq. (3.5). This extends the results of [84]. It is important to remark that in Eq. (3.14) we have included terms of

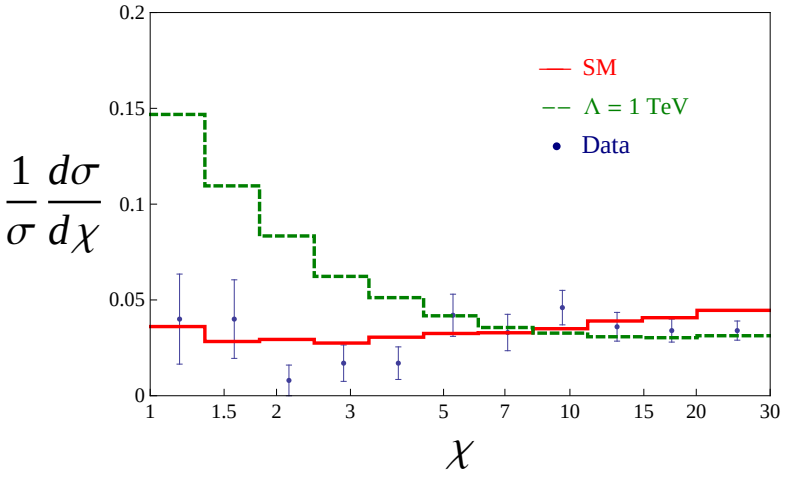

Figure 3.2: Dijet di erential cross section as a function of for $m_{jj} > 2$ TeV at the LHC with $\sqrt{s} = 7$ TeV. The QCD contribution is shown in solid red line, while the green dashed line includes the contribution from the operator $\mathcal{O}_{qq}^{(8)}$ with $c_{qq}^{(8)} = -0.5$ and $\Lambda = 1$ TeV.

order c_i^2/Λ^4; for $c_i \gg 1$ these terms are enhanced by an extra c_i factor with respect to the interference terms (of order c_i/Λ^2), compensating for the s/Λ^2 suppression factor. Therefore they should be considered in the calculations. Contributions from operators of dimension eight or larger are always smaller. For example, dimension-eight operators contributing to dijets involve at most four-fermions and extra derivatives, e.g. , and therefore their coe cients in front are not parametrically larger than those of dimension-six four-quark operators. They are then always suppressed by an extra $\sim s/\Lambda^2$.

As compared to the SM contribution Eq. (3.13), the BSM contribution Eq. (3.14) is enhanced at large s and large CM scattering angle , or equivalently, for large (negative) $t = -s(1 - \cos)/2$. It is convenient to define the angular variable $= (1 + \cos)/(1 - \cos) = -(1 + s/t)$ $[1, +)$ that can also be written as $= e^{y_1 - y_2}$ where $y_{1\,2}$ are the rapidity of the two jets. The QCD contribution to the differential cross section $d (pp jj)/d$ is almost flat in , while that of BSM grows for small values of , as can be appreciated in Fig. 3.2.

3.3.1 The F parameter

To put bounds on BSM four-quark operators, we will follow the method used by the ATLAS collaboration [68, 69]. This is based on the variable F defined as the quotient of events with $1 < < {}_c$ 3.32, the central region in the detector, over

those with $1 < \quad < \quad_{max} \quad 30$:

$$F^{m_{jj}^{cut}} = \frac{N(\quad < \quad_c, m_{jj} > m_{jj}^{cut})}{N(\quad < \quad_{max}, m_{jj} > m_{jj}^{cut})}\,, \tag{3.16}$$

where m_{jj}^{cut} is the cut over the invariant mass of the two-jet pair. Many systematic effects cancel in this ratio, providing an optimal test of QCD and a sensitive probe of hard new physics. It is also useful to write the analytic expression for this observable. Defining the integrated differential cross section over the angular region from 1 to $\quad_0$ as

$$\int_1^{\quad_0} d\quad \frac{d\quad}{d\quad}\bigg|_{pp\quad jj}^{m_{jj}^{cut}}\,, \tag{3.17}$$

we have

$$F^{m_{jj}^{cut}} = \frac{(\quad_c^{m_{jj}^{cut}})}{(\quad_{max}^{m_{jj}^{cut}})} \simeq \frac{(\quad_c^{m_{jj}^{cut}})_{SM} + (\quad_c^{m_{jj}^{cut}})_{BSM}}{(\quad_{max}^{m_{jj}^{cut}})_{SM}}\,, \tag{3.18}$$

where we have split the contribution of the SM from that of the BSM, and considered that the SM contribution, being almost flat, dominates in the denominator. By making this approximation the deviation from the exact value of F is of order 10%. Using Eqs. (3.13) and (3.14), and performing the integration over , we obtain the result

$$F^{m_{jj}^{cut}} \simeq (F^{m_{jj}^{cut}})_{SM} - \frac{1}{\Lambda^2} A \quad \mathcal{P} + \frac{1}{\Lambda^4} B \quad \mathcal{Q}\,, \tag{3.19}$$

where

$$\begin{aligned} A &= (A_1^u, A_2^u, A_1^d, A_2^d, A_3, A_4)\,, \\ B &= (B_1^u, B_2^u, B_1^d, B_2^d, B_3, B_4)\,, \end{aligned} \tag{3.20}$$

and

$$\begin{aligned} \mathcal{P} &\simeq (0.36P_{uu}, 0.12P_{uu}, 0.36P_{dd}, 0.12P_{dd}, 0.17P_{ud}, 0.074P_{ud})\,\text{TeV}^2\,, \\ \mathcal{Q} &\simeq (0.013Q_{uu}, 0.0069Q_{uu}, 0.013Q_{dd}, 0.0069Q_{dd}, 0.0024Q_{ud}, 0.00097Q_{ud})\,\text{TeV}^4\,, \end{aligned}$$

where $(F^{m_{jj}^{cut}})_{SM}$ is the SM value of $F^{m_{jj}^{cut}}$ and the coe cients $P_{q_iq_j}$ and $Q_{q_iq_j}$ encode the integration over the parton distribution functions (PDF):

$$P_{q_iq_j} = \frac{1}{(\quad_{max}^{m_{jj}^{cut}})_{SM}} \int d\quad \int dx\, f_{q_i}(x) f_{q_j}(\quad/x) \frac{\quad_s(\quad s)}{x} + (i \quad j \text{ for } i = j)\,, \tag{3.21}$$

$$Q_{q_iq_j} = \frac{1}{(\quad_{max}^{m_{jj}^{cut}})_{SM}} \int d\quad \int dx\, f_{q_i}(x) f_{q_j}(\quad/x) \frac{s}{x} + (i \quad j \text{ for } i = j)\,, \tag{3.22}$$

where $s =$ s is the center of mass energy of the partons $q_i q_j$ that initiate the collision, with $\overline{s} = 7$ TeV the center of mass energy of the colliding protons. To calculate these coe cients we use MadGraph/MadEvent 4.4.57 [85] and implement the cuts taken in [69]. For this analysis we use the CTEQ6L1 PDF set and fix both the renormalization and factorization scales to $m_{jj}^{cut} = 2\,\text{TeV}$. We obtain:

$$\begin{aligned} &P_{uu} \simeq 0.23\,\text{TeV}^2\ , \quad P_{dd} \simeq 0.038\,\text{TeV}^2\ , \quad P_{ud} \simeq 0.28\,\text{TeV}^2\,, \\ &Q_{uu} \simeq 23\,\text{TeV}^4\ , \quad Q_{dd} \simeq 3.8\,\text{TeV}^4\ , \quad Q_{ud} \simeq 19\,\text{TeV}^4\,, \end{aligned} \tag{3.23}$$

and $(F^{2\,\text{TeV}})_{SM} \simeq 0.067$, $(\ ^{2\,\text{TeV}}_{max})_{SM} \simeq 0.016\,\text{TeV}^{-2}$. We have checked the consistency of these results by numerically integrating over the MSTW2008 PDFs [86] using our analytical formulae for the cross sections Eqs. (3.13) and (3.14) and implemeting the cuts in [69], which translate into the integration limits x $[\ \ ^{-}e^{-y_B^{cut}}, 1]$, $[(m_{jj}^{cut})^2/s, e^{-2y_B^{cut}}]$ and x $[\ , 1]$, $[e^{-2y_B^{cut}}, 1]$, where $y_B^{cut} = 1.1$ is the cut on the rapidity boost of the partonic center of mass, $y_B\ = \frac{1}{2}\ y_1 + y_2$ y_B^{cut}. The variation of renormalization and factorization scales (by twice and half) introduces a theoretical uncertainty of the order of $10 - 15\%$. We have not computed the errors arising from the PDFs, and have not taken into account hadronization or showering effects since it is reasonable to neglect them for high dijet invariant masses [87].

3.4 Bounds

ATLAS has reported angular distributions of dijets for several m_{jj} [69]. We are interested in those with the largest invariant masses that correspond to $m_{jj} >$ 2 TeV and are given in Fig. 3.2. Using this data and Eq. (3.16), we obtain $F^{2\,\text{TeV}} =$ 0.053 0.015, and therefore the 95% CL bound

$$0.023 < F^{2\,\text{TeV}} < 0.083\,. \tag{3.24}$$

Using this value and the prediction Eq. (3.19) one can obtain bounds on the scales suppressing the operators Eq. (3.12). We instead derive the bounds using the coe cients of Eq. (3.23) but without making any approximation on the denominator of Eq. (3.18). The results are shown in Table 3.1. Few comments are in order. These bounds are obtained by taking the coe cient in front of the corresponding operator to be $c_i =$ 1. For other values we must rescale the bound by a factor $\sqrt{c_i}$. Since we are working in the approximation in which the energy of the physical process is assumed to be smaller than the masses of the BSM states Λ, we must require $\Lambda > m_{jj}^{cut}$. This implies that our bounds can only strictly be applied if $c_i\ > (2\ \text{TeV}/\Lambda\ )^2$. We recall that large values of c_i are in principle

Operator	Λ_-(TeV)	Λ_+(TeV)
$\mathcal{O}^{(1)}_{uu}$	3.2	2.1
$\mathcal{O}^{(1)}_{dd}$	1.8	1.5
$\mathcal{O}^{(1)}_{ud}$	1.5	1.5
$\mathcal{O}^{(8)}_{ud}$	1.3	0.8
$\mathcal{O}^{(1)}_{qq}$	3.5	2.4
$\mathcal{O}^{(8)}_{qq}$	2.5	1.3
$\mathcal{O}^{(1)}_{qu}$	1.7	1.7
$\mathcal{O}^{(8)}_{qu}$	1.4	1.0
$\mathcal{O}^{(1)}_{qd}$	1.3	1.3
$\mathcal{O}^{(8)}_{qd}$	1.0	0.8

Table 3.1: Bounds at 95% CL on the scale suppressing the four-quark interactions. We denote by $\Lambda_\pm$ the bound on this scale obtained when taking the coe cient in front of the operator $c_i = \ 1$, and considering the e ects of the operators one by one.

possible since $c_i \quad 16\pi^2$. Also, we notice that for $c_i < 0$ the interference between the BSM contribution and the QCD contribution is constructive (with the exception of $\mathcal{O}^{(1)}_{ud\,qu\,qd}$ where the interference is null), and as a consequence the bound is stronger than for a positive c_i.

These bounds are subject to a set of theoretical errors. The uncertainty in the parameters Eq. (3.23) estimated by changing the factorization and renormalization scales results in a $\sim 5\%$ uncertainty in the bounds. Also the NLO QCD correction to $(F^{2\,\mathrm{TeV}})_{BSM}/(F^{2\,\mathrm{TeV}})_{SM}$ has shown to be as large as $\sim 30\%$ [88], what amounts to a $\sim 10\%$ uncertainty in the bounds on Λ. Finally, it has been recently shown in [89] that electroweak corrections reduce the SM prediction of F by a $\sim 2\%$ for large invariant masses $m_{jj} \sim 2\,\mathrm{TeV}$. We therefore expect that our calculations for the bounds on Λ can be trusted within a $\sim 10\%$ margin of error.

3.4.1 Bounds on composite quarks

As we mentioned in section 3.2, previous experiments have not been able to probe the compositeness of quarks beyond the TeV scale. Data from dijets at the LHC can however improve this situation and put stronger constraints on their compositeness scale.

We will focus on models in which quarks arise as composite states of a strong sector whose global symmetry is $\mathcal{G} \quad SU(3)_c \quad SU(2)_L \quad U(1)_Y \quad G_F$, where G_F is given in Eq. (3.9). In these theories we expect to have massive vector resonances

Composite	$c_{uu}^{(1)}/g^2$	$c_{dd}^{(1)}/g^2$	$c_{ud}^{(1)}/g^2$	$c_{ud}^{(8)}/g^2$	$c_{qq}^{(1)}/g^2$	$c_{qq}^{(8)}/g^2$	$c_{qu}^{(1)}/g^2$	$c_{qu}^{(8)}/g^2$	$c_{qd}^{(1)}/g^2$	$c_{qd}^{(8)}/g^2$
u_R	$-37/72$	0	0	0	0	0	0	0	0	0
d_R	0	$-7/18$	0	0	0	0	0	0	0	0
u_R, d_R	$-37/72$	$-7/18$	$2/9$	-1	0	0	0	0	0	0
q_L	0	0	0	0	$-5/36$	-1	0	0	0	0
q_L, u_R	$-37/72$	0	0	0	$-5/36$	-1	$-1/9$	-1	0	0
q_L, d_R	0	$-7/18$	0	0	$-5/36$	-1	0	0	$1/18$	-1
q_L, u_R, d_R	$-37/72$	$-7/18$	$2/9$	-1	$-5/36$	-1	$-1/9$	-1	$1/18$	-1

Table 3.2: Coe cients of the operators of Eq. (3.12) induced from integrating out heavy vector resonances for di erent composite quark scenarios. We have taken $\Lambda = m$.

Composite States	f (TeV)
d_R	1.1
u_R	2.3
u_R, d_R	2.6
q_L	2.7
q_L, d_R	2.9
q_L, u_R	3.5
q_L, u_R, d_R	3.8

Table 3.3: 95% CL bounds on the scale $f = m \quad g$ for di erent composite quark scenarios.

associated to the current operators of $\mathcal{G}$, and then transforming in the adjoint representation of $\mathcal{G}$. This is in fact the case of the five-dimensional analogs based on the AdS/CFT correspondence [29]. Following Ref. [73], we will assume that all the vector resonances have equal masses and couplings, m and g respectively. Let us first consider the case in which only the right-handed up-type quarks u_R are composite states, with charges under the global group $\mathcal{G}$ equal to $(\mathbf{3}, \mathbf{1}, \mathbf{2}/\mathbf{3}, \mathbf{1}, \mathbf{1}, \mathbf{2})$. In this type of models, as we said before, the Higgs could also be composite without affecting our conclusions. Now, integrating out the heavy vector resonances at tree level (an approximation valid in the large-N limit or, equivalently, $g \quad 4\pi$), we find that the four-quark operators of Eq. (3.12) are induced with coe cients given in Table 3.2, where we have fixed $\Lambda = m$. Constraints from dijets give $f \quad m/g \quad 2$ TeV. For $g \gg 1$, we see that this bound is stronger than that coming from the S-parameter that requires $f \quad 4\pi v/g$ in theories of composite Higgs [73].

Similarly, we can assume a scenario where only the right-handed down-type quarks d_R are composite with quantum numbers under $\mathcal{G}$ equal to $(\mathbf{3}, \mathbf{1}, -\mathbf{1}/\mathbf{3}, \mathbf{1}, \mathbf{3}, \mathbf{1})$.

Again the coe cients of the four-quark operators induced are given in Table 3.2. We obtain the bound f 1 TeV. In the case of both u_R and d_R composite the bound goes up to f 2.5 TeV.

For composite left-handed quarks q_L with $\mathcal{G}$-charges $(\mathbf{3},\mathbf{2},\mathbf{1/6},\mathbf{3},\mathbf{1},\mathbf{1})$, the bound is f 3 TeV. Bounds on other composite quark scenarios are given in Table 3.3.

For weakly-coupled resonances (g 1) with masses close to m_{jj}^{cut} stronger bounds can be obtained from dijet resonance searches at the LHC [81]. This is just a consequence of the resonant enhancement of the cross section for a narrow region of invariant masses, where the resonances sit. This feature however is lost when the resonances are too broad.

3.4.2 Bounds on heavy gauge bosons

Heavy gauge bosons at the TeV-scale coupled to first family quarks generate four-quark operators that can be constrained by the dijet LHC data. Here we provide some examples. For a gauge boson Z gauging baryon number or hypercharge we obtain respectively

$$\frac{M_{Z'_B}}{g_B} \quad 1.2\,\text{TeV}\,, \qquad \frac{M_{Z'_Y}}{g_Y} \quad 1.6\,\text{TeV}\,, \tag{3.25}$$

while for the gauge bosons W of a $SU(2)_R$ symmetry, where $q_R = (u_R, d_R)$ is assumed to transform as a doublet, we get

$$\frac{M_{W'}}{g_R} \quad 1.6\,\text{TeV}\,. \tag{3.26}$$

As mentioned before, the fact that we work within an effective theory Eq. (3.5), implies that our bounds only apply to resonances with masses above $m_{jj}^{cut} = 2$ TeV. Gluonic resonances G^A coupled to first family quarks as

$$\mathcal{L}_{int} = G^A \left[g_L \bar{q}_L T^A \quad q_L + g_R \bar{q}_R T^A \quad q_R \right] , \tag{3.27}$$

with $T_A = \ _A/2$ where $\ _A$ are the Gell-Mann matrices, can also be constrained. This kind of resonances have been recently advocated (see for example Ref. [90]) to accommodate the discrepancy in the top forward-backward asymmetry measured at Tevatron. In Fig. 3.3 we show the excluded region of the parameter space. It can be seen that, for a resonance of mass $M_{G'} = 2.5$ TeV, the allowed range for the couplings is -1.5 $g_{L\,R}$ 1.5 at 95% CL. Similar bounds have been also obtained in Ref. [91].

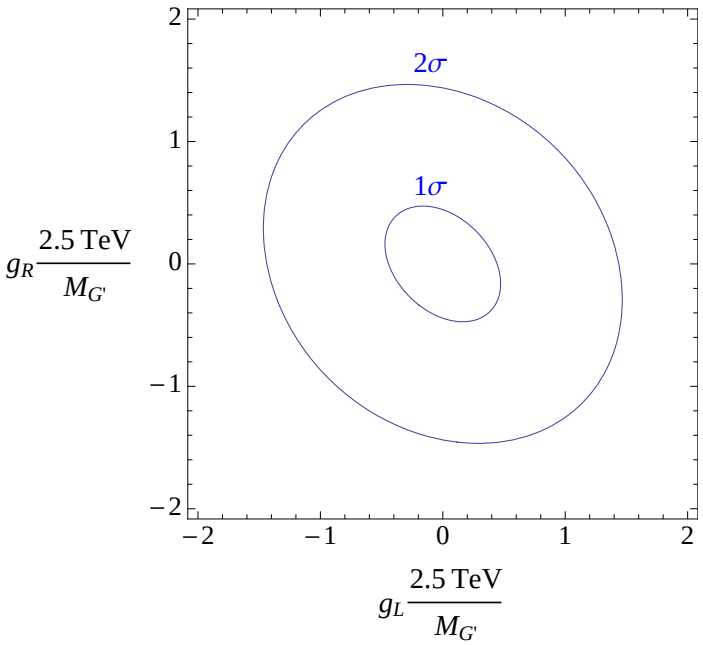

Figure 3.3: Excluded region in the $g_L - g_R$ plane by the $m_{jj} > 2$ TeV dijet analysis.

3.4.3 Bounds on oblique parameters Y, W and Z

The electroweak precision parameters Y, W and Z [82] can be regarded as a measure of the compositeness of the transversal components of the $SU(2)_L$, $U(1)_Y$, and $SU(3)_c$ gauge bosons respectively. They manifest themselves as deviations of the self-energies of such vector bosons, and can be parametrized by the following higher dimensional operators:

$$\frac{-Y}{4m_W^2}(\quad B\quad)^2, \quad \frac{-W}{4m_W^2}(D\ W^I\ )^2, \quad \frac{-Z}{4m_W^2}(D\ G^A\ )^2\,. \tag{3.28}$$

At large momenta as compared to the masses of the gauge bosons, these operators induce effective four-fermion operators, equivalent to those arising from integrating out a very heavy copy of the corresponding gauge boson. Therefore our dijet analysis can be conveniently used to put bounds on these parameters. We show in Fig. 3.4 our results in the W-Y plane. Although bounds from LEP [82] are still stronger, this analysis shows that LHC will be competitive when running at a higher energy. Regarding the Z-parameter our analysis gives the strongest bound up to date:

$$-3\quad 10^{-3}\quad Z\quad 6\quad 10^{-4}. \tag{3.29}$$

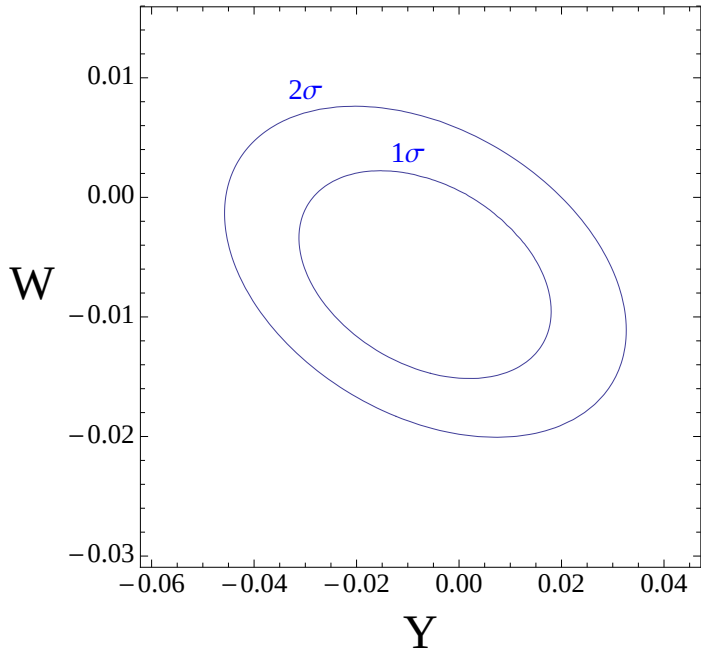

Figure 3.4: Excluded region in the W-Y plane by the $m_{jj} > 2$ TeV ATLAS dijet analysis.

3.4.4 Bounds on new interactions for the A_{FB} of the top

The recent discrepancy between the measured A_{FB} of the top and its SM prediction [76, 77] has boosted the search for BSM that could explain it. Dijet angular distributions can be useful to constrain these models. As an example, we consider the proposal of Refs. [92, 93] where the measured value of the top asymmetry was explained by the following new interaction:

$$\mathcal{L}_{eff} = \frac{c_A^{(8)}}{\Lambda^2}\mathcal{O}_A^{(8)} = \frac{c_A^{(8)}}{\Lambda^2}(u\,T^A \quad {}^5u)(t\,T^A \quad {}^5t)\,. \tag{3.30}$$

In terms of chirality eigenstates the operator $\mathcal{O}_A^{(8)}$ reads

$$\begin{aligned}\mathcal{O}_A^{(8)} =&(u_R \quad T^A u_R)(t_R \quad T^A t_R) - (u_L \quad T^A u_L)(t_R \quad T^A t_R)\\ &- (u_R \quad T^A u_R)(t_L \quad T^A t_L) + (u_L \quad T^A u_L)(t_L \quad T^A t_L)\,.\end{aligned} \tag{3.31}$$

If these operators arise from BSM that are invariant under the SM gauge group and G_F (up to small effects v^2/Λ^2 and Yukawa couplings), the presence of $c_A^{(8)} = 0$ requires, in the basis D.1.1,

$$c_{ut}^{(8)} = -c_{qt}^{(8)} = -c_{qu}^{(8)} = c_{qq}^{(8)} = c_A^{(8)}\,. \tag{3.32}$$

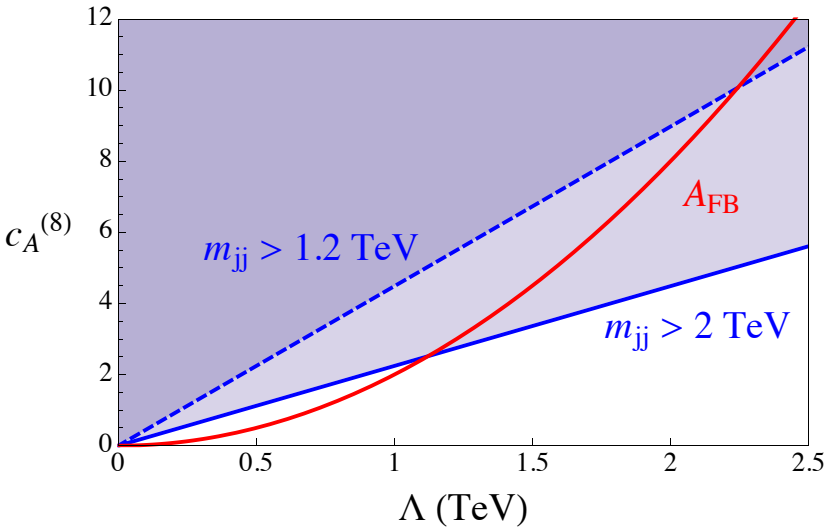

Figure 3.5: The red line shows the value of $c_A^{(8)}$ as a function of Λ that fits the A_{FB} of the top [93]. The shaded regions delimited by the solid and dashed blue lines show the excluded region due to our dijet angular distribution analysis with cuts $m_{jj}^{cut} = 2\,\text{TeV}$ and $m_{jj}^{cut} = 1.2\,\text{TeV}$ respectively.

In other words, the flavor symmetry requires that if the operator $\mathcal{O}_A^{(8)}$ is generated, also operators involving four up-quarks must be present. Bounds from our dijet analysis (mostly from the bounds on $c_{qu}^{(8)}$ and $c_{qq}^{(8)}$) lead then to

$$\frac{c_A^{(8)}}{\Lambda^2} \lesssim \frac{0.4}{\text{TeV}^2}\,, \tag{3.33}$$

excluding the possibility to fit the recent top asymmetry measurement which requires $c_A^{(8)}/\Lambda^2 \sim 2\ \text{TeV}^{-2}$ [93].

If we relax the assumption of flavor invariance of the BSM sector, an operator involving four up-quarks can still be generated from $\mathcal{O}_A^{(8)}$ at the one-loop level. The one-loop contribution, involving tops, is divergent and therefore sensitive to physics at the BSM scale Λ. We can get an estimate by regulating the divergence with a hard cut-off taken to be Λ. We obtain

$$c_{qq}^{(8)} = \frac{1}{3} c_{uu}^{(8)} = -2 c_{qu}^{(8)} \simeq -\frac{(c_A^{(8)})^2}{4\pi^2}\,. \tag{3.34}$$

In Fig. 3.5 we show the region of the parameter space that fits the A_{FB} of the top with the region excluded by dijets using Eq. (3.34). One can see that dijets with $m_{jj} > 2$ TeV exclude a large region of the parameter space, although, as we mentioned before, these results cannot be strictly applied if $\Lambda < m_{jj}$. For this reason we also show the exclusion region arising from dijets with smaller invariant masses, $m_{jj} > 1.2$ TeV.

3.5 Conclusions

We have shown that the present dijet LHC data is already testing all the quark sector of the SM at almost the same level of accuracy as leptons were tested at LEP after a decade of data collection. This is due to the very high-energy of the dijet scattering at the LHC that enhances the effects from four-quark interactions. We have used the F parameter, defined in Eq. (3.16), to put bounds on all possible four-quark operators. Our results, presented in Table 3.1, show bounds on the scales suppressing these operators $\Lambda/\sqrt{c_i}$ ranging between $1 - 3$ TeV.

Among the most interesting BSM scenarios to be tested by dijet angular distributions are theories in which strong dynamics are postulated to solve the hierarchy problem. These theories demand a composite scale Λ around the TeV-scale. We have seen that if the SM quarks are composite states arising from a new strong sector, Λ 50 TeV $(g\ /4\pi)$. Other possibilities are also significantly constrained, as can be seen from Table 3.3. We also derive the best bounds on the Z-parameter, Eq. (3.29), that measures the degree of compositeness of the gluons.

We also show that extra gauge bosons with sizable couplings to quarks are constrained to lie above the TeV scale, limiting then their possible contribution to the A_{FB} of the top.

Finally, we would like to stress that these results are based on the 2010 LHC data corresponding to 36 pb^{-1} of integrated luminosity [69]. It is expected that the 2011 LHC data set, containing more luminosity, will significantly improve all the bounds derived throughout this analysis.

Appendix A

The Effective Action for the Pion

In this appendix we will compute the effective action for the pion at $\mathcal{O}(p^4)$. Given that a complete treatment of the $U(1)_A$ anomaly is not included in the model, in the following we will neglect the Goldstone boson related to this symmetry, namely the field, and we will only consider a model with a chiral symmetry $SU(2)_L \quad SU(2)_R$.

An e cient way to perform the computation is to use the holographic approach presented in [42]. At tree-level, the holographic action for the pion is given by the 5d action for the gauge and the scalar fields (eqs. (2.22) and (2.25)), where the 5d fields satisfy the bulk EOM's with the usual IR boundary conditions given in eqs. (2.28) and (2.29). The UV conditions are modified as

$$\begin{cases} L \quad_{z_{\rm UV}} = U(x)(l \ + i \quad)U(x) \\ R \quad_{z_{\rm UV}} = r \\ \quad_{z_{\rm UV}} = U(x)\left(\frac{z_{\rm UV}}{z_{\rm IR}}\right) \ ^{-} M_q \mathbb{1} \end{cases} , \tag{A.1}$$

where $U(x)$ represents the 4d Goldstone matrix, which transforms as

$$U(x) \qquad g_R U(x) g_L \tag{A.2}$$

under a chiral $SU(2)_L \quad SU(2)_R$ 4d transformation. Notice that we are not interested in possible terms involving the scalar and pseudoscalar sources, so we did not include any source term in the UV condition for the scalar field in eq. (A.1).

To derive the complete effective action for the pion one would need to solve the full bulk EOM for the 5d fields. However, due to the presence of interaction terms, this can be done only perturbatively. As usually done in **PT**, we use an expansion in powers of the momentum p and we treat the external sources l and r as $\mathcal{O}(p)$ terms, while M_q will be treated as an $\mathcal{O}(p^2)$ term.

We expand the solutions of the EOM using a mixed momentum space representation

$$\begin{cases} V &= f_V^0(z)\widehat{V}\ (p) + V^{(3)}(p,z,\widehat{V},\widehat{A},U,M_q)\,, \\ A &= f_A^0(z)\widehat{A}\ (p) + A^{(3)}(p,z,\widehat{V},\widehat{A},U,M_q)\,, \\ &= \ {}^{(0)}(z) + \ {}^{(2)}(p,z,\widehat{V},\widehat{A},U,M_q) + \ {}^{(4)}(p,z,\widehat{V},\widehat{A},U,M_q)\,, \end{cases} \tag{A.3}$$

where we denoted by $\widehat{V}$ and $\widehat{A}$ the values of the vector and axial gauge fields at the UV boundary. Notice that, due to the tensorial structure, the gauge field solutions start at $\mathcal{O}(p)$ and their next to leading terms are of $\mathcal{O}(p^3)$, while the scalar field can be expanded in terms of $\mathcal{O}(p^{2n})$. All the terms in the expansion of the gauge fields satisfy the same IR boundary conditions as the original fields:

$$\begin{cases} \ {}_zV\ (x,z_{\rm IR}) = 0\,, \\ A\ \ (x,z_{\rm IR}) = 0\,. \end{cases} \tag{A.4}$$

Instead, for the scalar field we have

$$\begin{cases} \ {}^{(0)}(x,z_{\rm IR}) = \ \ \mathbb{1}\,, \\ \ {}^{(i)}(x,z_{\rm IR}) = 0 \qquad \text{for } i \quad 2\,. \end{cases} \tag{A.5}$$

The UV boundary conditions for the gauge fields are chosen so that the higher terms in the expansion vanish, while for the leading terms we have

$$f_{V\,A}^0(z_{\rm UV}) = 1\,. \tag{A.6}$$

For the scalar field we impose

$$\begin{cases} \ {}^{(0)}(z_{\rm UV}) = 0\,, \\ \ {}^{(2)}(z_{\rm UV}) = U\left(\dfrac{z_{\rm UV}}{z_{\rm IR}}\right)^{-} M_q\mathbb{1}\,, \\ \ {}^{(4)}(z_{\rm UV}) = 0 \qquad \text{for } i \quad 4\,. \end{cases} \tag{A.7}$$

By using the bulk EOM's and the boundary conditions for the fields, one can verify that the terms of $\mathcal{O}(p^3)$ in the expansion for the gauge fields and the ones of order $\mathcal{O}(p^4)$ in the expansion for the scalar field do not contribute to the effective action for the pion at $\mathcal{O}(p^4)$ (see the discussion in [42]).

As a first step of the derivation of the effective action, we will consider the contributions coming from the 5d gauge action in eq. (2.22). It is convenient to rewrite eq. (2.22) in the form

$$\begin{aligned} S_g \ &= \ -2M_5\int_{UV} d^4x\ a(z_{\rm UV})\,{\rm Tr}\,[V\ \ {}_zV\ \ + A\ \ {}_zA\ ] \\ &\quad -M_5\int d^4x\ \int dz a(z)\,{\rm Tr}\,[L\ \ L\ \ + R\ \ R\ \ ]\,. \end{aligned} \tag{A.8}$$

The leading terms in the expansion of the 5d fields satisfy the equations

$$\begin{cases} {}_z\left(a(z)\ {}_z f_V^0(z)\right) = 0\,, \\ {}_z\left(a(z)\ {}_z f_A^0(z)\right) - 2a^3(z)(\ {}^{(0)})^2 f_A^0(z) = 0\,, \\ {}_z\left(a^3(z)\ {}_z\ {}^{(0)}(z)\right) - a^5(z)M^2\ {}^{(0)}(z) = 0\,. \end{cases} \tag{A.9}$$

The solution for the ${}^{(0)}$ field can be obtained from eqs. (2.31) and (2.32) by setting $M_q = 0$. The equation for the vector gauge field admits the simple solution $f_V^0(z) = 1$, while the equation for f_A^0 in general can not be solved analytically.

By substituting the above expressions in the gauge action and using the relation

$$\widehat{A}\ = \frac{i}{2} U\,(D\ U)\ = -\frac{i}{2}\,(D\ U)\,U \qquad u\ , \tag{A.10}$$

we find that the first line in eq. (A.8) gives the kinetic term for the pion, from which we can extract the pion decay constant

$$f^2 = -2M_5 a(z)\ {}_z f_A^0(z)\Big|_{z=z_{\rm UV}}\ . \tag{A.11}$$

From the second line in eq. (A.8) we get contributions to the $\mathcal{O}(p^4)$ terms in the pion effective Lagrangian. In the standard form of **PT** [47] we get the following contributions

$$\begin{cases} L_1^{(g)} = \dfrac{M_5}{16}\displaystyle\int dz\, a(z)\left(1-(f_A^0)^2\right)^2 \\ L_{10}^{(g)} = -\dfrac{M_5}{2}\displaystyle\int dz\, a(z)\left(1-(f_A^0)^2\right) \end{cases}\ , \qquad \begin{cases} L_2^{(g)} = 2L_1^{(g)} \\ L_3^{(g)} = -6L_1^{(g)} \\ L_9^{(g)} = -L_{10}^{(g)} \end{cases}\ . \tag{A.12}$$

Now we consider the contributions to the effective action coming from the scalar action in eq. (2.25). To derive the action we need to compute the ${}^{(2)}$ term in the expansion of the 5d scalar field. This term satisfies the bulk EOM

$$-\frac{1}{a^3(z)}\ {}_z\left(a^3(z)\ {}_z\ {}^{(2)}\right) + a^2(z)M^2\ {}^{(2)} = -2\ {}^{(0)}\left[-2(f_A^0)^2 u\ u\ - i f_A^0 D\ u\ \right]\,, \tag{A.13}$$

where we defined $D\ u \qquad u\ - i[\widehat{V}\,, u\ ]$. The solution can be split into two parts:

$${}^{(2)} = \ {}^{(2)}_{M} + \ {}^{(2)}_{0}\,, \tag{A.14}$$

where ${}^{(2)}_{M}$ is a solution of the homogeneous part of eq. (A.13) with boundary conditions

$${}^{(2)}_{M}(z_{\rm UV}) = U\left(\frac{z_{\rm UV}}{z_{\rm IR}}\right)^{-} M_q \mathbb{1}\,, \qquad {}^{(2)}_{M}(z_{\rm IR}) = 0\,, \tag{A.15}$$

while $\overset{(2)}{0}$ satisfies eq. (A.13) with boundary conditions

$$\overset{(2)}{0}(z_{\rm UV}) = \overset{(2)}{0}(z_{\rm IR}) = 0\,. \tag{A.16}$$

The solution for $\overset{(0)}{M}$ is simply given by eqs. (2.31) and (2.32) with the choice $= 0$. The solution for $\overset{(0)}{0}$ can not be found analytically, and we will parametrize it as

$$\overset{(0)}{0} = f_R^{(2)}(z)u\ u\ + f_I^{(2)}(z)D\ u\ . \tag{A.17}$$

From the action for the scalar field we get an $\mathcal{O}(p^2)$ contribution to the pion effective action, which can be written as

$$S^{(2)} = M_5 \int_{UV} d^4x\, a^3(z) {\rm Tr}\left[\ \overset{(2)}{M}\ \ _z\ \ \overset{(0)}{} + {\rm h.c.}\right]. \tag{A.18}$$

To obtain this expression we integrated by parts the terms containing derivatives with respect to z and we used the bulk EOM and the boundary conditions for the terms in the scalar field expansion. Eq. (A.18) corresponds to a mass term for the pion, which in the limit $z_{\rm UV}$ 0 becomes

$$S^{(2)} = 2\frac{M_5}{L} \int d^4x\, {\rm Tr}\left[U M_q + M_q U\ \right]. \tag{A.19}$$

The expression for the pion mass and for the pion decay constant can be easily computed as an expansion in the parameter . Some approximate expressions are reported in eq. (2.50).

Computing the $\mathcal{O}(p^4)$ terms in the action we get

$$\begin{aligned} S^{(4)} \ = \ & M_5 \int d^4x \int dz\, a^3(z) \Big\{ 2{\rm Tr}\left[\ \overset{(0)}{} f_I^{(2)}(z) f_A^0(z) D\ u\ D\ u\ \right] \\ & + 4{\rm Tr}\left[\ \overset{(0)}{} f_R^{(2)}(z)(f_A^0(z))^2 u\ u\ u\ u\ \right] \\ & + i{\rm Tr}\left[\ \overset{(0)}{}\left(\ \overset{(2)}{M}\ -\ \overset{(2)}{M}\right) f_A^0(z) D\ u\ \right] \\ & + 2{\rm Tr}\left[\ \overset{(0)}{}\left(\ \overset{(2)}{M}\ +\ \overset{(2)}{M}\right)(f_A^0(z))^2 u\ u\ \right] \Big\} \\ & + \frac{M_5}{2} \int_{UV} d^4x\, a^3(z) {\rm Tr}\left[\ _z(f_R^{(2)}(z)u\ u\ - i f_I^{(2)}(z) D\ u\ )\ \overset{(2)}{M} + {\rm h.c.}\right] \end{aligned} \tag{A.20}$$

The $\mathcal{O}(p^4)$ action for the pion can be simplified by using the EOM for the pion field coming from the $\mathcal{O}(p^2)$ effective action. Using the standard notation of **PT** [47], the kinetic and mass terms for the pion are written as

$$\mathcal{L} = \frac{f^2}{4}\left\{ {\rm Tr}\left[(D\ U)\ D\ U\right] + {\rm Tr}\left(\ \ U + \ \ U\ \right)\right\}. \tag{A.21}$$

From this Lagrangian we get the EOM for U:

$$(D\ D\ U)U\ -U(D\ D\ U)\ +U\quad -\quad U\ =0\,, \tag{A.22}$$

which can be rewritten as

$$4iD\ u\ =\ U\ -U\quad . \tag{A.23}$$

Moreover, by comparing eq. (A.21) and eq. (A.19), we can extract the relation between M_q and , which, in the $z_{\rm UV}$ 0, limit reads

$$M_q = \frac{L}{M_5}\frac{f^2}{8}\quad . \tag{A.24}$$

By using these relations we get the scalar contributions to the coe cients of the $\mathcal{O}(p^4)$ effective pion action

$$\begin{cases} L_3^{(\ )} = \dfrac{M_5}{8}\displaystyle\int dz\ a^3(z)\mathrm{Tr}\left(\ \ ^{(0)}\right) f_R^{(2)}(z)(f_a^0(z))^2\,, \\ L_5^{(\ )} = \dfrac{M_5}{8}\left\{a^3(z)f_M^{(2)}(z)\ \ {}_z f_R^{(2)}(z)\Big|_{z_{\rm UV}} + 2\displaystyle\int dz\ a^3(z)f_M^{(2)}(z)(f_a^0(z))^2\mathrm{Tr}\left(\ \ ^{(0)}\right)\right\}\,, \\ L_8^{(\ )} = \dfrac{M_5}{16}\left\{2\ \ a^3(z)f_M^{(2)}(z)\ \ {}_z f_I^{(2)}(z)\Big|_{z_{\rm UV}} - \displaystyle\int dz\ a^3(z)f_a^0(z)(f_I^{(2)}(z) - 2\ \ f_M^{(2)}(z))\mathrm{Tr}\left(\ \ ^{(0)}\right)\right\}\,, \end{cases} \tag{A.25}$$

where is defined by the relation $M_q =$.

Appendix B

The Equations of Motion

In this appendix we report the EOM for the 2d fields which appear in the ansatz for the zero-mode soliton fluctuations in eqs. (2.53), (2.70) and (2.72), and we summarize the notation used in the paper.

B.1 The Equations of Motion

Before writing the EOM's for the 2d fields, it is useful to recall the residual symmetries which survive after we choose the ansatze for the Skyrmion solution. As already discussed in Sec. 2.1.5, the ansatz preserves a $U(1)$ local symmetry with 2d gauge field A , which corresponds to the 5d gauge transformations given in eq. (2.57). The fields , , and are charged under this symmetry, thus it is convenient to write the action and the EOM in terms of their covariant derivatives

$$\begin{array}{lllllll} D & = & -iA & , & D & = & -iA \quad , \\ D & = & -iA & , & D & = & -iA \quad . \end{array} \tag{B.1}$$

There is also a second residual $U(1)$ generated by the $U(1)_{L\,R}$ 5d transformations of the form $\widehat{g}_R = \widehat{g}$ and $\widehat{g}_L = \widehat{g}$ with

$$\widehat{g} = \exp\left[i \;\; (r,z)(k \;\; \widehat{x})\right] , \tag{B.2}$$

whose associated gauge boson is B (see [21]). The field transforms as a Goldstone boson under this symmetry, so we can define its covariant derivative as

$$D \quad = \quad -B \;\; . \tag{B.3}$$

The EOM's for the 2d fields can be easily found by substituting the ansatz for the Skyrmion solution into the 5d action. The EOM's for the fields which appear in the static soliton case

$$\begin{cases} D\ (a(z)D\quad) + \dfrac{a(z)}{r^2}\ (1-\quad^2) + \dfrac{a^3(z)}{4}\ (\quad -\quad) + i\ L\quad \left(\dfrac{s}{r}\right) D\quad = 0 \\ \quad \left(r^2 a(z) A\quad\right) - a(z)\left(i\quad D\quad + h.c.\right) - \dfrac{i}{4}a^3(z) r^2 \left[\quad (D\quad) - (D\quad)\quad\right] \\ \qquad +\ L\quad \left(\frac{s}{r}\right)(\quad^2 - 1) = 0 \\ \quad \left(a(z)\quad s\right) - \dfrac{L}{2r}\quad \left[\quad (-i\quad D\quad + h.c.) + A\quad\right] = 0 \\ D\ (r^2 a^3(z) D\quad) - a^3(z)\ (\quad -\quad) - a^5(z) r^2 M_{Bulk}^2\quad = 0 \end{cases}, \tag{B.4}$$

while the equations for the fields which are turned on for the rotating Skyrmion are

$$\begin{cases} \quad (r^2 a(z)\quad w) - 2a(z)\left[w(1+\quad^2) -\quad -\quad\right] +\ L\quad \left[\dfrac{1}{2}(\quad^2 - 1)B\quad + rQA\quad\right] = 0 \\ D\ (r^2 a(z) D\quad) + a(z)\left[2w\quad - (1+\quad^2)\ \right] + \dfrac{1}{4}a^3(z) r^2\ (\quad -\quad) \\ \qquad -\ L\quad (D\quad)\,[i\quad (rQ) + D\quad] = 0 \\ \dfrac{1}{r}\quad (r^2 a(z)\quad Q) - \dfrac{2}{r}a(z) Q \\ \qquad -\dfrac{L}{2}\quad \left[(iD\quad (D\quad) + h.c.) + \dfrac{1}{2}A\quad (2w -\quad -\quad) - \dfrac{2}{{}_2}D\quad \left(\dfrac{s}{r}\right)\right] = 0 \\ \quad (a(z)D\quad) - \dfrac{1}{4}a^3(z)\left[(\quad +\quad) - 2i\ (\quad -\quad)\right] \\ \qquad -\dfrac{L}{2}\quad \left[\left(D\quad (D\quad) + h.c.\right) + \dfrac{i}{2}A\quad (\quad -\quad) + \dfrac{2}{{}_2}\quad (rQ)\quad \left(\dfrac{s}{r}\right)\right] = 0 \\ \quad \left(r^2 a(z) B\quad\right) + 2a(z) D\quad + \dfrac{1}{4}r^2 a^3(z)\left[2\quad D\quad + \left(\ (D\quad) -\ (D\quad) + \text{h.c.}\right)\right] \\ \qquad +\ L\quad \left\{\left[(\quad - w\ )(D\quad) + h.c.\right] + (1-\quad^2)\quad w - \dfrac{2r}{{}_2}Q\quad \left(\dfrac{s}{r}\right)\right\} = 0 \\ D\ (a^3(z) r^2 D\quad) -\quad (a^3(z) r^2 D\quad) - 2a^3(z) r^2 (D\quad)(D\quad) \\ \qquad - a^3(z)\ (2+\quad^2) + a^3(z)\ (\quad + 4i\ ) - r^2 a^5(z) M_{Bulk}^2\quad = 0 \\ \quad (r^2 a^3(z)\quad) - a^3(z)\left[\ (1+\quad^2) - i(\quad -\quad)\right] - r^2 a^5(z) M_{Bulk}^2\quad = 0\,. \end{cases} \tag{B.5}$$

In order to find suitable equations for the numerical analysis of the solutions, the EOM's must be rewritten as a system of elliptic partial differential equations. For this purpose we need to choose a gauge fixing condition for the residual 2d

$U(1)$ gauge symmetries. A possible choice is a Lorentz gauge condition

$$A \ = 0\,, \qquad\qquad B \ = 0\,. \tag{B.6}$$

With this condition the equations for A become $J \ = \ (r^2 a A \ ) = r^2 a \ \ A \ + \ (r^2 a) A$ which is an elliptic equation and a similar result is obtained for B .

B.2 The Boundary Conditions

The derivation of the boundary conditions for the 2d fields has been discussed in section 2.1.5. Here we report the list of conditions we need to impose on the scalar field components as well as the conditions for the gauge fields, which are analogous to the ones for the massless case [21].

The IR and UV boundary conditions on the 2d fields follow from the boundary conditions for the 5d fields (eqs. (2.28) and (2.24) with vanishing sources for the gauge fields, eqs. (2.29) and (2.20) for the scalar) and from the gauge choice in eq. (B.6). They are given explicitly by

$$z = z_{\rm IR} \ : \quad \begin{cases} \ _1 = 0 \\ \ _2 \ _2 = 0 \\ A_1 = 0 \\ \ _2 A_2 = 0 \\ \ _2 s = 0 \\ \ = -2i \end{cases} \qquad \begin{cases} \ _1 = 0 \\ \ _2 \ _2 = 0 \\ \ _2 w = 0 \\ \ _2 Q = 0 \end{cases} \qquad \begin{cases} \ = 0 \\ B_1 = 0 \\ \ _2 B_2 = 0 \\ \ = 0 \\ \ = 0 \end{cases} , \tag{B.7}$$

and

$$z = z_{\rm UV} \ : \quad \begin{cases} \ = -i \\ A_1 = 0 \\ \ _2 A_2 = 0 \\ s = 0 \\ \ = 2i M_q \, (z_{\rm UV}/z_{\rm IR}) \ ^- \end{cases} \qquad \begin{cases} \ = i \\ w = -1 \\ Q = 0 \end{cases} \qquad \begin{cases} \ = 0 \\ B_1 = 0 \\ \ _2 B_2 = 0 \\ \ = 0 \\ \ = 0 \end{cases} . \tag{B.8}$$

The boundary conditions at $r =$ are obtained by the requirement that the energy of the solution minus the vacuum energy for the scalar field is finite. To obtain a soliton solution with $B = 1$ one imposes

$$r = \quad : \quad \begin{cases} \ = -ie^{i \ (z - z_{\rm UV}) \ (z_{\rm IR} - z_{\rm UV})} \\ \ _1 A_1 = 0 \\ A_2 = \pi/(z_{\rm IR} - z_{\rm UV}) \\ s = 0 \\ \ = 2iv(z) e^{i \ (z - z_{\rm UV}) \ (z_{\rm IR} - z_{\rm UV})} \end{cases} \qquad \begin{cases} \ = ie^{i \ (z - z_{\rm UV}) \ (z_{\rm IR} - z_{\rm UV})} \\ w = -1 \\ Q = 0 \end{cases} \qquad \begin{cases} \ = 0 \\ \ _1 B_1 = 0 \\ B_2 = 0 \\ \ = 0 \\ \ = 0 \end{cases} . \tag{B.9}$$

On the $r = 0$ boundary of the domain we must require the 2d solution to give rise to regular 5d fields and the gauge choice in eq. (B.6) to be fulfilled. These conditions are fulfilled with the choice

$$r = 0 \ : \quad \begin{cases} {}_1/r \quad A_1 \\ (1 + \ {}_2)/r \quad 0 \\ A_2 = 0 \\ \ {}_1 A_1 = 0 \\ s = 0 \\ \ {}_1 = 0 \\ \ {}_1 \ {}_2 = 0 \end{cases} \qquad \begin{cases} \ {}_1 = 0 \\ \ {}_1 \ {}_2 = 0 \\ w = - \ {}_2 \\ Q = 0 \end{cases} \qquad \begin{cases} \ /r \quad B_1 \\ \ {}_1 B_1 = 0 \\ B_2 = 0 \\ \ {}_1 = \\ \ {}_2 = 0 \\ \ {}_1 \ = 0 \end{cases} . \tag{B.10}$$

Appendix C

The QCD Anomaly

In this appendix we describe different forms of the QCD anomaly and discuss the relation with the CS term included in the 5d theory. Part of the material that follows overlaps with appendix A of [38].

The CS term (2.23) can be written as

$$S_{CS} = -\frac{N_c}{24\pi^2}\int d^5x\,[\,\bar{}_5(\mathbf{L}) - \bar{}_5(\mathbf{R})]\ , \tag{C.1}$$

where $\bar{}_5$ differs by a total differential from the standard text-book CS form:

$$\begin{aligned} {}_5(\mathbf{A}) &= i\,\mathrm{tr}\left[\mathbf{A}\,(\mathrm{d}\mathbf{A})^2 + \frac{3}{2}\mathbf{A}^3\mathrm{d}\mathbf{A} + \frac{3}{5}\mathbf{A}^5\right] \\ &= i\,\frac{1}{4}\,A(\mathrm{d}\widehat{A})^2 + i\frac{3}{2}\,\widehat{A}\,\mathrm{tr}\left[F^2\right] + i\,\mathrm{d}\left[\widehat{A}\ \mathrm{tr}\left[A\,F - \frac{1}{4}A^3\right]\right] \qquad \bar{}_5(\mathbf{A}) + \mathrm{d}X(\mathbf{A}) \end{aligned} \tag{C.2}$$

The variation of the CS is given by eq. (2.27), where the 4-form

$$\bar{}^1_4(\boldsymbol{\alpha},\mathbf{A}) = \frac{1}{4}\widehat{}\left(\mathrm{d}\widehat{A}\right)^2 + \frac{3}{2}\widehat{}\ \mathrm{tr}\left[F^2\right]\ , \tag{C.3}$$

is defined from the relation $\bar{}_5 = \mathrm{d}\bar{}^1_4$ and it is related to the standard $^1_4$ by

$$\bar{}^1_4(\boldsymbol{\alpha},\mathbf{A}) = {}^1_4(\boldsymbol{\alpha},\mathbf{A}) - X(\mathbf{A})\,, \tag{C.4}$$

where

$${}^1_4(\boldsymbol{\alpha},\mathbf{A}) = \mathrm{tr}\left[\boldsymbol{\alpha}\,\mathrm{d}\left(\mathbf{A}\mathrm{d}\mathbf{A} + \frac{1}{2}\mathbf{A}^3\right)\right]\ . \tag{C.5}$$

Provided the IR term in eq. (2.27) is cancelled, the CS variation gives the anomaly of eq. (2.18), which however does not coincide with the standard text-book QCD anomaly that is normally put in the "symmetric" form

$$\mathcal{A}_{sym} = \frac{N_c}{24\pi^2}\int\left[\ {}^1_4(\boldsymbol{\alpha}_L,\mathbf{l}) - {}^1_4(\boldsymbol{\alpha}_R,\mathbf{r})\right]\ . \tag{C.6}$$

The two forms of the anomaly ($\mathcal{A}$ and $\mathcal{A}_{sym}$) are equivalent because they only differ by a local counterterm

$$\mathcal{A} = \mathcal{A}_{sym} - \frac{N_c}{24\pi^2}\left[\ {}_{\boldsymbol{\alpha}_L}X(\mathbf{L}) - \ {}_{\boldsymbol{\alpha}_R}X(\mathbf{R})\right] . \tag{C.7}$$

Obviously we may equivalently have added the X local counterterm to the 5d Lagrangian and kept the standard form of the QCD anomaly. This would have not affected any of our results because X only depends on the 4d $\mathbf{l}$ and $\mathbf{r}$ sources, whose physical value is zero.

Similarly, the QCD anomaly could be also put in the Adler Bardeen form. Starting from the symmetric anomaly, this is achieved by the addition of the Adler Bardeen counterterm, as explained in [42].

Appendix D

Dimension six operators involving quarks

Here we list the set of independent higher-dimensional operators involving SM quarks. As explained in section 3.2, we assume a flavor symmetry for the three left-handed quarks q_L, the three right-handed down-quarks d_R, and the two lightest right-handed up-quarks u_R, given by $U(3)_q \quad U(3)_d \quad U(2)_u$. The top right-handed quark t_R will be considered a singlet of the flavor symmetry. We use the following notation. We label with A, I and F the color, electroweak and flavor index respectively in the adjoint representation. The contraction of the indices in the fundamental representation of these symmetries is understood within the fields in parenthesis, and flavor indices can also be contracted with Yukawa matrices $Y_{u\,d}$. We identify $T_A = \ _A/2$, being $\ _A$ the Gell-Mann matrices, and $\ _I = \ _I/2$, where $\ _I$ are the Pauli matrices.

We classify the operators according to their expected suppression. First, we show the list of independent operators unsuppressed by Yukawa couplings (those generated in the massless quark limit). Following the discussion of section 3.2, we separate these operators as those of first class and second class, Eq. (3.6) and Eq. (3.7) respectively. We finally show the list of independent operators suppressed by Yuwaka couplings.

D.1 First class operators

D.1.1 Four-quark operators

$$
\begin{aligned}
\mathcal{O}_{dd}^{(1)} &= (d_R \quad d_R)(d_R \quad d_R) \\
\mathcal{O}_{ud}^{(1)} &= (u_R \quad u_R)(d_R \quad d_R) & \mathcal{O}_{td}^{(1)} &= (t_R \quad t_R)(d_R \quad d_R) \\
\mathcal{O}_{uu}^{(1)} &= (u_R \quad u_R)(u_R \quad u_R) & \mathcal{O}_{ut}^{(1)} &= (u_R \quad u_R)(t_R \quad t_R) \\
& & \mathcal{O}_{tt}^{(1)} &= (t_R \quad t_R)(t_R \quad t_R) \\
\mathcal{O}_{qu}^{(1)} &= (q_L \quad q_L)(u_R \quad u_R) & \mathcal{O}_{qt}^{(1)} &= (q_L \quad q_L)(t_R \quad t_R) \\
\mathcal{O}_{qd}^{(1)} &= (q_L \quad q_L)(d_R \quad d_R) \\
\mathcal{O}_{qq}^{(1)} &= (q_L \quad q_L)(q_L \quad q_L) \\
\mathcal{O}_{qq}^{(3_W)} &= (q_L \quad {}^I q_L)(q_L \quad {}^I q_L) \\
\mathcal{O}_{qq}^{(8_F)} &= (q_L \quad T^P q_L)(q_L \quad T^P q_L) \\
\mathcal{O}_{uu}^{(8)} &= (u_R \quad T^A u_R)(u_R \quad T^A u_R) & \mathcal{O}_{ut}^{(8)} &= (u_R \quad T^A u_R)(t_R \quad T^A t_R) \\
\mathcal{O}_{dd}^{(8)} &= (d_R \quad T^A d_R)(d_R \quad T^A d_R) \\
\mathcal{O}_{ud}^{(8)} &= (u_R \quad T^A u_R)(d_R \quad T^A d_R) & \mathcal{O}_{td}^{(8)} &= (t_R \quad T^A t_R)(d_R \quad T^A d_R) \\
\mathcal{O}_{qq}^{(8_C)} &= (q_L \quad T^A q_L)(q_L \quad T^A q_L) \\
\mathcal{O}_{qu}^{(8)} &= (q_L \quad T^A q_L)(u_R \quad T^A u_R) & \mathcal{O}_{qt}^{(8)} &= (q_L \quad T^A q_L)(t_R \quad T^A t_R) \\
\mathcal{O}_{qd}^{(8)} &= (q_L \quad T^A q_L)(d_R \quad T^A d_R)
\end{aligned}
\tag{D.1}
$$

For physics involving only the first family quarks, that as explained in section 3.3 mainly corresponds to the LHC dijet data $pp \quad jj$, we can reduce the above set of four-quark operators to the set of Eq. (3.12). In this reduction, we have

$$
\begin{aligned}
c_{uu}^{(1)} + \frac{1}{3} c_{uu}^{(8)} \qquad & c_{uu}^{(1)} \\
c_{dd}^{(1)} + \frac{1}{3} c_{dd}^{(8)} \qquad & c_{dd}^{(1)} \\
c_{qq}^{(1)} - \frac{1}{12} c_{qq}^{(3_W)} + \frac{1}{3} c_{qq}^{(8_F)} \qquad & c_{qq}^{(1)} \\
c_{qq}^{(8_C)} + c_{qq}^{(3_W)} \qquad & c_{qq}^{(8)}
\end{aligned}
\tag{D.2}
$$

D.1.2 Higgs-quark operators

$$\begin{aligned}
\mathcal{O}_{Hu} &= i(H \quad D \quad H)(u_R \quad u_R) \qquad\qquad \mathcal{O}_{Ht} = i(H \quad D \quad H)(t_R \quad t_R) \\
\mathcal{O}_{Hd} &= i(H \quad D \quad H)(d_R \quad d_R) \\
\mathcal{O}^{(1)}_{Hq} &= i(H \quad D \quad H)(q_L \quad q_L) \\
\mathcal{O}^{(3)}_{Hq} &= i(H \quad {}^I D \quad H)(q_L \quad {}^I q_L)
\end{aligned} \tag{D.3}$$

Notice that we just consider the antisymmetric part of the corresponding operators in [33]. This is so because the symmetric part of the above operators can be put in the form $(\ H\ ^2)(\qquad)$, where $\quad = (q_L, d_R, u_R, t_R)$. It can be shown that this kind of operators can be expressed in terms of operators appearing in D.3.

D.2 Second class operators

$$\begin{aligned}
\mathcal{O}_{uB} &= (u_R \quad u_R) \quad B \qquad\qquad \mathcal{O}_{tB} = (t_R \quad t_R) \quad B \\
\mathcal{O}_{dB} &= (d_R \quad d_R) \quad B \\
\mathcal{O}_{qB} &= (q_L \quad q_L) \quad B \\
\mathcal{O}_{qW} &= (q_L \ {}^I \quad q_L) D \ W^I
\end{aligned} \tag{D.4}$$

As explained in [94] this kind of operators can be rewritten, by using the equations of motion (EOM) for the field strengths, as four-fermion operators involving quarks and leptons. Also notice that operators involving gluons are not included since they can be rewritten as four-quark operators.

D.3 Yukawa-suppressed operators

The Yukawa couplings break the flavor symmetry and generate extra dimension-six operators. Assigning to the 3 3 Yukawa matrices, Y_d and Y_u, the following quantum numbers under G_F: $Y_d \quad (\mathbf{3}, \mathbf{3}, \mathbf{1})$, $Y_u \quad (Y_u)_{ik} \quad (\mathbf{3}, \mathbf{1}, \mathbf{2})$ $(i = 1, 2, 3;\ k = 1, 2)$ and $Y_t \quad (Y_u)_{i3} \quad (\mathbf{3}, \mathbf{1}, \mathbf{1})$, we can write the following G_F-invariant operators $(\widetilde{H} = i \ {}_2 H^{\ *})$:

(i)

$$\begin{aligned}
\mathcal{O}_{uH} &= (H^{\ *} \ H)(q_L Y_u \widetilde{H} u_R) \qquad\qquad \mathcal{O}_{tH} = (H^{\ *} \ H)(q_L Y_t \widetilde{H} t_R) \\
\mathcal{O}_{dH} &= (H^{\ *} \ H)(q_L Y_d H d_R)
\end{aligned} \tag{D.5}$$

(ii)

$$\begin{aligned}
\mathcal{O}_{uGH} &= (q_L Y_u \quad T^A u_R)\widetilde{H} G^A \qquad & \mathcal{O}_{tGH} &= (q_L Y_t \quad T^A t_R)\widetilde{H} G^A \\
\mathcal{O}_{uWH} &= (q_L Y_u \quad {}^I u_R)\widetilde{H} W^I & \mathcal{O}_{tWH} &= (q_L Y_t \quad {}^I t_R)\widetilde{H} W^I \\
\mathcal{O}_{uBH} &= (q_L Y_u \quad u_R)\widetilde{H} B & \mathcal{O}_{tBH} &= (q_L Y_t \quad t_R)\widetilde{H} B \\
\mathcal{O}_{dGH} &= (q_L Y_d \quad T^A d_R) H G^A \\
\mathcal{O}_{dWH} &= (q_L Y_d \quad {}^I d_R) H W^I \\
\mathcal{O}_{dBH} &= (q_L Y_d \quad d_R) H B
\end{aligned} \tag{D.6}$$

(iii)

$$\begin{aligned}
\mathcal{O}_{uDH} &= (q_L Y_u u_R) D \;\; D \;\; \widetilde{H} \qquad & \mathcal{O}_{tDH} &= (q_L Y_t t_R) D \;\; D \;\; \widetilde{H} \\
\mathcal{O}_{dDH} &= (q_L Y_d d_R) D \;\; D \;\; H
\end{aligned} \tag{D.7}$$

By applying the EOM of H these operators could be rewritten as other operators of the list plus four-fermion operators involving leptons.

(iv)

$$\begin{aligned}
\mathcal{O}_{Hud} &= i(\widetilde{H} \;\; D \;\; H)(u_R Y_u Y_d \quad d_R) \\
\mathcal{O}_{Htd} &= i(\widetilde{H} \;\; D \;\; H)(t_R Y_t \; Y_d \quad d_R)
\end{aligned} \tag{D.8}$$

(v)

$$\begin{aligned}
\mathcal{O}^{(1)}_{qud} &= (q_L Y_u u_R)(q_L Y_d d_R) \\
\mathcal{O}^{(1)}_{qtd} &= (q_L Y_t t_R)(q_L Y_d d_R) \\
\mathcal{O}^{(8)}_{qud} &= (q_L Y_u T^A u_R)(q_L Y_d T^A d_R) \\
\mathcal{O}^{(8)}_{qtd} &= (q_L Y_t T^A t_R)(q_L Y_d T^A d_R)
\end{aligned} \tag{D.9}$$

Bibliography

[1] T. Kaluza, Sitzungsber. Preuss. Akad. Wiss. Berlin (Math. Phys.) **1921** (1921) 966; O. Klein, Z. Phys. **37** (1926) 895 [Surveys High Energ. Phys. **5** (1986) 241].

[2] O. Domenech, M. Montull, A. Pomarol, A. Salvio and P. J. Silva, JHEP **1008** (2010) 033 [arXiv:1005.1776 [hep-th]].

[3] O. Domenech, G. Panico and A. Wulzer, Nucl. Phys. A **853** (2011) 97 [arXiv:1009.0711 [hep-ph]].

[4] O. Domenech, A. Pomarol and J. Serra, arXiv:1201.6510 [hep-ph].

[5] T. Gherghetta, arXiv:1008.2570 [hep-ph].

[6] J. M. Maldacena, Adv. Theor. Math. Phys. **2** (1998) 231 [Int. J. Theor. Phys. **38** (1999) 1113] [hep-th/9711200].

[7] N. Arkani-Hamed, S. Dimopoulos and G. R. Dvali, Phys. Lett. B **429** (1998) 263 [hep-ph/9803315].

[8] I. Antoniadis, N. Arkani-Hamed, S. Dimopoulos and G. R. Dvali, Phys. Lett. B **436** (1998) 257 [hep-ph/9804398].

[9] L. Randall and R. Sundrum, Phys. Rev. Lett. **83** (1999) 3370 [hep-ph/9905221].

[10] L. Randall and R. Sundrum, Phys. Rev. Lett. **83** (1999) 4690 [hep-th/9906064].

[11] E. Witten, Adv. Theor. Math. Phys. **2** (1998) 253 [hep-th/9802150].

[12] S. S. Gubser, I. R. Klebanov and A. M. Polyakov, Phys. Lett. B **428** (1998) 105 [hep-th/9802109].

[13] N. Arkani-Hamed, M. Porrati and L. Randall, JHEP **0108** (2001) 017 [hep-th/0012148].

[14] R. Rattazzi and A. Zaffaroni, JHEP **0104** (2001) 021 [hep-th/0012248].

[15] M. Perez-Victoria, JHEP **0105** (2001) 064 [hep-th/0105048].

[16] G. 't Hooft, Nucl. Phys. B **72** (1974) 461.

[17] E. Witten, Nucl. Phys. B **160** (1979) 57.

[18] T. H. R. Skyrme, Proc. Roy. Soc. Lond. A **260** (1961) 127.

[19] A. Pomarol and A. Wulzer, JHEP **0803** (2008) 051 [arXiv:0712.3276 [hep-th]].

[20] A. Pomarol and A. Wulzer, Nucl. Phys. B **809** (2009) 347 [arXiv:0807.0316 [hep-ph]].

[21] G. Panico and A. Wulzer, Nucl. Phys. A **825** (2009) 91 [arXiv:0811.2211 [hep-ph]].

[22] L. Da Rold and A. Pomarol, Nucl. Phys. B **721**, 79 (2005) [arXiv:hep-ph/0501218].

[23] T. Gherghetta and A. Pomarol, Nucl. Phys. B **586** (2000) 141 [hep-ph/0003129].

[24] F. London and H. London, Proc. Roy. Soc. (London) **A149**, 71 (1935).

[25] V. L. Ginzburg and L. D. Landau, "On the Theory of superconductivity," Zh. Eksp. Teor. Fiz. **20**, 1064 (1950).

[26] J. Bardeen, L. N. Cooper and J. R. Schrieffer, "Theory Of Superconductivity," Phys. Rev. **108**, 1175 (1957).

[27] *For a review see, for example,* S. A. Hartnoll, Class. Quant. Grav. **26** (2009) 224002 [arXiv:0903.3246 [hep-th]]; C. P. Herzog, J. Phys. A **42** (2009) 343001 [arXiv:0904.1975 [hep-th]]; G. T. Horowitz, arXiv:1002.1722 [hep-th].

[28] K. Nakamura *et al.* [Particle Data Group Collaboration], "Review of particle physics", J. Phys. G **G37** (2010) 075021.

[29] K. Agashe, R. Contino and A. Pomarol, Nucl. Phys. B **719** (2005) 165 [hep-ph/0412089].

[30] D. B. Kaplan and H. Georgi, "SU(2) X U(1) Breaking By Vacuum Misalignment", Phys. Lett. B **136** (1984) 183; D. B. Kaplan, H. Georgi and S. Dimopoulos, "Composite Higgs Scalars", Phys. Lett. B **136** (1984) 187.

[31] J. Mrazek, A. Pomarol, R. Rattazzi, M. Redi, J. Serra and A. Wulzer, Nucl. Phys. B **853** (2011) 1 [arXiv:1105.5403 [hep-ph]].

[32] K. Agashe, R. Contino, L. Da Rold and A. Pomarol, Phys. Lett. B **641** (2006) 62 [hep-ph/0605341].

[33] W. Buchmuller and D. Wyler, Nucl. Phys. B **268** (1986) 621.

[34] J. Polchinski and M. J. Strassler, JHEP **0305** (2003) 012 [arXiv:hep-th/0209211]; D. T. Son and M. A. Stephanov, Phys. Rev. D **69** (2004) 065020 [arXiv:hep-ph/0304182]; A. Karch, E. Katz, D. T. Son and M. A. Stephanov, Phys. Rev. D **74** (2006) 015005 [arXiv:hep-ph/0602229];

[35] J. Erlich, E. Katz, D. T. Son and M. A. Stephanov, Phys. Rev. Lett. **95**, 261602 (2005) [arXiv:hep-ph/0501128].

[36] L. Da Rold and A. Pomarol, JHEP **0601**, 157 (2006) [arXiv:hep-ph/0510268].

[37] J. Hirn and V. Sanz, JHEP **0512**, 030 (2005) [arXiv:hep-ph/0507049];

[38] D. Becciolini, M. Redi and A. Wulzer, arXiv:0906.4562 [hep-ph].

[39] M. A. B. Beg and A. Zepeda, Phys. Rev. D **6** (1972) 2912.

[40] A. Cherman, T. D. Cohen and M. Nielsen, Phys. Rev. Lett. **103** (2009) 022001 [arXiv:0903.2662 [hep-ph]].

[41] E. Witten, Nucl. Phys. B **223** (1983) 422.

[42] G. Panico and A. Wulzer, JHEP **0705** (2007) 060 [arXiv:hep-th/0703287].

[43] E. Katz and M. D. Schwartz, JHEP **0708** (2007) 077 [arXiv:0705.0534 [hep-ph]].

[44] B. R. Holstein, Phys. Lett. B **244** (1990) 83.

[45] J. Bijnens and J. Prades, Nucl. Phys. B **490** (1997) 239 [arXiv:hep-ph/9610360].

[46] A. Pich, arXiv:hep-ph/9806303.

[47] J. Gasser and H. Leutwyler, Nucl. Phys. B **250** (1985) 465.

[48] R. D. Amado, R. Bijker and M. Oka, Phys. Rev. Lett. **58** (1987) 654.

[49] T. Sakai and S. Sugimoto, Prog. Theor. Phys. **113** (2005) 843 [arXiv:hep-th/0412141]; *ibid.* **114** (2005) 1083 [arXiv:hep-th/0507073].

[50] T. Imoto, T. Sakai and S. Sugimoto, arXiv:1005.0655 [hep-th].

[51] S. A. Hartnoll, C. P. Herzog and G. T. Horowitz, Phys. Rev. Lett. **101** (2008) 031601 [arXiv:0803.3295 [hep-th]].

[52] P. Basu, A. Mukherjee and H. H. Shieh, Phys. Rev. D **79** (2009) 045010 [arXiv:0809.4494 [hep-th]]; C. P. Herzog, P. K. Kovtun and D. T. Son, Phys. Rev. D **79** (2009) 066002 [arXiv:0809.4870 [hep-th]].

[53] E. Witten arXiv:hep-th/0307041.

[54] S. A. Hartnoll, C. P. Herzog and G. T. Horowitz, JHEP **0812** (2008) 015 [arXiv:0810.1563 [hep-th]].

[55] T. Albash and C. V. Johnson, JHEP **0809** (2008) 121 [arXiv:0804.3466 [hep-th]]. E. Nakano and W. Y. Wen, Phys. Rev. D **78** (2008) 046004 [arXiv:0804.3180 [hep-th]]. K. Maeda and T. Okamura, Phys. Rev. D **78** (2008) 106006 [arXiv:0809.3079 [hep-th]]. X. H. Ge, B. Wang, S. F. Wu and G. H. Yang, arXiv:1002.4901 [hep-th].

[56] M. Montull, A. Pomarol and P. J. Silva, Phys. Rev. Lett. **103** (2009) 091601 [arXiv:0906.2396 [hep-th]].

[57] V. Keranen, E. Keski-Vakkuri, S. Nowling and K. P. Yogendran, arXiv:0912.4280 [hep-th].

[58] T. Albash and C. V. Johnson, arXiv:0906.0519 [hep-th]; T. Albash and C. V. Johnson, Phys. Rev. D **80** (2009) 126009 [arXiv:0906.1795 [hep-th]].

[59] S. Weinberg, Prog. Theor. Phys. Suppl. **86** (1986) 43.

[60] W. H. Kleiner, L. M. Roth and S. H. Autler, Phys. Rev. A**133** (1964) 1226.

[61] G. T. Horowitz and M. M. Roberts, Phys. Rev. D **78** (2008) 126008 [arXiv:0810.1077 [hep-th]].

[62] See http://www.comsol.com.

[63] K. Maeda, M. Natsuume and T. Okamura, Phys. Rev. D **81** (2010) 026002 [arXiv:0910.4475 [hep-th]].

[64] B. D. Josephson, Phys. Lett. **1** (1962) 251.

[65] S. S. Gubser and S. S. Pufu, JHEP **0811** (2008) 033 [arXiv:0805.2960 [hep-th]]; M. M. Roberts and S. A. Hartnoll, JHEP **0808** (2008) 035 [arXiv:0805.3898 [hep-th]]; M. Ammon, J. Erdmenger, M. Kaminski and P. Kerner, Phys. Lett. B **680** (2009) 516 [arXiv:0810.2316 [hep-th]]; JHEP **0910** (2009) 067 [arXiv:0903.1864 [hep-th]].

[66] K. Balasubramanian and J. McGreevy, Phys. Rev. Lett. **101** (2008) 061601 [arXiv:0804.4053 [hep-th]]; S. Kachru, X. Liu and M. Mulligan, Phys. Rev. D **78** (2008) 106005 [arXiv:0808.1725 [hep-th]]; M. Taylor, arXiv:0812.0530 [hep-th].

[67] See, for example, Henri Bachacou's talk at the Lepton-Photon Symposium, Mumbai, August 2011.

[68] G. Aad [ATLAS Collaboration], Phys. Lett. **B694** (2011) 327-345 [arXiv:1009.5069 [hep-ex]].

[69] G. Aad *et al.* [ATLAS Collaboration], arXiv:1103.3864 [hep-ex].

[70] V. Khachatryan *et al.* [CMS Collaboration], Phys. Rev. Lett. **105** (2010) 262001 [arXiv:1010.4439 [hep-ex]].

[71] V. Khachatryan *et al.* [CMS Collaboration], arXiv:1102.2020 [hep-ex].

[72] E. Eichten, K. D. Lane and M. E. Peskin, Phys. Rev. Lett. **50** (1983) 811.

[73] G. F. Giudice, C. Grojean, A. Pomarol and R. Rattazzi, JHEP **0706** (2007) 045 [hep-ph/0703164]; see also recent examples in J. Mrazek *et al.*, Nucl. Phys. B **853** (2011) 1 [arXiv:1105.5403 [hep-ph]].

[74] M. Gabella, T. Gherghetta and J. Giedt, Phys. Rev. D **76** (2007) 055001 [arXiv:0704.3571 [hep-ph]]; T. Gherghetta and A. Pomarol, JHEP **1112** (2011) 069 [arXiv:1107.4697 [hep-ph]].

[75] F. Bazzocchi, U. De Sanctis, M. Fabbrichesi and A. Tonero, arXiv:1111.5936 [hep-ph].

[76] T. Aaltonen *et al.* [CDF Collaboration], Phys. Rev. D **83** (2011) 112003 [arXiv:1101.0034 [hep-ex]].

[77] V. M. Abazov *et al.* [D0 Collaboration], Phys. Rev. D **84** (2011) 112005 [arXiv:1107.4995 [hep-ex]].

[78] For the case of the top quark, see B. Lillie, J. Shu and T. M. P. Tait, JHEP **0804** (2008) 087 [arXiv:0712.3057 [hep-ph]]; A. Pomarol and J. Serra, Phys. Rev. D **78** (2008) 074026 [arXiv:0806.3247 [hep-ph]].

[79] M. Bona *et al.* [UTfit Collaboration], JHEP **0803** (2008) 049 [arXiv:0707.0636 [hep-ph]].

[80] K. Kumar, W. Shepherd, T. M. P. Tait and R. Vega-Morales, JHEP **1008** 052 (2010) [arXiv:1004.4895 [hep-ph]].

[81] M. Redi and A. Weiler, JHEP **1111** (2011) 108 [arXiv:1106.6357 [hep-ph]].

[82] R. Barbieri, A. Pomarol, R. Rattazzi and A. Strumia, "Electroweak symmetry breaking after LEP1 and LEP2", Nucl. Phys. B **703** (2004) 127 [arXiv:hep-ph/0405040].

[83] E. Eichten, I. Hinchliffe, K. D. Lane *et al.*, Rev. Mod. Phys. **56** (1984) 579-707.

[84] R. S. Chivukula, A. G. Cohen and E. H. Simmons, Phys. Lett. B **380** (1996) 92 [arXiv:hep-ph/9603311].

[85] J. Alwall, P. Demin, S. de Visscher, R. Frederix, M. Herquet, F. Maltoni, T. Plehn, D. L. Rainwater *et al.*, JHEP **0709** (2007) 028 [arXiv:0706.2334 [hep-ph]].

[86] A. D. Martin, W. J. Stirling, R. S. Thorne and G. Watt, Eur. Phys. J. C **63** (2009) 189 [arXiv:0901.0002 [hep-ph]].

[87] M. Perelstein, arXiv:1002.0274 [hep-ph].

[88] J. Gao, C. S. Li, J. Wang, H. X. Zhu and C. -P. Yuan, Phys. Rev. Lett. **106** (2011) 142001 [arXiv:1101.4611 [hep-ph]].

[89] A. V. Manohar and M. Trott, arXiv:1201.3926 [hep-ph].

[90] E. Alvarez, L. Da Rold, J. I. S. Vietto and A. Szynkman, JHEP **1109** (2011) 007 [arXiv:1107.1473 [hep-ph]].

[91] U. Haisch and S. Westhoff, JHEP **1108** (2011) 088 [arXiv:1106.0529 [hep-ph]].

[92] C. Degrande, J. -M. Gerard, C. Grojean, F. Maltoni and G. Servant, JHEP **1103** (2011) 125 [arXiv:1010.6304 [hep-ph]].

[93] C. Delaunay, O. Gedalia, Y. Hochberg, G. Perez and Y. Soreq, JHEP **1108** (2011) 031 [arXiv:1103.2297 [hep-ph]].

[94] J. A. Aguilar-Saavedra, Nucl. Phys. B **812** (2009) 181 [arXiv:0811.3842 [hep-ph]].